

**An shRNA expression system to interrogate the role of
PTEN proximal genes in BRAF^{V600E}-driven melanoma
malignancy *in vitro***

Angeline de Bruyns
Department of Biology, McGill University

July 2015

A thesis submitted to McGill University in partial fulfillment of the requirements of the degree
of Master of Science

© Angeline de Bruyns, 2015

Table Of Contents

i. Abstract	4
English	4
French	5
ii. Acknowledgements	7
iii. Preface	8
Background	8
Authors Contributions	9
1. Introduction	10
1.1. Introduction to Melanoma	10
1.2. Genetic and Environmental Interactions in Melanomagenesis	11
1.3. The MAPK Signaling Pathway in Melanoma	12
1.4. The PI3K/AKT Signaling Pathway in Melanoma	14
1.5. BRAF ^{V600E} Therapeutic Inhibition and Mechanisms of Resistance	17
1.6. PI3K-AKT-mTOR Therapeutic Inhibition and Resistance	19
1.7. Research Objectives	22
2. Materials and Methods	25
2.1. Manipulation of DNA/Plasmid Preparation	25
2.1.1. Bacterial Growth	25
2.1.2. Sequencing	25
2.1.3. Gateway LR Reaction (pCheck2, pTREG, and pLEG)	25
2.1.4. Cloning of shRNA into pBEG shTest	26
2.1.5. pCheck2 Plasmids	27
2.1.6. Generation of pBEG miRNA-E	28
2.2. Tissue Culture	28
2.2.1. Culture of Mammalian Cells	28
2.2.2. Transfections	29
2.2.3. Luciferase Assay	29
2.2.4. Lentivirus Production	30
2.2.5. Lentivirus Production for Concentration by Ultracentrifugation	30
2.2.6. Lentivirus Titration – Puromycin-Resistant Colonies	31
2.2.7. Lentivirus Titration – TurboRFP Positive Colonies	31
2.2.8. Lentivirus Infection	32
2.2.9. Doxycycline Treatment	33
2.2.10. Resazurin Viability Assays	33
2.2.11. Western Blots	33
2.2.12. Microscopy	34
3. Results	35
3.1. PTEN Proximal Gene Knockdown	35
3.1.1. shRNA Triaging with a Luciferase Reporter System	35
3.1.2. shRNA Delivery	40
3.1.2.1. Transient PTEN Proximal Gene Knockdown	40
3.1.2.2. Stable and Inducible PTEN Proximal Gene Knockdown	41
3.1.3. The miRNA-E Backbone	47
4. Discussion	49
4.1. Optimization of shRNA Delivery	49

4.2. Future Work	51
5. Conclusion	54
6. Bibliography	55
7. Appendix.....	72
7.1. Optimizing pTREG shRNA Knockdown.....	72
7.1.1. Insufficient Knockdown with pTREG	72
7.1.2. Lentiviral Infection Cytotoxicity.....	75
7.1.2.1. Viral Pseudotyping and Serum-less Medium for Virus Production and Infection.....	80
7.1.2.1. Underestimation of Lentiviral Titer/Redefining MOI	86
7.1.3. Doxycycline Toxicity	90
7.2. Appendix Tables.....	93

Table Of Figures

Figure 1.1. Experimental approach.	23
Figure 3.1 Rapid triage of novel shRNAs.	36
Figure 3.2. Luciferase assay triaging results for shRNAs targeting PTEN Proximal genes.....	39
Figure 3.3. Transient pBEG shRNA-mediated endogenous protein knockdown in 293T cells.	40
Figure 3.4. Overview of Gateway cloning of shRNAmirs into pLEG and pTREG lentiviral vectors.	42
Figure 3.5. pLEG and pTREG shRNA-mediated knockdown of targeted genes.	45
Figure 3.6. Western blot analysis of PTEN Proximal protein expression in melanoma cells and knockdown in pLEG shRNA cell lines.	46
Figure 3.7. Evaluating the efficacy of shRNA-mediated target knockdown in the miRNA-30 and miRNA-E backbones.	48
Figure 7.1. pTREG-mediated knockdown in melanoma cells.	74
Figure 7.2. Troubleshooting cytotoxicity associated with lentiviral transduction.	77
Figure 7.3. Affect of increased MOI on pTREG-mediated TurboRFP expression and target knockdown.	80
Figure 7.4. Affect of lentiviral vector pseudotyping and serum-less media on the infectivity and cytotoxicity of infection.	82
Figure 7.5. Presence of serum in virus production and transduction affects viral cytotoxicity.	86
Figure 7.6. Characterization of pTREG-mediated target knockdown at different MOIs.	89
Figure 7.7. Effect of doxycycline concentration on pTREG expression and cell viability.....	91

Table Of Tables

Table 1. Sequencing primers for shRNA sequence confirmation in shRNAmir containing plasmids.	93
Table 2. Cloning primers to construct TOPO compatible AKT2 cDNA PCR product.	93
Table 3. DNA oligonucleotides for shRNA sequences used in the pBEG system.	94
Table 4. The miRNA-30 and miRNA-E backbones.	95
Table 5. Melanoma lines and their mutation status.....	96
Table 6. Primers for qRT-PCR analysis of PTEN Proximal gene mRNA expression.....	97

i. Abstract

English

Despite valiant clinical efforts, metastatic melanoma remains as one of the most difficult cancers to treat, possessing abysmal 5-year survival rates (<20 %). Melanoma accounts for less than 5% of skin cancer cases, but is responsible for the vast majority of skin cancer deaths. To develop more effective targeted therapies, uncovering the genetic underpinnings for the initiation and progression of malignant melanoma is of utmost importance. The *BRAF*^{V600E} mutation has been identified as one of the earliest and most frequent oncogenic events in melanoma. *BRAF*^{V600E} stimulates sustained activation of the MAPK pathway, promoting cellular proliferation and survival. However, oncogenic *BRAF* activation is known to be insufficient for full malignant conversion because of oncogene induced senescence. Progression to malignant melanoma is invariably accompanied by silencing of one or more tumour suppressor genes, such as *PTEN*. *PTEN* negatively regulates the PI3K-AKT pathway which promotes cellular proliferation and survival parallel to the MAPK pathway. It has been shown that *BRAF*^{V600E} cooperates with *PTEN* loss to induce metastatic melanoma. Furthermore, *PTEN* loss and subsequent hyperactivation of the PI3K-AKT signalling pathway contributes to the therapeutic resistance that develops in *BRAF* mutant melanoma treated with *BRAF*^{V600E} inhibitors. Using shRNA-mediated knockdown technologies, this research aims to investigate which molecules immediately upstream and downstream of *PTEN* in the PI3K-AKT pathway (*PTEN* Proximal proteins) are required for mediating the signals responsible for the malignant phenotype of *BRAF*^{V600E}-driven melanoma *in vitro*. Thus, the ultimate goal of this research is to identify potentially druggable contributors to melanoma formation, progression, and drug resistance. Towards this goal, I have used a unique shRNA luciferase-reporter triaging system to identify shRNAs that would effectively and specifically knockdown expression of *PTEN* Proximal proteins. I created lentiviral shRNA targeting constructs and optimized the delivery of these constructs into *BRAF*^{V600E} melanoma cell lines. The remainder of the my research involved the optimization of an inducible lentiviral expression system to ensure adequate knockdown of *PTEN* proximal proteins can be achieved as this will be required to properly assess their role in the melanoma malignancy.

French

Malgré les efforts cliniques soutenus, le mélanome métastatique demeure un des cancers les plus difficiles à traiter, laissant une espérance de vie maximale de 5 ans aux personnes qui en sont atteintes (<20%). Le mélanome compte pour moins de 5 % des cas de cancer de la peau, mais est responsable de la majorité des mortalités dues à ce type de cancer. Afin de développer des thérapies plus efficaces, découvrir la génétique impliquée dans l'initiation et la progression du mélanome malin est de la première importance. La mutation BRAF^{V600E} a été identifiée comme étant un des événements les plus courants chez le mélanome. BRAF^{V600E} active constitutivement la voie de signalisation MAPK, ce qui promouvoit la prolifération et la survie de la cellule. Par contre, l'activation de BRAF est insuffisante pour le développement en tumeur maligne et la cellule progresse plutôt vers la sénescence. La progression vers le mélanome malin est invariablement accompagnée par la suppression d'un ou plusieurs gènes suppresseurs de tumeurs tels que PTEN (20% des mélanomes). PTEN inhibe la voie de signalisation PI3K-AKT, laquelle promouvoit la prolifération et la survie de la cellule, parallèlement à la voie de signalisation MAPK. Il a été démontré que BRAF^{V600E} agit en coopération avec la perte de PTEN afin d'induire un mélanome métastatique. De plus, la perte de PTEN et l'hyperactivation de la voie PI3K-AKT qui en résulte contribuent à offrir une résistance thérapeutique qui se développe chez les mélanomes arborant une mutation de BRAF et qui sont traités à l'aide d'inhibiteurs de BRAF^{V600E}. À l'aide d'une technologie permettant de diminuer significativement l'expression d'un gène *in vitro* (sh-RNA), les expérimentations exposées ici avaient pour but de déterminer quelles sont les molécules immédiatement avant ou après PTEN dans la voie de signalisation PI3K-AKT (protéines proximales de PTEN) qui sont requises pour transmettre les signaux responsables du phénotype malin du mélanome causé par BRAF^{V600E}. Le but ultime étant l'identification de protéines cibles contribuant à la formation, la progression ou la résistance aux agents thérapeutiques. À l'aide d'un système unique de shRNA utilisant la luciférase comme gène rapporteur, j'ai identifié des shRNAs qui pouvaient efficacement et spécifiquement diminuer l'expression de protéines proximales de PTEN. Afin d'en savoir davantage, ces shRNA ont été livrés à l'aide de lentivirus dans des lignées cellulaires de mélanomes possédant la mutation BRAF^{V600E}. Dû à des complications, le reste de mon projet de recherche a impliqué l'optimisation de l'expression à l'aide de lentivirus afin de m'assurer d'une

diminution significative des protéines proximales de PTEN, ce qui est requis afin de connaître leur rôle chez le mélanome malin.

ii. Acknowledgements

First and foremost, I would like to extend my sincerest appreciation to my supervisor Dr. David Dankort for all of the support and mentorship he has provided during my graduate studies at McGill. I would like to thank him for providing the means to work on such an interesting project and for always making himself available to any project-related queries I had. I am truly grateful for his advice on the research and encouragement along the way. This has been an invaluable learning experience and an enjoyable one at that, especially since Dr. Dankort always advocated for a positive lab environment and the well being of his graduate students. I would also like to extend by appreciation to the members of my supervisory committee, Dr. Joe Teodoro and Dr. Nam-Sung Moon, for their advisement on my research.

I would like to thank the previous members of the Dankort lab, Guillame Vandal and Ben Geiling, for their instruction on techniques that were new to me when I first started in the lab. Separately, I would like to thank the efforts of a former undergraduate student in the lab, Cristina Jamieson, who under my supervision assisted with many aspects of my project. Her contribution undoubtedly allowed the project to progress more smoothly. I would also like to thank current members of the lab, Sam Garnett, Kendall Dutchak, and Kyle Lewis for their help on aspects of the research and their continued companionship. Additionally, I would like to extend my thanks to our lab manager Eve Bigras, who always made sure the lab was running smoothly for our use and for translating my abstract to French.

Thank you to all of the members of the Bellini 2nd floor labs for being immensely welcoming upon the start of my time at McGill and for their continued friendship and camaraderie. Furthermore, I greatly appreciate all the occasions when neighboring lab members were willing to lend me equipment, reagents, or expertise for my research needs. Lastly, I would like to say thank you to all my friends and family for their continued support during my studies at McGill.

iii. Preface

Background

Incidence of melanoma is on the rise world-wide, with the highest incidence occurring in North America, North and Western Europe, and Australia/New Zealand[2]. In 2012, melanoma accounted for 232,000 new cancer cases and 55,000 cancer-related deaths world-wide[2]. Melanoma is by far the deadliest form of skin cancer owing to its resistance to therapeutic treatment (conventional and targeted), aggressive clinical behaviour, and tendency to result in lethal metastasis. Genetically, melanoma is a complex disease[3], the management of which will likely require an in-depth understanding of the molecular biology underlying its initiation, progression, and resistance to therapeutics. Mutations that activate oncogenes and/or deactivate tumour suppressor genes can lead to the formation of malignant tumours. In melanoma, the proto-oncogene *BRAF* is frequently mutated and expression or function of the tumour suppressor gene *PTEN* is commonly lost or reduced. BRAF is an activator of the MAPK pathway and PTEN negatively regulates the PI3K-AKT pathway. Both of these pathways mediate extracellular signals that stimulate cellular proliferation and survival. Alterations resulting in concurrent oncogenic activation of *BRAF* and loss of *PTEN* function are prevalent in human melanoma [4-7]. While patients receiving a specific BRAF inhibitor often have astounding initial responses, invariably these patients become resistant to the drug[8-10]. This has prompted researchers to redouble their efforts to identify additional targets for combined therapies that will overcome the mechanisms of resistance.

During my graduate work at McGill, I set out to investigate how one of the most common oncogenic mutations in melanoma, *BRAF*^{V600E}, cooperates with members of the PI3K-AKT pathway to contribute to the malignant characteristics and drug resistance of melanoma cells *in vitro*. I planned to systematically ablate the expression of specific PI3K-AKT signaling to assess their effect on the proliferative potential, viability, and malignant transformation of *BRAF*^{V600E} melanoma cells. Towards this goal, I have identified shRNAs that effectively and specifically target these genes in cell culture. Additionally, I constructed lentiviral shRNA expression vectors and optimized the delivery of these targeting constructs into melanoma cell lines. The established protocols will provide the framework for finding druggable targets in the PI3K-AKT pathway

informing the development of new targeted and effective therapeutic options in the treatment of melanoma.

Authors Contributions

This thesis was written entirely by myself (Angeline de Bruyns). The work represented herein is the research effort for my graduate degree and was my own work unless otherwise stated. I would like to recognize Ben Geiling for the work he did to prepare the luciferase assay shRNA triaging system and the Gateway compatible pLEG lentiviral vector construction system. Also, thank you to Kendall Dutchak for preparing the Gateway compatible pCheck2 plasmid. I would like to recognize the successful effort made by Samantha Garnett of the Dankort lab who made the pTRIPz plasmid Gateway compatible to create the pTREG vector that I used extensively during the course of this work. I would also like to recognize efforts of Cristina Jamieson, a former undergraduate student under my supervision, in assisting with many parts of the project along the way including the cloning of shRNAs into the pTREG plasmid, designing and testing qRT-PCR primers to assess mRNA expression of the PTEN Proximal genes (Appendix, Table 6), and for running the Western blot with samples I prepared to make Figure 7.3B. And lastly, I would like to recognize Kyle Lewis for his contributions to experiments involving the optimization of the pTREG system, specifically for making lentivirus, performing the infections, and taking photos to prepare Figure 7.4 (A, B, and D), for performing the WM1617 Western blots and assisting with preparing Figure 7.6C, for performing the doxycycline time course experiment and Western blots to produce Figure 7.6D, and for performing the luciferase assay, doxycycline time course, and Western blot to prepare Figure 3.7.

1. Introduction

1.1. Introduction to Melanoma

Melanoma arises as cancer of melanocytes that predominantly reside in the skin. Cutaneous melanoma accounts for most melanoma cases although melanoma can also result from the non-cutaneous melanocytes residing in the pigmented parts of the eye (uveal melanoma) or internal mucosal membranes (mucosal melanoma). These latter melanomas are relatively rare (<10%)[11, 12]. In comparison to other skin cancers, such as basal and squamous cell carcinoma which total 2 – 3 million cases per year worldwide, melanoma accounts for less than five percent of skin cancer cases[13]. However, melanoma is the deadliest form of skin cancer, causing the vast majority of skin cancer deaths (61% in 2010)([14, 15]. Additionally, melanoma incidence rates continue to rise worldwide, notably in the United States where there has been a 300% increase over the past 40 years[16, 17]. Melanoma cancers are known for their resistance to therapeutic treatment, aggressive clinical behaviour, and tendency to result in lethal metastasis[18]. Surgical resection of early melanoma has a 98% 5-year survival rate. This number drops to an abysmal 16% when the disease metastasizes to distant organs[19]. The rising incidence and poor prognosis of this cancer has motivated research aimed towards uncovering the genetic underpinnings for malignant melanoma initiation, progression, and resistance to therapeutic intervention. Indeed, melanoma is a genetically heterogeneous disease, exhibiting some of the highest mutation rates compared to nearly all other solid tumour types[3, 20, 21]

Clinical and histological studies have shown that development of metastatic melanoma is often a multistep process. Stages in melanoma-genesis are generally characterized by additionally acquired genetic aberrations that can instill a proliferative, invasive, and/or survival advantage[22-24]. Melanoma can arise from precursor lesions such as benign nevi (typical moles) or dysplastic nevi (atypical moles). Nevi develop as a result of an oncogenic mutation causing an initially uncontrollable proliferation of melanocytes. These melanocytic lesions occur within the outer layer of the skin (the epidermis), above the basement membrane and the dermis, where melanocytes are typically found [23]. Moles are thought to be benign precursors of melanoma. Fortunately, the majority of moles remain arrested for the lifetime of the individual due to a phenomenon known as oncogene induced senescence (OIS)[25, 26] . However, likely

due to subsequent genetic/epigenetic changes they can progress to the radial growth phase (RGP) and/or vertical growth phase (VGP). RGP, defined as outward growth within the epidermis, arises as a result of rogue melanocytes that have acquired additional genetic/epigenetic aberrations causing sustained proliferation. Surgical resection at this stage is often curative. Vertical growth phase (VGP) is a step in melanoma-genesis, wherein the melanocytes become capable of breaking through the basement membrane to invade the dermis and subcutaneous tissues[22-24]. The transition to VGP is a crucial step in the evolution of melanoma, because once melanocytes have entered VGP they have acquired mutations that allow for anchorage-independent growth and metastasis[23, 27]. This facilitates local invasion and metastatic spread, which are the main cause of melanoma morbidity and mortality.

1.2. Genetic and Environmental Interactions in Melanomagenesis

Both genetic and environmental factors contribute to the transformation of a melanocyte into melanoma. One of the most significant melanoma risk factors is a family history of melanoma. Familial inactivating mutations of the *CDKN2A* gene occur in 20 – 40 % of cases of melanoma-prone families[28]. From the same locus, *CDKN2A* encodes two gene products, p16^{INK4A} (INK4A) and p14^{ARF} (ARF), both of which are negative regulators of the cell cycle. INK4A inhibits cyclin dependent kinase 4 (CDK4)- and CDK6- mediated phosphorylation of retinoblastoma protein (pRB), prohibiting progression from G1 to S phase in the cell cycle[29]. ARF inhibits mouse double minute 2 homolog (Mdm2)-mediated degradation of p53[30, 31]. Thus, ARF acts to stabilize the tumour suppressor p53 that also functions to prohibit cell cycle progression from G1 to S phase, but additionally activates DNA damage repair and induce apoptosis in response to DNA damage and other cellular stressors[30-32]. Thus, inactivation of INK4A and ARF due to mutation at the *CDKN2A* locus can result in unrestricted cell cycle progression and subsequent oncogenic transformation. The cyclin dependent kinase 4 (*CDK4*) locus has also been identified as a high risk melanoma susceptibility gene, although to a much lesser extent than *CDKN2A*[33-37].

In addition to genetic predisposition to melanoma, exposure to the sun is a major environmental risk factor associated with melanomagenesis. It is thought that, melanoma is usually caused by DNA damage resulting from UV radiation from the sun or other sources, such as tanning beds[38, 39]. An important genetic-environmental interaction that contributes to the

genesis of melanoma is the role of polymorphisms in the melanocortin receptor 1 (*MC1R*) gene in sensitivity to sun exposure (i.e. UV light)[40, 41]. This membrane receptor mediates the skin's ability to protect against DNA damage caused by UV radiation. Exposure to sunlight stimulates *MC1R* resulting in the production of melanin, the UV-protective pigmentation produced by melanoma cells[42]. Hair and skin colour, and the degree of pigmentation produced in response to UV radiation (the UV pigmentation/tanning response) are in part mediated by germline polymorphisms in the *MC1R* gene. These variants of the *MC1R* gene, and the resulting impairment in melanin production, contribute to the light-skin, red/blonde hair, inability to tan, and freckled phenotype[23, 42-46]. Not surprisingly, it follows that this phenotype is associated with an increased risk for melanoma development and is associated with the number and severity of melanoma tumours in familial and sporadic cases[23, 40, 41, 47]. Although certain genes have been clearly linked to a heritable increased risk for melanoma, only 5 – 10% of melanoma cases occur in a familial setting[48]. Silencing of *CDKN2A* also occurs in 20 % of sporadic melanomas due to chromosomal deletions and promoter inactivation[49-52]. Another pathway that controls progression through the cell cycle, the mitogen-activated protein kinase (MAPK) signaling pathway, is commonly mutated in sporadic melanoma and other cancers. The MAPK pathway transmits extracellular signals to cytoplasmic and nuclear effectors that act to mediate cell cycle progression, cellular survival, and cellular differentiation[53-55]. The relevance of the most common MAPK activating mutations in melanoma will be addressed below.

1.3. The MAPK Signaling Pathway in Melanoma

The MAPK pathway consists of the RAS-RAF-MEK-ERK signaling cascade. This cascade is stimulated by upstream receptor tyrosine kinases (RTKs), cytokines, and heterotrimeric G-protein-coupled receptors in response to growth factors[56]. These factors activate the membrane localized GTPase protein RAS (HRAS, KRAS, and NRAS in humans) by facilitating the switch from GDP bound RAS to GTP bound Ras. Activated Ras can then recruit the serine-threonine kinase RAF (ARAF, BRAF, and CRAF in humans) to the plasma membrane where a complex mechanism involving conformational changes and phosphorylation events activates their protein kinase activity[56]. Active RAF kinase then phosphorylates MEK1/2 kinases that subsequently phosphorylates a downstream kinases such as ERK and other proteins. Activated ERK phosphorylates numerous cytosolic and nuclear effector proteins that regulate the

cellular response to the original signal[53-55]. Besides regulating proliferation, apoptosis/survival, differentiation and senescence, MAPK signaling also mediates cell shape, malignant invasion, and metastasis[57]. In comparison to what is observed for melanocytes, in melanoma ERK is hyperactivated in 90% of cases by receptor overstimulation and mutationally activated upstream signaling components such as RAS and RAF[58-60]. Oncogenic mutations in melanocytes occur frequently in the *BRAF* and *NRAS* genes, found in approximately 50% and 20% of melanomas, respectively[60, 61]. In addition to activating the MAPK pathway, *NRAS* activates the phosphoinositide 3-kinase (PI3K)/AKT pathway that functions in parallel to the MAPK pathway to elicit proliferation and survival along with many other essential physiological and cellular processes such as growth, metabolism, motility, and angiogenesis[62-64]. Oncogenic *BRAF* and *NRAS* mutations are typically mutually exclusive in human melanoma, suggesting double mutants may not provide an advantage for melanoma initiation or progression or are potentially selected against in tumorigenesis [5, 65-67]. This may also be a product of the type of sun damage that most often produces each of these mutations. Melanomas harbouring *NRAS* mutations are more frequently found in areas of chronic sun exposure (e.g. lower extremity) whereas melanoma harbouring *BRAF* mutations are associated with areas that experience intense intermittent exposures to the sun (e.g. trunk and back)[68-71].

Of the oncogenic genetic aberrations causing hyperactivation of the MAPK pathway in human melanoma, mutational activation of *BRAF* is the most common and often the earliest oncogenic event in melanoma-genesis. *ARAF* and *CRAF* mutational activation is extremely rare in human cancer likely because of a fundamental difference in how they are regulated compared to *BRAF*. Because of their structure and activation mode, *ARAF* and *CRAF* require two mutations for oncogenic activation, whereas *BRAF* requires only one mutational alteration in order to become activated[56, 60, 72]. Over 80% of the *BRAF* mutations in melanoma are the result of a single base mutation from a T to an A at position 1799 of the *BRAF* gene, substituting a glutamic acid for valine at the codon 600 (*BRAF*^{V600E})[60, 73]. This mutation results in a ~400 to 600-fold increase in *BRAF* activity relative to wildtype *BRAF* stimulating constitutive ERK signaling [55, 72, 73]. In addition to stimulating proliferation, survival, and transformation, studies have demonstrated *BRAF*^{V600E} signaling is important in promoting angiogenesis, invasiveness, and metastatic spread in melanoma[57, 74]. Considering the significant role of oncogenic *BRAF* in melanoma malignancy, interestingly, expression of oncogenic *BRAF* alone

is insufficient for full malignant conversion. This notion is consistent with the observation that BRAF is mutated in up to 80% of benign nevi (moles). Moles are thought to rarely progress to melanoma because they are locked in growth arrested state brought on by the engagement of OIS[73, 75-77]. OIS is mediated by the engagement of tumour suppressive mechanisms, often acting through the p53 and pRb pathways [27]. Progression to malignant melanoma is most often accompanied by the silencing of one or more tumour suppressor genes such as *CDKN2A*, *P53*, or *PTEN*[77, 78]. As mentioned above, loss of *CDKN2A* expression is common in sporadic cases of melanoma (~20%)[52, 65]. Somatic mutations of *P53* appear to be less frequent (~13%) and mutually exclusive of *CDKN2A* mutations in human melanoma[52]. This is thought to be because silencing of *CDKN2A* effectively inactivates both the p53 and pRb pathways and loss of *CDKN2A* expression is so common in melanoma there is less genetic pressure for mutation at the *P53* locus in melanoma tumorigenesis[79, 80]. Silencing of the tumour suppressor PTEN is also common in melanoma. PTEN acts as a negative regulator of the PI3K/AKT pathway, a pathway whose deregulation has been heavily implicated in the malignant progression of many human cancers including melanoma[63, 81, 82]. The prevalence of mutations in *PTEN* and other components of the PI3K/AKT pathway will be discussed in detail below.

1.4. The PI3K/AKT Signaling Pathway in Melanoma

The PI3K/AKT cascade controls a myriad of cellular functions, notably proliferation and survival. This pathway is stimulated in response to growth factors or other extracellular stimuli that act through a number of different membrane associated proteins, including RTKs, RAS, G protein-coupled receptors (GPCRs), and integrins[83, 84]. These signals activate the catalytic subunit of the class I PI3Ks (p110 α , β , δ , and γ , encoded for by *PIK3CA*, *PIK3CB*, *PIK3CD*, and *PIK3CG*, respectively). Activated PI3Ks phosphorylate plasma membrane bound phosphatidylinositols at the 3' OH group. The 3'phospholipids interact with intracellular proteins that contain the plekstrin homology (PH) domain, recruiting them to the plasma membrane. Phosphoinositide-dependent kinase 1 (PDK1) and AKT (isoforms AKT1, AKT2, and AKT3) are recruited to the plasma membrane in this manner. Recruitment to the plasma membrane results in the sequential activation of PDK1 and AKT. For full activation, AKT must be phosphorylated at 2 critical residues, Thr308 (catalytic domain) and Ser473 (regulatory domain). The Thr308 residue of AKT is phosphorylated by membrane recruited PDK1 and the Ser473 residue by the

mTORC2 (mechanistic target of rapamycin (mTOR) complex 2). Through its serine/threonine protein kinase activity, activated AKT phosphorylates several effector proteins, thereby regulating multiple key cellular processes, including proliferation, apoptosis, growth/size, metabolism, motility, angiogenesis, invasion, and metastasis [63, 81, 83-87]. As a lipid phosphatase, PTEN directly antagonizes PI3Kinase activity by dephosphorylating phosphoinositols at the 3' position[88]. Thus, the overall activity of the PI3K/AKT pathway is regulated by PTEN. Several independent studies have illustrated that without interference from PTEN, the PI3K/AKT pathway is hyper-activated[82, 89]. Perhaps the most compelling evidence of PTEN's tumour suppressive role in cancer is the occurrence of tumour syndromes (Cowden Syndrome) as clinical manifestations of PTEN germline mutations resulting in decreased or dysfunctional PTEN. Individuals with Cowden Syndrome develop multiple benign tumours termed hamartomas and are at increased risk for developing breast, thyroid, uterus, brain, and renal cancer[90].

Oncogenic events that activate the PI3K-AKT pathway occur frequently in a variety of cancers. In comparison to normal melanocytes, AKT is overexpressed ($\geq 60\%$) and hyper-activated (43%) in a large proportion of melanomas[91-93]. Studies have identified that AKT3 is the predominant overexpressed and hyperactivated AKT isoform in melanoma[93]. The deregulated expression and activity of AKT3 was demonstrated to be attributable to increased copy number of the *AKT3* gene and reduced PTEN protein activity[93]. Although more common in other types of cancer, mutational activation of PI3K or AKT are rare in melanoma ($\sim 1-3\%$, refs [94-96]). Activating somatic mutations RTKs functioning upstream of the PI3K/AKT pathway, such as c-Kit ($\sim 7.5\%$) and ERBB4 ($\sim 20\%$), have also been identified and implicated in the hyperactivity of the pathway[97-99]. The two most common and studied oncogenic events that activate the PI3K-AKT pathway in melanoma are activating mutations in the *NRAS* oncogene and loss of expression and/or function of the tumour suppressor *PTEN*. Lost or reduced expression of PTEN occurs in 20-40% of melanomas[4, 100]. Many mechanisms, including epigenetic silencing, inactivating missense or nonsense mutations, focal or chromosomal deletions, or frameshift mutations disrupting translation have been identified as causes for reduced PTEN expression and function[89, 101-103]. Adenoviral transfer of wild-type PTEN into melanoma cells lacking PTEN protein inhibits Akt phosphorylation and elicits tumour-specific apoptosis or growth inhibition[104, 105]. Additionally, ectopic expression of

PTEN can reduce the invasive potential of melanoma cells[89, 106]. Taken together these data reinforce PTENs role as an important tumour suppressor in melanoma, and are consistent with findings that PTEN functional loss is common in late-stage melanoma[89].

Similar to oncogenic *NRAS* and *BRAF* mutations, *NRAS* mutations and *PTEN* mutations/deletions are most often mutually exclusive. Whereas coinciding *BRAF* and *PTEN* mutations, and consequent activation of both the MAPK and PI3K-AKT pathways, occur frequently in melanoma cases (~20%, refs [4-7]). Since NRAS functions upstream of both the MAPK and PI3K-AKT pathway, the fact that it can activate both of these pathways is generally thought to be the reason for the mutual exclusivity of *NRAS* and *BRAF* mutations and *NRAS* and *PTEN* mutations in melanoma. Cooperativity of activating BRAF mutations and PTEN loss in melanoma tumourigenesis has been demonstrated *in vitro* and *in vivo*. Typically, in melanocytes expressing a lentiviral BRAF^{V600E} insert, OIS is triggered, marked by increased expression of senescence associate β -galactosidase (SA- β -gal) and decreased proliferative potential[107]. However, shRNA depletion of PTEN in BRAF^{V600E}-expressing cultured melanocytes prevents these cells from undergoing senescence as detected by decreased levels of SA- β -gal and increased proliferation[107]. An *in vivo* study utilizing genetically engineered mouse models (GEMMs) demonstrated that BRAF^{V600E} expression cooperates with PTEN loss to induce invasive and metastatic melanoma[77]. AKT3-BRAF cross-talk is another mechanism by which BRAF^{V600E} and the PI3K-AKT pathway cooperate in melanomagenesis[108]. AKT3 can directly phosphorylate BRAF^{V600E} on residues S364 and S428, lowering BRAF activity. These inhibitory phosphorylation events by AKT3 reduces BRAF^{V600E} activity to levels promoting, rather than inhibiting, anchorage-independent growth and proliferation. In this way, aberrant AKT3 activity relieves high levels of BRAF^{V600E}-mediated MAPK signaling responsible for engaging OIS, thus contributing to the transformation of BRAF^{V600E}-expressing melanocytes[108]. Although AKT3 has been heavily implicated in the pathogenesis of melanoma, recent studies using GEMMs of melanoma have demonstrated the involvement of AKT2 in melanoma tumour development and metastasis[109, 110]. Moreover, both PTEN loss and aberrant AKT activity contribute to increased resistance to apoptosis in BRAF^{V600E} melanoma cells, providing a mechanism to bypass therapeutic inhibition of BRAF[92, 93, 105, 108]. As such, the role of the PI3K-AKT pathway in mediating resistance to BRAF^{V600E}-targeted therapies will be discussed below.

1.5. BRAF^{V600E} Therapeutic Inhibition and Mechanisms of Resistance

Since the discovery that about 50% of melanoma patients harboured the BRAF^{V600E} mutation, mutant BRAF became a favoured target for drug design[60, 111, 112]. After clinical testing, in 2011 vemurafinib became the first selective BRAF^{V600E} inhibitor to be approved for use in BRAF mutant melanoma patients[8, 9, 111, 113, 114]. This was a breakthrough in the treatment of advanced stage metastatic melanoma, which pre-2011 had an extremely poor prognosis of median overall survival of less than a year[115]. Before 2011, the DNA-damaging agent dacarbazine and immunomodulatory cytokines, interleukin-2 (IL-2) and interferon alpha-2B (IFN- α), had been approved for the treatment of advanced melanoma, but none of these had a significant effect on increasing overall patient survival[116-118]. Treatment of previously untreated BRAF mutant melanoma patients with vemurafinib provided much improved response rates (~48% patients had tumour shrinkage) over dacarbazine treatment (5% [8], reviewed in ref [115]). Clinical trials comparing the efficacies of vemurafinib and dacarbazine treatment showed improved progression-free survival (time between treatment initiation and tumour growth or patient death) of 5.3 months compared to 1.6 months, respectively, and improved median overall survival of 13.3 months and 10.0 months, respectively. Dabrafenib, a second generation BRAF inhibitor with more potency and some inhibitory activity on CRAF, has shown similarly impressive responses. Dabrafenib treatment improved progression-free survival over dacarbazine treatment (5.1 months versus 2.7 months, respectively) and when used in combination with vemurafinib achieved a 76% response rate in BRAF-mutant melanoma patients[119, 120]. Although survival rates for advanced stage melanoma have improved due to the successful use of targeted and immunotherapies, responses are usually neither complete nor durable (reviewed in ref [115]). Unfortunately, approximately 20% of BRAF mutant melanoma patients present with intrinsic resistance to BRAF inhibition (i.e. no tumour shrinkage)[10, 119]. Even in patients who initially respond to the drug (i.e. progression-free survival), in nearly all cases this response is short-lived with tumours acquiring resistance to BRAF-targeted therapy within a year (following 6-7 months of treatment)[8-10].

Besides development of resistance, treatment with BRAF inhibitors can cause increased occurrence of secondary skin cancers, colon cancers, and leukemias[121-124]. These cancers

arise due to the paradoxical activation of MEK by inhibitor driven formation of BRAF/CRAF homo- or hetero-dimers made up of an inhibitor-free partner and an inhibitor-bound partner. Dimerization is required in the normal activation of RAF proteins, but inhibitor binding promotes dimerization [125, 126]. In the presence of GTP-bound RAS, the inhibitor-bound partner facilitates scaffolding or conformational changes that promote RAS-mediated activation of the kinase activity of the inhibitor-free partner to drive MEK activation and subsequent ERK activation[125, 127, 128]. Similarly, the majority of cases of acquired resistance to BRAF-selective inhibitors involve ERK-dependent mechanisms wherein BRAF inhibition is bypassed by reactivation of the MEK-ERK pathway[111, 129]. To date, no secondary mutation in BRAF that would prevent inhibitor binding has been found in melanomas that have acquired resistance[130, 131]. However, amplification of the mutant BRAF gene can occur resulting in overexpression to levels that would overwhelm BRAF inhibition. In fact, mutant BRAF is amplified in ~20% of resistant tumours[132]. Truncated forms of BRAF^{V600E} resulting from alternative splicing can drive resistance by constitutive dimerization and activation of wildtype BRAF[133]. Other mechanisms of ERK-dependent acquired resistance include, but are not limited to, increased signaling by MAPK-activating RTKs, CRAF amplification, and acquisition of activating NRAS mutations (able to signal through CRAF) or MEK mutations[131, 134-141]. Many of these resistance mechanisms can be prevented by dual BRAF and MEK inhibition since they function upstream of ERK to sustain MAPK signaling. The treatment of melanoma patients with dabrafenib and a MEK inhibitor, trametinib, has shown improved response rates (64% with combination therapy compared to 51% with dabrafenib monotherapy), improved median progression free survival (11.4 months with combination therapy compared to 7.3 months with dabrafenib monotherapy), and an increase in overall survival rate (72% at 12 months with combination therapy compared to 65% with dabrafenib monotherapy)[142]. Additionally, formation of secondary cancers is less frequent when using this combinatorial treatment approach because addition of MEK inhibitor treatment is thought to block the paradoxical activation of the MAPK pathway[120]. Unfortunately, patients still relapse on this combined treatment regime, indicative of ERK-independent mechanisms of resistance are at play[120].

Multiple ERK-independent mechanisms of intrinsic or acquired resistance have been identified in melanomas refractory to BRAF or BRAF/MEK inhibition. Microphthalmia-associated transcription factor (MITF) is key regulator of melanocyte development functioning

downstream of MC1R and RTK stimulation to control cell proliferation, survival, and differentiation[130, 143]. Amplification of the *MITF* gene locus has been implicated in the progression of melanoma, being absent in benign nevi, but present in 10% of primary cutaneous and 21-40% of metastatic melanoma[7, 144]. MITF has been found to confer resistance to MEK and BRAF inhibitors in melanoma cells by regulating anti-apoptotic factors (such as BCL2A1, Bcl-2-related protein A1)[145]. Furthermore, increased expression of MITF was found in MEK inhibitor-resistant melanoma cells[146]. As a signaling pathway that functions in parallel with the MAPK pathway to transmit cellular proliferative and survival signals, not surprisingly, the PI3K/AKT pathway has been found to confer BRAF^{V600E} melanoma with resistance to BRAF inhibitors. Both *in vitro* and *in vivo* studies have determined several mechanisms by which components of the PI3K-AKT pathway confer resistance to BRAF or MEK inhibition (reviewed in [111, 130, 147]). Loss of PTEN expression has been shown to contribute to intrinsic and acquired resistance to drug inhibition, partially as a result of increased AKT signaling that suppressed the pro-apoptotic factor Bcl-2 associated death promoter (BAD)[148, 149]. Specifically, AKT3 overexpression in melanoma cells mediates resistance to apoptosis when BRAF is knocked down or inhibited[150]. In BRAF mutant melanoma, MEK inhibition can mediate AKT activation, increasing PI3K-AKT signaling[151]. Overexpression of insulin-like growth factor 1 receptor (IGF-1R) and platelet-derived growth factor receptor (PDGFR), RTKs acting upstream of PI3K-AKT signaling, has been linked to BRAF and MEK inhibitor resistance in resistant melanoma cell lines or tumour biopsies[131, 138]. These RTKs were able to confer resistance to inhibitor-induced apoptosis by activating the PI3K/AKT pathway, without concurrent activation of the MAPK pathway. Taken together, these studies further highlighted the importance of PI3K-AKT signaling in the malignancy and drug-refractory nature of melanoma and thus presenting a new avenue for targeted drug design.

1.6. PI3K-AKT-mTOR Therapeutic Inhibition and Resistance

Considering the contribution of PI3K-AKT pathway to malignant progression and development of resistance to therapeutic drugs, it has become an attractive target for therapeutic inhibition in melanoma and other cancers. To date, many inhibitors targeting this pathway have been designed and have undergone preclinical and clinical testing for efficacy in the treatment of various cancers[152-154]. Specific to melanoma, preclinical studies of PI3K-AKT pathway

inhibition on cultured melanoma cells and GEMMs of BRAF^{V600E}-driven melanoma have demonstrated the efficacy of these inhibitory drugs in decreasing melanoma malignancy and reversing resistance to MAPK inhibition[138, 151, 155-161]. In conjunction with MAPK inhibition, these studies the use of inhibitory drugs directed to specifically targeting PI3K, AKT, and/or mTOR (mechanistic target of rapamycin), a downstream effector of the PI3K-AKT pathway that stimulates increased cellular transcription and translation (i.e. growth). Co-targeting the MAPK and PI3K-AKT pathway proved successful in reducing proliferative potential and increasing levels of apoptosis when compared to independent pathway targeting. Unfortunately, in clinical trials combining MEK and PI3K/AKT/mTOR targeted therapies, the presence of overlapping toxicities has become problematic[63, 162, 163]. Because the PI3K-AKT pathway is also essential in non-tumour cells, establishing a tolerable dose and schedule for clinical co-administration with MAPK inhibitors has been a difficult undertaking. However, it remains to be tested whether targeting specific isoforms of PI3K or AKT can generate a sustained critical response with reduced toxicities.

Another issue with targeting components of the PI3K-AKT pathway is the emergence of resistance to inhibition due to feedback loops that reactivate the pathway (reviewed in[164]). Feedback induction of AKT activation due to mTORC1 inhibition is a prime example of one such loop. mTORC1 is a protein complex of mTOR (catalytic subunit) and several other proteins that is activated downstream of AKT, stimulating transcription and translation[165]. Normally, mTORC1 functions to negatively regulate insulin receptor substrate 1 (IRS1), a signaling adaptor protein that transmits signals from IGFR1 to PI3K. Inhibiting mTORC1 with rapamycin (mTOR inhibitor) relieves its negative regulation on IRS1, resulting in the subsequent activation of PI3K and AKT[166, 167]. In some cases, mTORC1 inhibitor-mediated activation of IRS1 can signal through the MAPK pathway to activate ERK signaling[168, 169]. This type of feedback has been seen in many types of cancers including melanoma, possibly explaining the ineffective clinical activity of single agent mTORC1 inhibitors in the treatment of metastatic melanoma, even when co-administered with RAF inhibitors[158, 170-172]. Dual mTORC1/mTORC2 targeting can mitigate this effect since mTORC2 functions to phosphorylate the regulatory domain of AKT, required for the full activation of AKT kinase activity. The protein complex of mTORC2 also contains mTOR as its catalytic subunit, but it carries out a different function by interacting with a different set of proteins than those in mTORC1[173]. Also, since PDK1 is required to

phosphorylate the catalytic subunit of AKT for complete activation of AKT kinase activity, targeting mTORC1 and PDK1 simultaneously could help overcome this mechanism of resistance. Using a GEMM of BRAF^{V600E}::PTEN^{-/-} driven melanoma, Scortegagna *et al.* demonstrated that deletion or inhibition of PDK1 delayed melanoma progression and reduced invasion and metastasis with little toxicity[174]. These results shed light on another node of the PI3K-AKT pathway that could be targeted in conjunction with MAPK inhibition for the treatment of melanoma.

In another feedback loop seen in breast, lung, and prostate cancer cell lines, inhibition of PI3K and AKT relieves the negative regulation on forkhead box protein O (FOXO) transcription factors permitting the transcription and overexpression of multiple RTKs, most often ERBB3 and IGF1R[175-177]. Upregulation of these RTKs can reactivate downstream MAPK and PI3K-AKT pathway signaling, reinforcing signals that promote proliferation and survival[175, 177]. A strategy to escape the feedback resistance mediated by both of these feedback loops would be to use dual PI3K/mTOR inhibitors. Pre-clinical studies in melanoma cell lines and GEMMs of melanoma have confirmed the efficacy single agent inhibitors that target both PI3K and mTOR, with or without concurrent MEK inhibition[158, 178]. Currently, various clinical trials are underway to assess the efficacy and safety of co-administration of MEK and dual PI3K/mTOR inhibitors to treat melanoma, although preliminary results suggest that toxicity of this combined treatment is still problematic[111, 163, 164, 179].

Since recurrent resistance to BRAF-specific inhibitors was realized, there has been a shift in the rational drug development for treating malignant melanoma. Multiple pathways have become simultaneously relevant in finding treatment options that will provide a sustained critical response. Researchers are now looking to use BRAF and/or MEK inhibitors in conjunction with other drugs that target multiple nodes of aberrant melanoma signaling pathways [180]. The PI3K-AKT pathway is a logical target for therapeutic intervention considering its well-documented role in melanoma-genesis and contribution to development of resistance to MAPK targeting chemotherapeutic drugs. Loss of PTEN expression has been implicated in both of these aspects of melanoma malignancy. Unfortunately, restoration of PTEN loss is not a therapeutic option with currently existing technologies. Therefore, the PI3K-AKT pathway activating molecules that function directly above PTEN (PI3K), and below PTEN (PDK1 and AKT), from henceforth referred to as PTEN proximal genes/proteins, have been heavily investigated to

determine their role in malignant progression and potential to be clinically targeted, especially in the context of BRAF mutant melanoma. As potentially druggable kinases, these signaling molecules present an opportunity for the rational development of inhibitors to effectively target this pathway.

In the treatment of melanoma, clinicians are currently faced with several problems in targeting the MAPK and PI3K-AKT pathways, including the emergence of resistance (due to feedback loops, pathway cross-talk, etc.) and toxicities associated with co-targeting these pathways. One strategy to potentially overcome toxicity and feedback loop resistance associated with targeting PI3K and AKT in cancer, would be to use isoform-specific inhibitors instead of pan-PI3K and pan-AKT targeted drugs. For instance, the immune system is largely dependent on PI3K-p110- δ and PI3K-p110- γ signaling, so using inhibitors to specifically target p110- α and/or p110- β could help avoid adverse chemotherapeutic effects on the immune system[63, 164]. A considerable amount of evidence exists that suggest that inhibiting a single PI3K or AKT isoform is sufficient to inhibit certain types of tumours[63, 164]. However, it remains to be tested whether targeting specific isoforms can generate a sustained critical response in the treatment of melanoma.

1.7. Research Objectives

To safely pursue these PTEN proximal signaling molecules as rational therapeutic targets, the PI3K/AKT pathway must be studied more extensively. Preclinical studies are required to gain a better understanding for how specific PI3K and AKT isoforms, along with PDK1, cooperate with BRAF activation to contribute to the initiation and progression of melanoma, and additionally, how these PTEN proximal signaling molecules contribute to intrinsic and acquired resistance to therapeutics. Following this logic, the goal of my research was to elucidate the role of PTEN proximal signaling molecules in BRAF^{V600E}-driven melanoma cell transformation, proliferation, and viability (Figure 1.1). Using a lentiviral delivery system, expression of PTEN proximal genes were systematically ablated *in vitro* with short hairpin RNAs (shRNAs) to be able to assess their contribution the malignant characteristics of melanoma cell lines. With these reagents we could determine whether knockdown of specific PTEN proximal genes could sensitize cells to BRAF/MEK inhibition. The knowledge gained from performing these experiments was to build upon the current model of melanoma

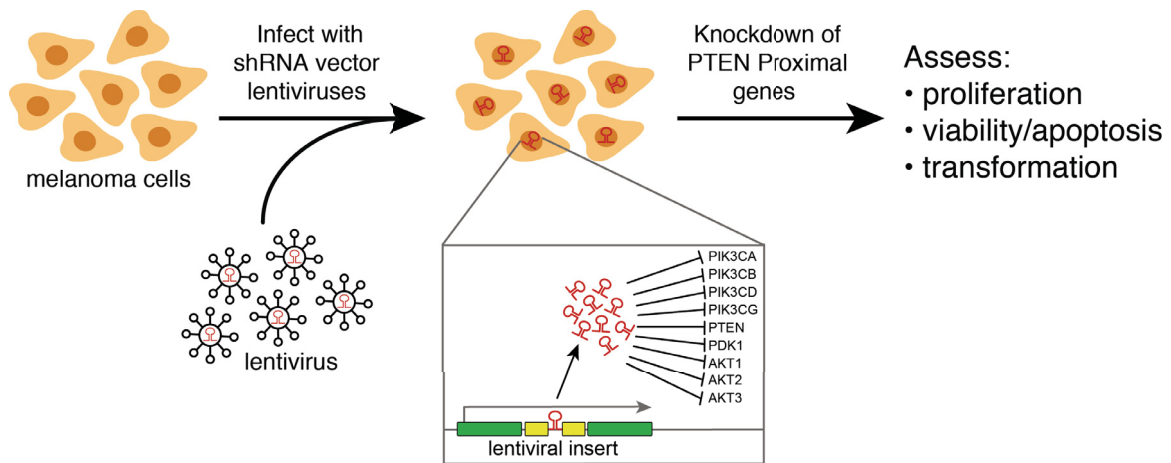


Figure 1.1. Experimental approach. Melanoma cells are infected with lentiviral shRNA vectors containing shRNAs targeting the PTEN proximal signalling molecules in the PI3K-AKT pathway. Cells that have stably incorporated the lentiviral insert are selected for. These cells are used in subsequent experiments to test the effect of shRNA-mediated target knockdown on the malignant phenotype of melanoma cells in vitro.

development and resistance, with the intention of informing efforts geared towards determining how to effectively and specifically target the PI3K-AKT pathway in a way that will produce a sustained and tolerable therapeutic response.

There exists a great level of homology within the catalytic domains of the PI3K isoforms and the AKT isoforms[181]. This makes it challenging to target individual isoforms specifically with small molecule inhibitors. At the onset of my Master's studies, isoform-specific inhibitors were in the early stages of development and commercialization and were not readily available[181]. To genetically determine the functional role of PTEN proximal genes in melanoma, I set out to use a genetic, shRNA-based approach. Furthermore, within the PI3K family and AKT family of signaling molecules, respectively, the isoforms have overlapping downstream targets, which would make it more difficult to monitor efficacy of isoform-specific pharmacological inhibition given their functional redundancy. With shRNA-mediated knockdown of each target, one can simply assay for adequate knockdown by detecting levels of mRNA or protein. Herein I describe the use of a luciferase-based approach to triage shRNAs for functional knockdown of target mRNA. Once identified, successful shRNAs were cloned into lentiviral targeting constructs. Further work was done to ensure the effective delivery and

expression of targeting constructs in melanoma cells using lentiviral integration to confer stable silencing of each PTEN Proximal gene. With this work, I sought to optimize the use of an inducible lentiviral expression system for the purposes of the aforementioned research.

2. Materials and Methods

2.1. Manipulation of DNA/Plasmid Preparation

2.1.1. Bacterial Growth

To prepare plasmid DNA for cloning and cell culture purposes, mostly DH10B (Invitrogen) and Mach1 (Invitrogen) bacteria were used. When growing a plasmid that contained a ccdB cassette, ccdB Survival™ 2 T1 Phage-Resistant bacteria (Invitrogen) were used. Bacteria were made chemically competent for transformation using the Zymo Research Mix & Go E. coli Transformation Kit (Zymo Research #T3001) as per the manufacturers instructions. Plasmid DNA transformations into competent bacteria were performed on ice for 5 – 30 minutes, then plated on LB agar plates containing the appropriate selection antibiotic. The antibiotic concentrations used for selection in LB growth medium or agar plates were 50 ng/mL Kanamycin, 50 ng/mL Carbenicillin and 12.5 ng/mL Chloramphenicol. For Kanamycin and Chloramphenicol encoding plasmids, transformed bacteria were first grown in antibiotic-free LB or SOC medium for an hour before plating on LB agar plates. To isolate plasmid DNA from bacterial cultures, standard miniprep and midiprep protocols were used. For minipreps, if cleaner plasmid preps were required, the BioBasic BS614 EZ-10 Spin Column Plasmid DNA kit was used. For midipreps, the Promega PureYield Plasmid Midiprep System (Promega #A2495) was used.

2.1.2. Sequencing

For sequence verification of prepared plasmids, all sequencing was performed by the McGill University and Genome Quebec Innovation Centre using Sanger sequencing. The sequencing primers are listed in the Appendix (Table 1).

2.1.3. Gateway LR Reaction (pCheck2, pTREG, and pLEG)

For two-plasmid LR recombination reactions Gateway LR Clonase II enzyme was used (Invitrogen #11791-020) in a 5 µL total reaction volume (10 fmol Entry vector, 20 fmol Destination vector, 1 µL LR Clonase II, and rest of volume with TE pH 8.0). For four-plasmid LR recombination reactions, Gateway LR Clonase II Plus enzyme was used (Invitrogen #12538-

120) in a 5 μ L total reaction volume (1 μ L of each of the Entry plasmids at 10 fmol, 1 μ L of the Destination plasmid at 20 fmol, 1 μ L LR Clonase II Plus, and TE to 5 μ L if needed. Reactions incubated at room temperature for 16 – 24 hours, and were terminated by adding 1 μ L Proteinase K (Invitrogen P/N 59895) and incubating at 37°C for 20 minutes. The 3 – 6 μ L of the reaction mix was then transformed into 50 – 100 μ L of competent ccdB-sensitive bacteria bacteria.

Two-plasmid LR reactions: recombining miRNA cassette from pBEG R3-shRNA-L4 into pTREG Dest L3-(ChlorR-ccdB)-R4 to make pTREG shRNA, recombining cDNA from pDONR201(L1-L2), pDONR221(L1-L2), or pENTR D(L1-L2) plasmids into pCheck2 Dest (R1-R2). Four-plasmid LR reaction: pENTR L1-dsRed-L2, pBEG R2-iPuro-L3, pBEG R3-shRNA-L4, and pLEG R1-(ChlorR-ccdB)-R4 to make pLEG-dsRed-iPuro-miRNA, referred to as pLEG shRNA below. Note: pLEG-eGFP-iPuro was obtained from Ben Geiling who had already constructed this plasmid.

2.1.4. Cloning of shRNA into pBEG shTest

Novel shRNAs were cloned into the pBEG shTest R3-miRNA(ChlorR-ccdB)-L4 plasmid in between XhoI/EcoRI sites flanked by the miRNA-30 cassette. The backbone of the pBEG shTest plasmid was prepared for shRNA insertion by restriction enzyme digest with XhoI/EcoRI, followed by gel extraction with BioBasic EZ-10 Spin Column Gel Extraction Kit (#BS654) of the resulting ChlorR-ccdB free backbone. The ~100 bp shRNA templates were ordered from Sigma Aldrich Custom DNA at a 0.05 μ mol scale using Reverse-Phase Cartridge Purification (RP1). The basic structure for the ordered shRNA template is as follows: TGCTGTTGACAGTGAGCG-A(shRNA Sequence)C-TGCCTACTGCCTCGAAT with a constant 19-bp loop sequence (X – TAGTGAAGCCACAGATGTA - X') flanked by 19 – 23 nucleotide sequences, X and X', homologous to the target (based on [182, 183]). For a list of PTEN Proximal gene targeting shRNA sequences, see the Appendix (Table 3). X represents the sense sequence (target sequence on mRNA from gene of interest) and X' represents the antisense sequence (portion that binds target sequence on mRNA to elicit knockdown). Bolded nucleotides vary depending on the target sequence. The **C** represents the last 3' nucleotide of the antisense sequence and should compliment the intended target sequence. The **A** represents the first 5' nucleotide of the sense sequence which should be changed to be uncomplimentary to whatever nucleotide replaces the **C** in the antisense sequence. The underlined sequences share homology

with universal primers (Fwd) 5'-CACCTCGAGAAGGTATATTG CTG TTG ACA GTG AG-3' and (Rev) 5'-CCCCTTGAATTCCGAGGCAGTAGGCA-3' and add flanking XhoI/EcoRI sites for subsequent cloning into pBEG shTEST (primers based on those used by Chang *et al.*[183]).

PCR amplification from the ~100 nucleotide shRNA template was performed using 0.5 units Phusion polymerase (NEB #M05305), 200 nM dNTP, 400 nM of each primer, 400 nM shRNA template, 704 nM DMSO in a total 25 µl PCR volume with 30 cycles (10 seconds at 98°C, 30 seconds at 60°C and 60 seconds at 72°C). The Phusion polymerase was then inactivated with Proteinase K (Invitrogen P/N 59895, 1 uL in 25 uL PCR volume) for 30 minutes at 37 °C, followed by a Proteinase K inactivation incubation for 10 minutes at 95 °C. Of the PCR product, 10 µL is digested with XhoI/EcoRI for 2 hours at 37°C, followed by incubation for 20 minutes at 85°C to inactivate the restriction enzymes. Digested shRNA PCR product (3 µL) was then ligated to the gel extracted pBEG shTest backbone (3 µL) with T4 DNA Ligase (NEB #M0202S) for at least 1 hour. The ligation mix (2.0 to 4.0 uL) was then transformed into 50 µL of competent bacteria to plate on LB agar plates. Colonies were subsequently picked for pBEG shRNA minipreps to isolate plasmid DNA for the luciferase assay shRNA triaging process.

2.1.5. pCheck2 Plasmids

PTEN Proximal gene human cDNA sequences were inserted into the pCheck2 Dest (R1-R2) plasmid (psiCHECK2 made Gateway compatible by Kendall Dutchak, Addgene #48955) for use in the luciferase assay shRNA triaging. cDNA sequences were cloned out of plasmids obtained from Addgene: pJP1520-PIK3CA (HsCD00038080), pDNR-Dual-PIK3CB (HsCD00001636), pDNR-Dual-PIK3CD (HsCD00022410), pDNR-Dual-PIK3CG (HsCD00005739), pDONR201-PTEN (HsCD00001438), pDONR221-PDK1 (HsCD00296763), pDONR221-AKT1 (HsCD00296490), pDNR-Dual-AKT2 (HsCD00022399), and pDONR201-AKT3 (HsCD00305207). Upon my arrival, Kendall Dutchak (PhD student in Dankort lab) had already made the pCheck2-AKT1 and pCheck3-AKT3 plasmids with Gateway LR recombination from the addgene cDNA plasmids into the pCheck2 Dest (R1-R2) plasmid. I prepared the pCheck2 PTEN and pCheck2 PDK1 plasmids in the same manner. These cDNA sequences were flanked by L1-L2 recombination sites, therefore only one Gateway LR recombination reaction was required to the pCheck2 plasmid. The AKT2 cDNA was PCR

amplified with TOPO-directional compatible primers (See Appendix Table 1) and subsequently cloned into pENTR D-TOPO (Invitrogen pENTR-TOPO-D Kit #K2400-20) as per the manufacturers instructions. The L1-L2 flanked AKT2 cDNA was the cloned by Gateway LR recombination into pCheck2. The PI3K cDNA sequences were cloned into pCheck2 using standard restriction enzyme cloning methods. I obtained the pCheck2-P53 from Ben Geiling who had constructed this plasmid previously.

2.1.6. Generation of pBEG miRNA-E

The miRNA-E cassette was synthesized by BioBasic (in pUC57). See Appendix for more detailed description of modifications to the miRNA-30 cassette to give miRNA-E. The miRNA-E cassette was cut out of pUC57 with BglII/MluI before being ligated into the pBEG shTEST backbone cut with BamHI/MluI. This ligation would destroy the 5' BamHI site in pBEG shTEST, allowing for the easy discrimination between pBEG shTest miRNA-30 and pBEG shTest miRNA-E by restriction enzyme screening for the missing BamHI site. This was followed by cloning a chloramphenicol-ccdB cassette into the XhoI/EcoRI sites in the miRNA-E cassette to give pBEG shTest R3-miRNA-E(ChlorR-ccdB)-L4. Existing shRNA oligos were PCR amplified with the following primers to make them compatible with the miRNA-E backbone: (Fwd) 5'- TGA ACTCGAGAAGGTATATTGCTGTTGACAGTGAGCG-3' and (Rev) 5'- TCTCGAATTCTAGCCCCTTGAAGTCCGAGGCAGTAGGC-3'. From this PCR product I proceed with the same steps used to miRNA-30 shRNAs into pBEG shTest.

2.2. Tissue Culture

2.2.1. Culture of Mammalian Cells

Cells were grown in a humidified incubator at 37°C and 5% CO₂. HEK 293T (human embryonic kidney) and A375 cells (melanoma) were cultured in DMEM (Wisent) containing 10% v/v FBS (Wisent) and 1% w/v penicillin/streptomycin (P/S, Wisent), unless otherwise stated. WM279, WM1617, WM9, and WM35 melanoma cells were cultured in 2% Tumour Medium (Tu 2%: 80% MCDB 153 medium, 20% Leibovitz's L-15 media, 5 µg/ml bovine insulin and 1.68 mM CaCl₂) containing 2% heat-inactivated FBS (56°C for 20 minutes) and 1% P/S. Sk-mel-2 melanoma cells were cultured in EMEM containing 10% FBS and 1% P/S. All cells were maintained in 100 mm tissue culture coated dishes with 10 mL of media and sub-

cultured every 3 - 4 days when appropriate. When trypsinizing cells, 0.25% w/v trypsin-EDTA solution was used for 293T cells, and 0.05% w/v trypsin-EDTA was used for the melanoma cell lines.

2.2.2. Transfections

In a 100 mm dish, 5×10^6 293T cells were transfected using a polyethyleneimine (PEI, 42 μ L of 1 mg/mL solution) along with a total of 16 μ g of plasmid DNA diluted in 550 μ L OMEM (Invitrogen #11058-021). In a 150 mm dish a total of 36 μ g of DNA was transfected after dilution in 1200 μ L of OMEM and 96 μ L of PEI. The transfection mix was incubated at room temperature for 30 minutes before adding it to the 293T cells cultured in regular growth medium. When applicable transfections for virus production were performed using Lipofectamine 2000 transfection reagent (Invitrogen #11668-027) as per the manufacturers instructions. Transfections were performed overnight at 37°C and the medium was replaced the next morning.

2.2.3. Luciferase Assay

On Day 1, 5×10^4 293T cells/well were seeded in 24-well dishes. For the first round of triaging, to compare the efficiency of knockdown between shRNAs targeting the same reporter, pBEG shRNA plasmid DNA was prepared with BioBasic BS614 EZ-10 Spin Column Plasmid DNA kit using the low copy plasmid protocol. The pBEG shRNA and pCheck2 plasmid DNA to be used for transfections was standardized to 100 ng/ μ L. On Day 2, 293T cells were co-transfected with 0.46 μ g of pBEG shRNA DNA and 0.20 μ g of pCheck2 DNA per well. Before putting the DNA on the cells, the transfection mixture was prepared in 100 μ L of OMEM and 1.8 μ L of PEI and left to incubate at room temperature for 30 minutes. Transfections were performed overnight. On Day 3, the medium was replaced the in the morning for fresh DMEM. On Day 4, cells were washed 1X with PBS and then lysed with Passive Lysis Buffer (Promega #E194A) as per the manufacturers instructions. Of the lysate, 5 μ L from each sample was transferred to a 96-well plate (white flat-bottomed, Corning #3912). Firefly and Renilla luciferase activity was quantified using a Tecan 200 plate reader/injector running i-Control software. The luciferase assay solutions were made in the lab as described previously[184, 185]. Firefly solution is injected first (100 μ L/well), shaken for 2 seconds, and then the luminence is recorded over 10 seconds, followed by injection of the renilla luciferase solution (100 μ L/well), 2 seconds of shaking, and then renilla luminescence was recorded over 10 seconds. For the second round of

luciferase assays, 2-3 effective pBEG shRNA plasmids were chosen to midiprep and test for specificity amongst targets that are from a family of isoforms (e.g. PI3K isoforms). To test specificity the luciferase assays were set up the same way except pBEG shRNA plasmids are co-transfected with the pCheck2 reporter plasmids they specifically target and also the pCheck2 reporters of similar targets.

2.2.4. Lentivirus Production

Lentivirus was produced in 293T cells co-transfected of the packaging plasmids pAX.2 and pMDG (VSV-G encoding plasmid) with a lentiviral plasmid (pLEG or pTREG). When lentivirus of different pseudotype was required, either pLTR-RD114A (Addgene #17576), pHCMV-MokolaG (Addgene #15811), or pHCMV-LCMV-WE (Addgene #15793) replaced pMDG in the transfection. On Day 1, 5×10^6 and 12×10^6 293T cells were seeded in 100 mm and 150 mm dishes, respectively. On Day 2, for the 100 mm dish 293T cells were transfected with the following: 8.0 μg of the lentiviral plasmid, 2.8 μg of pMDG, and 5.2 μg of pAX.2 diluted in 550 μL of OMEM and 42 μL of PEI. For the 150 mm dishes the amounts were as follows: 18.0 μg of the lentiviral plasmid, 6.3 μg of pMDG, and 11.3 μg of pAX.2 diluted in 1200 μL of OMEM and 96 μL of PEI. The transfection mix was left to incubate at room temperature for 30 minutes before adding it to the 293T cells. Transfections were performed overnight. On day 3, the medium was replaced with fresh culture medium. On Day 4, the viral superantant was collected from the cells and filtered through a 0.45 μm filter to remove cells or other debris. The virus was either used for infections immediately thereafter or aliquoted for storage in a -80°C freezer.

2.2.5. Lentivirus Production for Concentration by Ultracentrifugation

On Day 1, 10 x 175 cm^2 flasks were seeded with 12×10^6 293T cells each. On Day 2, each flask of cells was transfected with the following: 18.0 μg of the lentiviral plasmid, 6.3 μg of pMDG (or other envelope glycoprotein encoding plasmid for pseudotyping), and 11.3 μg of pAX.2 diluted in 1200 μL of OMEM and 96 μL of PEI. Transfections were performed overnight. On Day 3, the medium was replaced with 20 mL fresh serum containing or serum-free culture medium per flask. On Day 4, viral supernatant from all of the flasks was pooled and filtered through a bottle-top 0.22 μm filter to remove cells and other debris. To concentrate the virus, 32 mL was placed in each of six 38.5 mL polypropylene tubes (Beckman Coulter #326823) for

ultracentrifugation. A 4 mL layer of 20% sucrose was added to each tube to cushion the viral supernatant. Virus was centrifuged in a Beckman Coulter SW32Ti ultracentrifuge rotor at 25,900 RPM for 2 hours cooled to 4°C. After ultracentrifugation, the supernatant was removed by aspiration and 100 µL of PBS was added to each tube to resuspend the pellet. The tubes were kept at 4°C for 2 hours with occasional gentle vortexing. Lastly, the virus was pooled from all 6 tubes usually totaling ~1000 µL. This was aliquoted into microtubes for storage in a -80°C freezer.

2.2.6. Lentivirus Titration – Puromycin-Resistant Colonies

To titer virus by puromycin selection, on Day 1, 4×10^5 293T cells were seeded per well in 6 well dishes. The dishes were coated with poly-D-lysine as per manufacturer's instructions (Sigma Aldrich #P6407-5MG). One 6 well dish was required for each viral preparation to be titered. On Day 2, required volumes of virus were thawed on ice. 2 mL 10-fold serial dilutions of the virus was prepared (in microtubes) ranging from 10^{-2} to 10^{-6} . Virus was diluted in DMEM containing 8 µg/mL of polybrene for enhanced transduction. After removing the normal culture medium from the cells in the 6 well dishes, 1 mL of each serial dilution was put on the cells with one well containing just polybrene DMEM as a non-infected control. Cells were infected overnight. On Day 3, the virus was removed and replaced with fresh DMEM. On Day 4, media was replaced by DMEM containing puromycin at concentration of 4 µg/mL. Cells were cultured for 7 – 9 days in puromycin to allow for puromycin-resistant colonies to grow, replacing the medium with fresh puromycin containing DMEM every 2 – 4 days. To count resistant colonies, cells were washed once with 1X PBS, fixed with formalin for 1 hour, then stained with 0.1% crystal violet for 20 minutes, followed by two rinses with 1X PBS. Plates were left to dry overnight and crystal violet stained colonies were counted the following day. Colonies were counted under microscope visualization at 40X magnification. Viral titer was calculated by multiplying the number of colonies per well by the dilution factor (transducing units/mL, TU/mL). An average of calculated titers from all the countable wells was taken to give final viral titer.

2.2.7. Lentivirus Titration – TurboRFP Positive Colonies

Titration by this method was performed as explained in the pTRIPz technical manual[186], with a minor modifications. Briefly, on Day 1, 5×10^4 293T cells were seeded per

well in 24 well dishes in 0.5 mL/well of regular culture media (DMEM supplemented with serum). The dishes were pre-coated with poly-D-lysine as per manufacturer's instructions (Sigma Aldrich #P6407-5MG). For each viral preparation to be titered, 6 wells of cells were required. On Day 2, DMEM was replaced on the 293T cells with 225 μ L/well of DMEM containing 8 μ g/mL of polybrene. Required volumes of virus were thawed on ice (20 μ L per viral prep). 100 μ L 5-fold dilutions of each virus were prepared in a round bottom 96 well plate, with dilutions ranging from 5¹- to 5⁸-fold. Virus was diluted in DMEM containing 8 μ g/mL of polybrene. The first 5-fold dilution was made by diluting 20 μ L of the viral stock in 80 μ L of DMEM. After pipetting up and down 10 – 15 times, the pipette tip was discarded and a new tip was used to transfer 20 μ L of this dilution to the next well already containing 80 μ L of DMEM. These transfer/mixing steps were repeated until all the serial dilutions were prepared. If multiple viral preps were being titered at once, the serial dilutions were prepared using a multichannel pipettor. 25 μ L of each viral dilution ranging from 5³- to 5⁸-fold were transferred to the 24 well destination plate containing 293T cells. Cultures were incubated for transduction at 37°C for 4 hours. The transduction mix was removed and cells were rinsed very gently with once with 1X PBS. Gently, 1 mL of doxycycline containing DMEM (1 μ g/mL) was added to each well and incubated at 37°C for 72 hours. TurboRFP expressing cells or colonies of cells were counted under a fluorescence microscope. Each multi-cell colony was counted as 1 transduced cell, as the cells were dividing over the 72 hour culture period. To calculate viral titer, the following formula for used: # of TurboRFP positive colonies counted x dilution factor x 40 = # TU/ml. An average of calculated titers from all the countable wells was taken to give final viral titer.

2.2.8. Lentivirus Infection

To infect cells, 1 – 5 mL unconcentrated virus was diluted to 10 mL with fresh media containing polybrene at a concentration of 4 - 8 μ g/mL. For A375 and 293T cells 5 mL of virus was diluted in 5 mL of DMEM. For WM9 and WM1617 cells, less virus had to be used because of cytotoxicity issues (1 – 3 mL of unconcentrated virus in a total of 10 mL of Tu 2%). For infections at a specific MOI, first the # of TUs required were calculated: MOI x # cells to be infected. Then volume of the titered viral stock to be used for infection was calculated: (# of TUs required)/(viral titer in TU/mL). When heat-inactivation of the virus was required before introduction to cells, the virus was incubated at 50°C for 1 hour. Infections were performed at

37°C overnight. The following day the infection mix was removed and replaced with regular growth media. Two days post-infection, stable cell lines were selected by adding puromycin to the culture medium at 4 µg/mL for at least 4 days.

2.2.9. Doxycycline Treatment

Expression of shRNA in pTREG shRNA cell lines was induced with treatment of doxycycline at 1 µg/mL, unless otherwise stated. Doxycycline-containing medium was changed every other day for the duration of induction/assay time.

2.2.10. Resazurin Viability Assays

Cells were seeded in 96 well dishes at 2500 cells/well. The next day, growth medium was added containing 0 – 5.0 µg/mL of doxycycline. Each concentration was tested in replicates of 4. Cells were incubated in doxycycline for 5 days at 37°C, changing the medium every other day. At the end of the treatment period, resazurin (Sigma) prepared at 0.3 mg/mL was added at 10% volume of the medium in each well (e.g. 10 µL of resazurin in 100 µL of medium). The cells were incubated in resazurin for 3 hours at 37°C. Absorbance at 570 nm with reference at 600 nm was measured using a Tecan 200 plate reader. To analyze the data, the OD values of doxycycline treated samples (test samples) were divided by that of doxycycline-free control samples, i.e. the control samples were set as 100% viable and cell viability for the treated samples was calculated as: (OD of test samples)/(OD of control samples) x 100%.

2.2.11. Western Blots

Protein lysis was performed using PLC lysis buffer (50 mM HEPES pH 7.5, 150 mM NaCl, 10 % glycerol (v/v), 1% Triton X-100 (v/v), 1 mM EGTA, 1.5 mM MgCl₂, 10 mM NaF, and 10 mM Na₄P₂O₇, Aprotinin, Leupeptin, and Pepstatin at 1 µg/mL, 1 mM PMSF, 1 mM orthovanadate). In a 100 mm dish, cells were washed with ice cold PBS (2 x 5 mL), and then 500 µL of lysis buffer was added. Cells were incubated on ice for 20 minutes with occasional tapping to loosen the cells from the plate. A cell scraper was used to collect the cells in the lysis buffer into a microtube. Lysates were centrifuged at 16,100 g at 4°C. The supernatant was collected into a fresh tube and stored in the -80°C freezer until assayed for protein concentration (Novagen BCA Protein Assay Kit #CA82601-004). Samples were prepared in 1X Laemmli buffer (67 mM Tris pH 6.8, 10% v/v glycerol, 1.25% w/v SDS, 0.0025% w/v bromophenol blue and 2.5% v/v 2-

mercaptoethanol) to load onto gel, at 30 – 60 µg of protein per well. Once in Laemmli buffer, samples were boiled at 100°C for 5 minutes before loading.

Proteins were separated by SDS-PAGE on 10% acrylamide gels. The proteins were then transferred onto a PVDF membrane in transfer buffer (25 mM Tris base, 192 mM Glycine) containing 20% methanol (v/v). Transfers were run at 400 mA for 2 hours or overnight at 100 mA for 8 hours. Membranes were blocked using milk-TBS-T, TBS-T (50 mM Tris base, 150 mM NaCl and 0.05% v/v Tween-20) with 5% milk powder (w/v), for 1 hour at room temperature. After blocking, blots were incubated in primary antibody overnight at 4°C. Primary antibodies were diluted in TBS-T with 5% BSA (w/v). The primary antibodies and dilutions used were: PI3Kinase p110 α (Cell Signalling #4249, 1:500), PI3Kinase p110 β (Cell Signalling #3011, 1:500), PI3Kinase p110 δ (Santa Cruz #sc-7176, 1:1000), PI3Kinase p110 γ (Santa Cruz #sc-7177, 1:1000), PTEN (Cell Signalling #9188, 1:1000), PDK1 (Cell Signalling #3062 1:1000), AKT1 (Cell Signalling #2938, 1:1000), AKT2 (Cell Signalling #3063, 1:1000), AKT3 (Cell Signalling #8018, 1:1000), and α -Tubulin (Sigma #T5168, 1:8000).

The following day blots were washed with TBS-T (3 x 5 minutes) at room temperature and then incubated in horseradish peroxidase (HRP)-linked secondary antibody at a dilution of 1:5000 – 1:10000 in milk-TBS-T at room temperature for 1 hour. The secondary antibodies used were donkey anti-rabbit (GE Healthcare #NA934) or sheep anti-mouse (GE Healthcare #NA931). After this incubation, blots were washed with TBS-T (3 x 5 minutes) followed by ECL detection on X-Ray film using either Amersham ECL Western Blotting Detection Reagent (GE Healthcare #RPN2106) or Luminata Crescendo HRP Substrate (Millipore #WBLUR0100).

2.2.12. Microscopy

Cellular fluorescence was observed using a Leica DM IL LED inverted microscope with X-cite series 120 Q UV source. Fluorescent photos were captured using a QICAM Fast 1394 camera attachment (Q IMAGING) and filter sets from CHROMA: GFP: ET470/40x, ET525/50m, T495LPXR, dsRed or TurboRFP: ET545/30x, ET620/60m, T570lp.

3. Results

Before testing the effect of PTEN proximal gene knockdown on melanoma cell malignancy and resistance to therapeutic drugs *in vitro*, it was crucial to this goal that I ensure activity of the PTEN proximal genes targets could be effectively and specifically knocked down. Isoform-specific inhibitors for these targets were still in the early stages of development and commercialization at the onset of my Master's project[181]. The lack of commercially available selective pharmacological inhibitors was a contributing factor to my decision to target the PTEN proximal genes using a genetic approach (shRNA-mediated knockdown) rather than a pharmacological approach (protein kinase inhibition). Isoform-specific shRNA target sequences are accessible in the literature and can even be chosen using algorithms with set design criteria[187-189]. It is with this in mind that my initial efforts were focused on finding shRNAs that would effectively and specifically knockdown each of the PTEN proximal gene targets. Thereafter, lentiviral delivery of the targeting constructs was optimized to ensure adequate expression of shRNAs for effective target knockdown in melanoma cell lines.

3.1. PTEN Proximal Gene Knockdown

Below is a description of the methods used to screen shRNAs for efficacy and specificity in targeting PTEN Proximal genes using a dual-luciferase reporter system, followed by a description and characterization of the lentiviral vectors designed for the purposes of shRNA delivery for PTEN Proximal gene knockdown. The PTEN Proximal proteins whose knockdown I attempted are those directly upstream and downstream of PTEN: the Class I PI3Ks (p110- α , p110- β , p110- δ , and p110- γ), PDK1, and the AKT isoforms (AKT1, AKT2, and AKT3). Each individual target was to be knocked down using a miRNA30-embedded shRNA (shRNAmir). The utility of embedding shRNA sequences in an miRNA-30 backbone is that shRNAs can be stably expressed from any RNA polymerase II promoter[190]. With Pol II-driven transcription, lentiviral plasmids can be constructed to deliver non-transient shRNAmir expression under the control of constitutive, inducible, or tissue-specific promoters[183, 191].

3.1.1. shRNA Triage with a Luciferase Reporter System

Our lab has previously developed a novel method to rapidly and efficiently triage shRNAs using the psiCHECK2 luciferase reporter system[192]. The psiCHECK2 plasmid

contains two independently driven transcripts, one encoding Renilla luciferase and one coding for Firefly luciferase.(Figure 3.1A). Targeted cDNAs are cloned into psiCHECK2 downstream

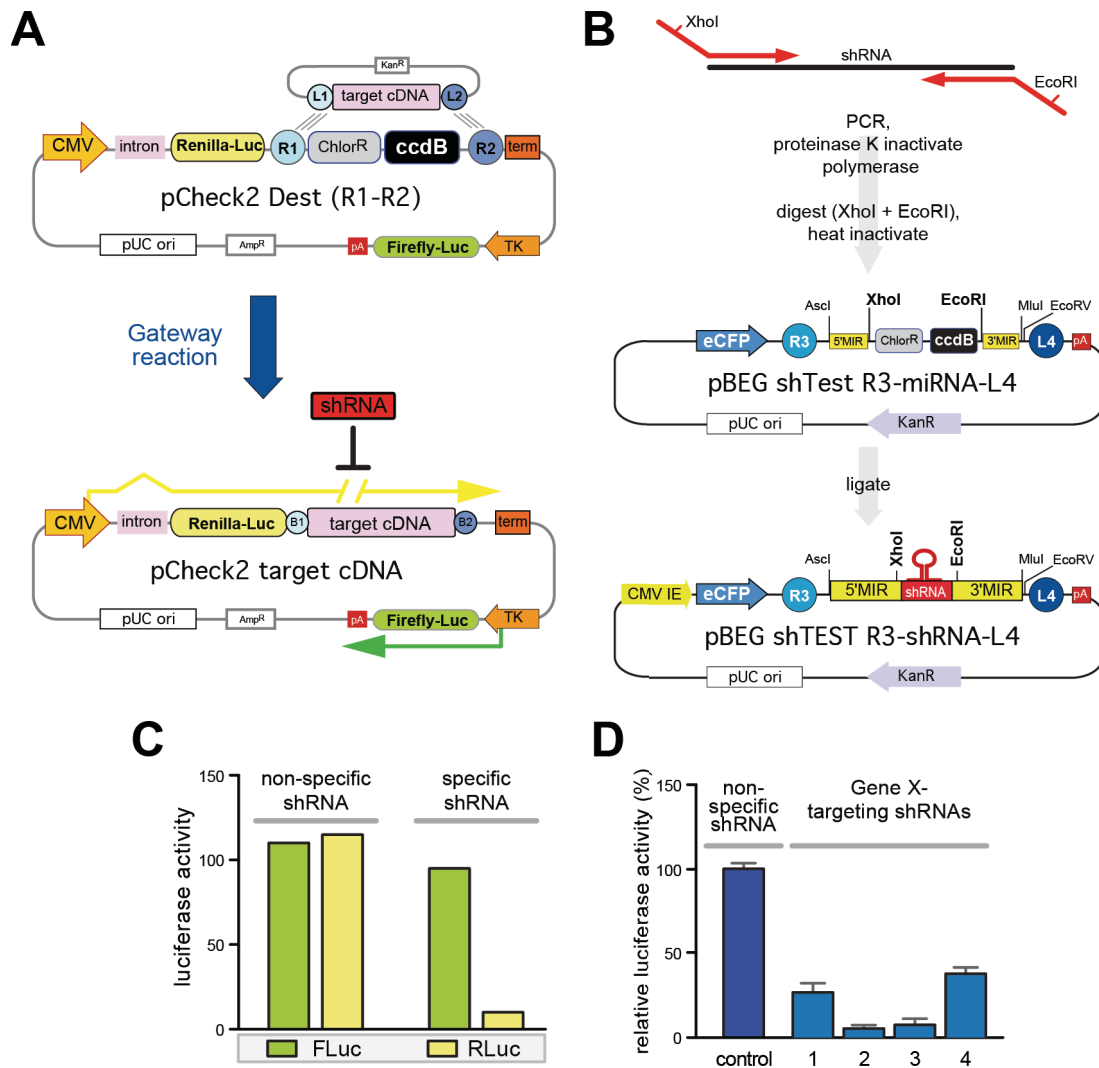


Figure 3.1 Rapid triage of novel shRNAs. (A) Target cDNAs are cloned into pCheck2 Dest (R1-R2) through Gateway recombination in between R1– R2 sites. The resulting plasmid produces a CMV-driven transcript (yellow arrow) encoding Renilla luciferase and a non-translated cDNA target and a Thymidine Kinase(TK)-driven transcript (green arrow) encoding Firefly luciferase to serve as an internal transfection control (adapted from [1]). (B) General method for the PCR amplification of novel shRNAs from a ~100 bp oligonucleotide core with two universal primers (red arrows). After high fidelity PCR, the polymerase is inactivated by Proteinase K treatment; the Proteinase k is heat inactivated and then the PCR product is digested with XhoI/EcoRI. The restriction enzymes are subsequently heat inactivated and the fragment is cloned into the corresponding sites of pBEG shTest R3-miRNA-L4 to create an R3-L4 based Entry vector pBEG R3-shRNA-L4. (C) Two different shRNAs are compared by normalizing for transfection efficiency via Firefly luciferase and then for specific knockdown by assessing renilla luciferase levels (mock data). (D) This data is normalized to the luciferases observed for the non-specific shRNA control (mock data is depicted here).

of Renilla luciferase but upstream of a polyadenylation (PolyA) sequence. The Renilla luciferase and target mRNA sequences are contained within the same mRNA transcript but separated by a stop codon. For mRNAs to be transcribed efficiently, a lariat structure must be formed between the 5'-cap and PolyA-tail of the transcript. shRNA-induced cleavage of the target sequence will prevent the efficient translation of the Renilla luciferase encoded upstream [193, 194]. Thus, in this assay Renilla luciferase activity is used as a readout of shRNA-mediated knockdown (Figure 3.1C and D). Firefly luciferase activity serves as an internal control for transfection since it is expressed independently of Renilla luciferase and has different substrate requirements to produce the bioluminescence. The bioluminescence produced by the Renilla and Firefly luciferases are measured sequentially from a single sample, allowing for Renilla activity to be normalized to Firefly activity. Normalizing to Firefly luciferase activity minimizes variability in experimental results caused by differences in cell viability and/or transfection efficiencies.

Recombination based, Gateway cloning allowed for the rapid construction of the plasmids required for the described shRNA triaging method. Briefly, Gateway technology is based on the site-specific recombination properties of bacteriophage λ [195, 196]. This phage inserts its DNA into the bacterial genome in between specific DNA attachment sites termed attPx (phage attachment site) and attBx (bacterial attachment site), creating attLx (left end of prophage) and attRx (right end of prophage) sites. This recombination system has been harnessed and commercialized as Gateway cloning technology (Invitrogen) to allow for the efficient, precise, and directional transfer of desired DNA sequences from one plasmid to another by site-specific recombination. Using LR recombination (between attL and attR sites), I created Expression plasmids by transferring a desired DNA fragment from a kanamycin-resistant Entry plasmid(s) into a Destination plasmid. Destination plasmids have both an attR-flanked *ccdB* selection cassette (toxic to most *E. coli* strains) for negative selection and an ampicillin selectable marker to select for the backbone [197].

Human cDNA sequences for the PTEN Proximal genes of interest were cloned into pCheck2 Dest R1-R2 (psiCHECK-2 made Gateway® compatible, Figure 3.1A). The second component to the shRNA triaging system, the pBEG shRNAmir-expressing vectors, were prepared by PCR and restriction enzyme capture from ordered shRNA oligonucleotides (Figure 3.1B). A literature search was performed to find published siRNA or shRNA sequences that had been shown to knock down my targets of interest. For those targets that had few functionally

verified shRNAs available in the literature (≤ 2 shRNAs), sequences were acquired from the CODEX RNAi library portal[198]. Targeting sequences were ordered as 93-105 nt single stranded DNA oligonucleotides designed to have a standard loop and overall structure as described previously[192]. The shRNA sequences had approximately 19-25 bases of homology with the target cDNA. Each shRNA to be tested was cloned into the miRNA-30 cassette of the pBEG shTest plasmid (Figure 3.1B). This plasmid was similar to an Entry vector, pBEG R3-miRNA-L4, designed to contain a shRNAmir cassette flanked by Gateway compatible attR3/L4 recombination sites to allow for one-step recombination into lentiviral expression vectors[192]. pBEG shTest R3-miRNA-L4 additionally contains the cytomegalovirus (CMV) promoter and eCFP (enhanced cyan fluorescent protein for visual tracking) upstream of the miR-30 cassette used in pBEG R3-miRNA-L4. An shRNA is cloned into the miRNA cassette of pBEG shTEST to give pBEG shTest R3-shRNA-L4. In this construction the presence of the attR3 and attL4 sites, which are 125 and 96 bp long, respectively, do not appreciably interfere with expression. Thus, these shTest plasmids function both as Entry Gateway vectors and as plasmids to express shRNAs when transfected into mammalian cells.

To initially assess shRNA efficacy, HEK-293T cells were co-transfected with the targeted pCheck2 Dest R1-R2 and shTest plasmids. Forty-eight hours post-transfection, cells were lysed to assay luciferase activity. Initially, five or six shRNAs were chosen for each target to put through this triaging process. This method of triaging shRNAs was optimized in our lab to be particularly rapid and efficient. Once the shRNA sequences are ordered (as DNA oligonucleotides) and received in our lab, cloning the sequences into the shTest plasmid and carrying out the first round of luciferase assay triaging could be completed in as little as five days. The initial round of the luciferase assays was used to identify the shRNA candidates most effective at targeting their respective mRNA transcripts. The most effective shRNAs (2-4 shRNAs per target) were selected to carry through a second round of luciferase assays in which candidate shRNAs were tested for target specificity within similar groups of targets (Figure 3.2). In other words, PI3K shRNAs were cross-tested against all of the PI3K reporter plasmids (Figure 3.2A). Likewise, AKT shRNAs were cross-tested against all of the AKT reporter plasmids (Figure 3.2B). PDK1 and PTEN shRNAs were cross-tested against each other to further illustrate the specificity for their intended target (Figure 3.2C).

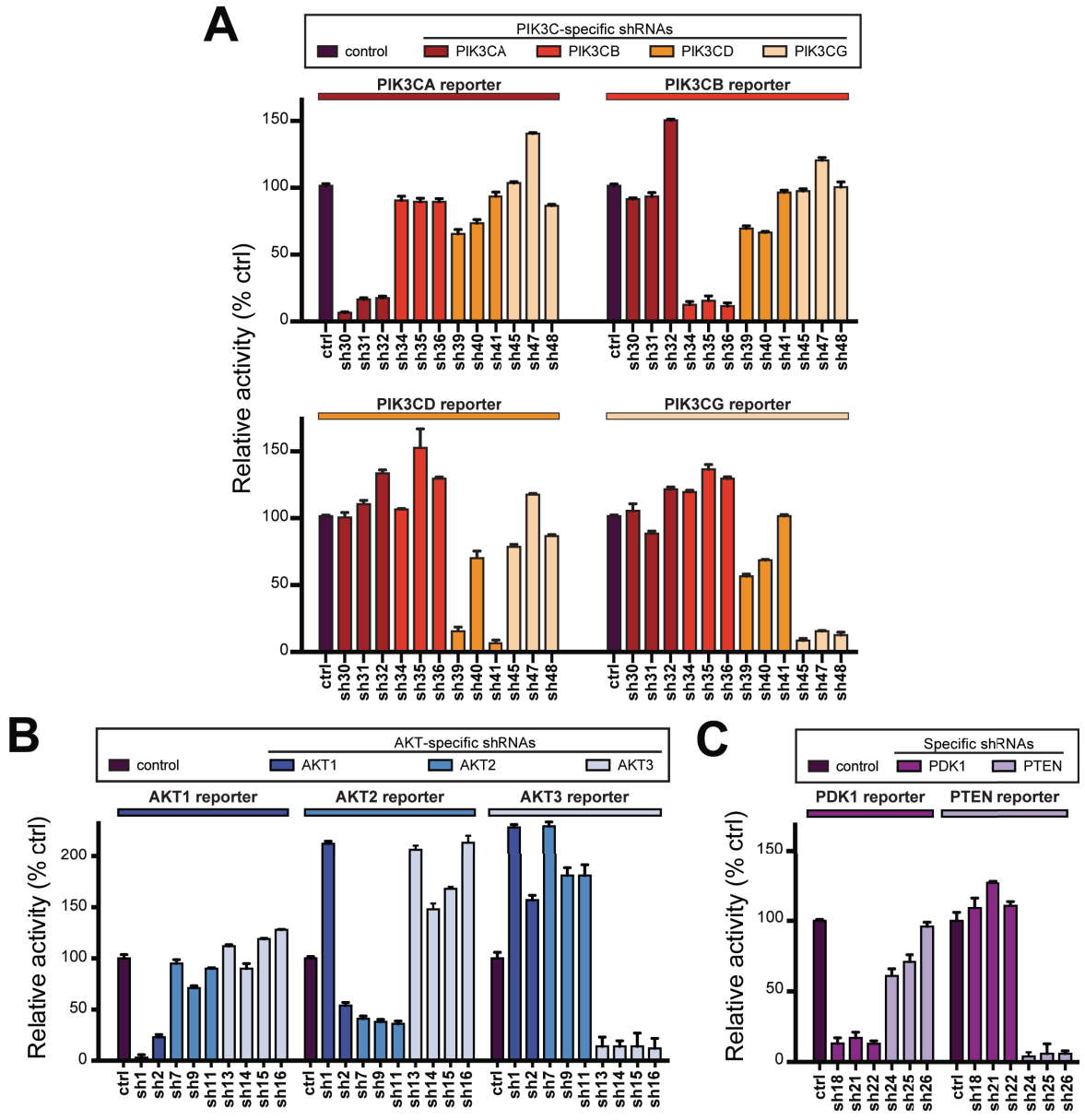


Figure 3.2. Luciferase assay triaging results for shRNAs targeting PTEN Proximal genes. After an initial round of testing candidate shRNAs, those producing the most efficient knockdown of their respective target were chosen to be tested again for the specificity of knockdown of their intended target. To test specificity, the selected pBEG shRNA plasmids were cross-tested against pCheck2 target cDNA plasmids containing the cDNA of targets within similar groups. To facilitate the cross-testing, pBEG shRNAs were co-transfected into 293T cells with pCheck2 reporter plasmids of similar targets. Transfections were done in triplicate. Renilla luciferase read-outs from the 293T cells were normalized to the Firefly luciferase internal control. Relative Renilla/Firefly activity was determined by standardizing to a non-targeting control shRNA (% ctrl). Colours of bars for relative activity indicate the specific reporter each shRNA is intended to target. (A) Luciferase assay readout of PI3K shRNA specificity. (B) Luciferase assay readout of AKT shRNA specificity. (C) Luciferase assay readout of PTEN and PDK1 shRNA specificity. Error bars represent relative standard error.

3.1.2. shRNA Delivery

By way of luciferase reporter assays, I was able to identify shRNAs that should effectively target each PTEN proximal gene of interest and do so in a specific manner. One or two of these shRNAs were selected to further characterize their efficacy and specificity when knocking down targeted protein in cultured cells (See Appendix Table 3 for a list of shRNAs chosen to further study). This was assessed by means of transient and stable shRNAmir delivery as described below.

3.1.2.1. Transient PTEN Proximal Gene Knockdown

Using transient transfection of shRNAmir expressing shTest plasmids, shRNAmirs were tested for their ability to knockdown endogenous protein levels in 293T cells. 293T cells were used because they are transfected with high efficiency and under the CMV promoter from which the shTest shRNAmirs are expressed, transcription is driven strongly in this cell type[199]. This step essentially served two purposes: 1) Ensured endogenous protein knockdown is achievable with the shRNAs that produced promising results in the luciferase assay experiments, 2) To test antibodies on 293T lysates to ensure the antibodies we have effectively and reliably detect their appropriate targets on Western blots. One or two shRNAs were tested for each PTEN proximal gene of interest (Figure 3.3). Generally, the shRNAs appeared to be effective at knocking down

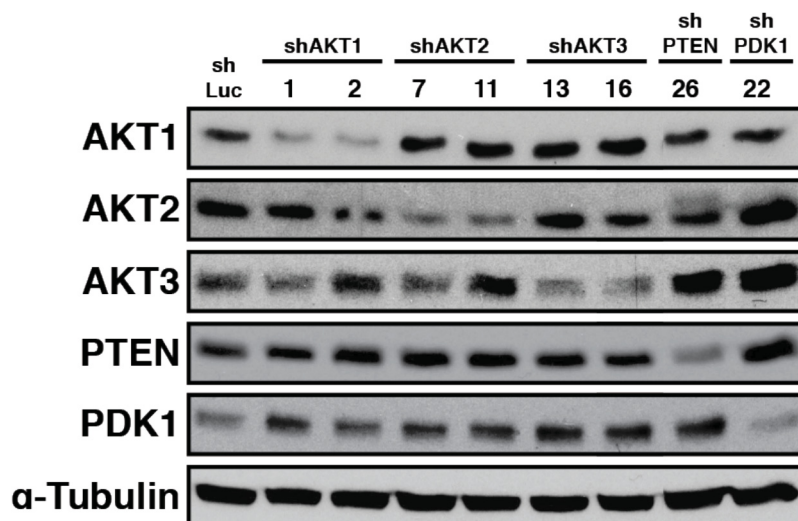


Figure 3.3. Transient pBEG shRNA-mediated endogenous protein knockdown in 293T cells. 293T cells were transfected with pBEG shRNA plasmids targeting AKT1, AKT2, AKT3, PTEN, or PDK1. shRNAs were selected based on results from the luciferase assay shRNA triage. Cells were lysed 72 hours post transfection and the protein lysates were used for Western blot analysis of target protein knockdown. These results are representative of at least two sets of transfection experiments.

their endogenous protein targets. Some results regarding shRNA efficacy and specificity were inconclusive, presumably due to the variability inherent of transiently delivering shRNAmirs. Also, levels of some PTEN proximal proteins were below detection levels in 293T cells (p110- α and p110- γ) as has been seen by others for these proteins in 293T cells[200, 201]. However, I was able to detect p110- α protein in other cell lines using the p110- α on hand (not shown). After confirming that the shRNAmir expression was functional in producing endogenous protein knockdown by mere transient delivery, I further investigated the efficacy and specificity of protein knockdown by means of lentiviral delivery for stable integration of shRNAs targeting the PTEN proximal genes. A description of the lentiviral vectors at my disposal and characterization of their utility in producing target knockdown follows below.

3.1.2.2. Stable and Inducible PTEN Proximal Gene Knockdown

To properly elucidate the role of each PTEN Proximal gene on melanoma malignancy, I required a method to produce sustained knockdown of the aforementioned genes of interest in melanoma cells. Transient transfection of shRNAmir-expressing plasmids would not allow for sustained and completely reliable knockdown of genes. Thus I chose lentiviral vectors to deliver stable integration of viral shRNAmir-encoding DNA constructs into the host genome for long-term expression of shRNA *in vitro*. Moreover, lentiviruses can be used to infect actively dividing as well as growth arrested and differentiated cells[202]. Using Gateway recombination, I constructed two lentiviral vectors that when integrated into the host genome would allow either constitutive or inducible shRNA expression (Figure 3.4). Our lab had previously developed a system based on MultiSite Gateway cloning technology with which one could rapidly generate viral vectors that could simultaneously express desired cDNAs, selectable markers, and shRNAmirs[1]. Using this system, I constructed pLEG shRNA lentiviral vectors for my experimental purposes (Figure 3.4A). pLEG is a modified version of the lentiviral pLEX vector (OpenBiosystems) made Gateway-compatible[1]. Using Gateway recombination, I could clone triaged shRNAs directly from the shTest plasmid into a recombinant pLEG vector. Additionally, the four-plasmid recombination reaction facilitated simultaneous cloning of a fluorophore and selectable marker into the pLEG vector. After recombination, all three of these elements are transcribed from the constitutively active CMV promoter. The fluorophore (dsRed, *Discosoma sp.* Red fluorescent protein) would allow for assessment of transduction efficiency and shRNA

expression, and the resistance marker (puromycin resistance) would allow for the selection of successfully transduced cells.

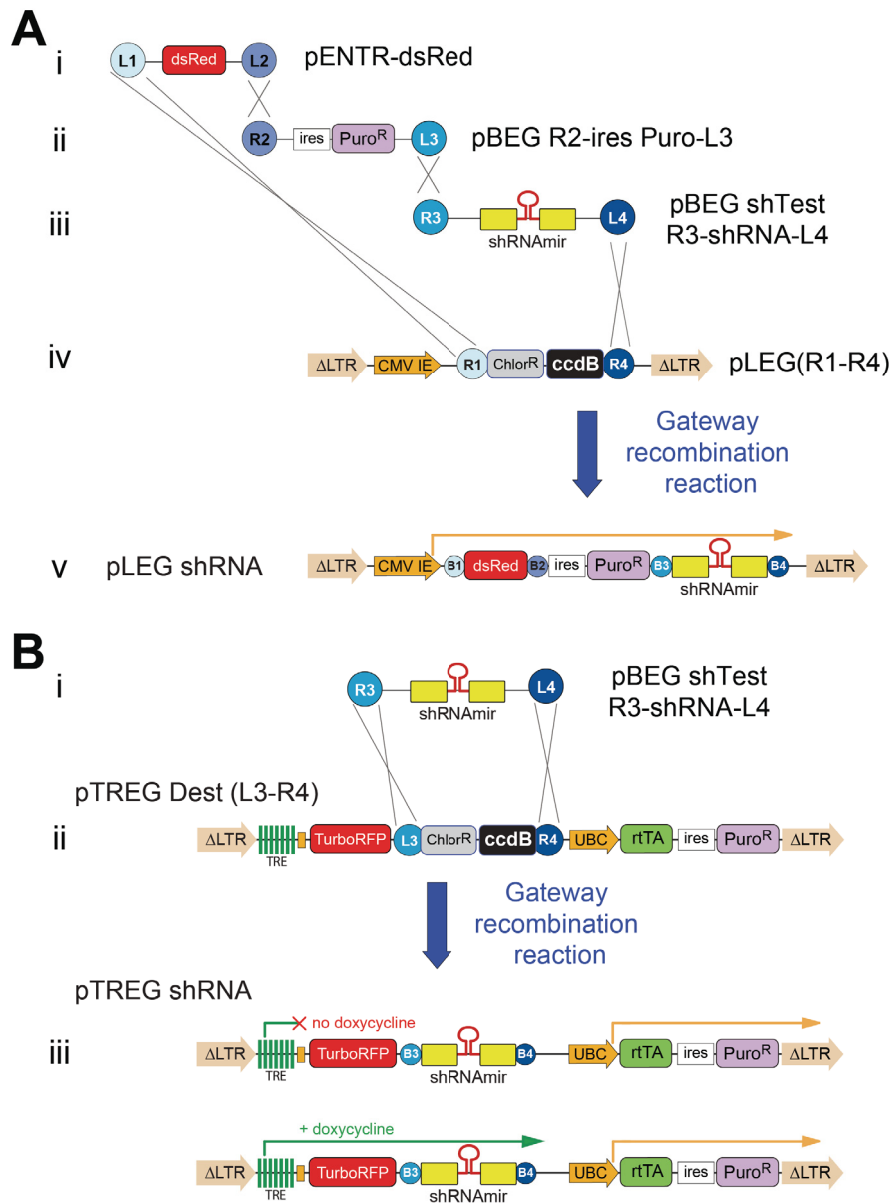


Figure 3.4. Overview of Gateway cloning of shRNAmirs into pLEG and pTREG lentiviral vectors. (A) A four-plasmid Gateway® LR recombination reaction showing the insertion of the dsRed fluorophore (i), Puromycin selection marker (ii) and miRNA cassette (iii) into pLEG(R1-R4) (iv) to produce a recombinant lentiviral pLEG shRNA expression vector (v). When integrated, pLEG shRNA will allow constitutive expression of the shRNA driven by the CMV promoter (B) A two-plasmid Gateway LR recombination reaction between pBEG shRNA (i) and TREG Dest(L3-R4) (ii) to produce TREG shRNA (iii), a pTRIPz-derived shRNA lentiviral vector. When integrated, TREG shRNA will allow doxycycline-regulated expression of the shRNA under control of the Tet-responsive element (TRE)(adapted from [1]).

While constitutively expressed shRNAs are useful for many of the experiments, inducible knockdown is ideal when studying genes essential for viability. Since the PI3K/AKT pathway is known to mediate anti-apoptotic signals within the cell, knockdown of signaling components in this pathway could very well result in cell death[83, 203]. This could be especially pertinent if PTEN proximal genes mediate drug resistance by conferring decreased susceptibility to apoptosis, as supported by the previous research[138, 155, 156, 160, 204, 205]. To more tightly control and monitor the lethality of PTEN proximal gene knockdown on BRAF^{V600E} melanoma cells, I made use of a pTRIPz-derived vector (Open Biosystems), the pTREG plasmid, that allows for Tet-On inducible shRNA expression. The Tet-On system requires binding of reverse tetracycline transactivator (rtTA) to the TetO operator sequences of the Tet-responsive element (TRE) to activate downstream gene expression (i.e. downstream shRNAmir expression). However, rtTA will only bind to TetO in the presence of tetracyclines (such as doxycycline, a more stable tetracycline analogue)[206]. Thus, with the pTREG vector, shRNA expression can be controlled in a doxycycline-dependent manner. The pTRIPz lentiviral vector was modified to pTREG to contain Gateway compatible sites so any gene or shRNAmir could be inserted through recombination in between these sites downstream of the TRE inducible promoter (Figure 3.4B). These Gateway sites were chosen to be compatible with the shTest plasmids so that the shRNAmir cassettes could simply be cloned into pTREG downstream of the TetO promoter with one Gateway recombination reaction. Like the pLEG vector, pTREG also encodes a fluorophore and a selectable marker. However, expression of the fluorophore, TurboRFP in this case, is controlled under the doxycycline inducible TRE allowing for visual confirmation of shRNA expression. Expression of a selectable marker encoding for puromycin resistance is constitutively expressed under the human ubiquitin C (UBC) promoter. The UBC promoter also drives constitutive expression of rtTA required for doxycycline-dependent induction of the TRE promoter.

With the pLEG shRNA and pTREG shRNA vectors at my disposal, I could create BRAF^{V600E} melanoma cell lines that would constitutively or inducibly express shRNAs targeting PTEN proximal genes. The successful shRNA candidates triaged by luciferase assays could be cloned into either vector using one Gateway reaction. I performed a preliminary assessment of shRNA knockdown produced by the pLEG and pTREG lentiviral transductions to compare the efficacy of each expression system (Figure 3.5). I chose to conduct the test with just one shRNA

to simplify the process. An AKT2 shRNA was chosen (shRNA #11), because it appeared to specifically and effectively knock down its intended target in both the luciferase assay and Western blot experiments in transient transfections. 293T cells were infected with pLEG shRNA or pTREG shRNA lentivirus containing either the AKT2 shRNA or an shRNA targeting Firefly luciferase. This would facilitate a qualitative and quantitative comparison between the pLEG shRNA and pTREG shRNA target knockdown.

To assess AKT2 knockdown, the luciferase shRNA would serve as a negative control in a Western blot experiment wherein I would be blotting for AKT2. Here, I compared AKT2 protein knockdown between pLEG and pTREG infected 293T cell lines (Figure 3.5A). pTREG infected cells were treated with doxycycline for up to five days to induce AKT2 shRNA expression prior to Western blot analysis. AKT1 and AKT3 were also blotted for to assess the specificity of this AKT2 shRNA for knockdown of its target. Both pLEG and pTREG shRNA expression effectively knocked down AKT2 protein levels, with pLEG shRNA expression producing slightly greater knockdown of AKT2 than the pTREG inducible knockdown. This is likely attributable to the constitutive nature of shRNA expression produced by the pLEG vector. The shRNA is expressed immediately upon integration into the recipient cell's genome prolonging the shRNA expression period as compared to pTREG-mediated shRNA expression which only occurs at the onset of doxycycline induction. Nonetheless, both lentiviral expression systems produced suitable knockdown of the intended target.

To quantify the level of shRNA-mediated knockdown between pLEG and pTREG transduced cells, AKT2 shRNA expressing 293T cells served as a control for Firefly luciferase knockdown in luciferase assays. A pCheck2 luciferase reporter plasmid was transfected into these cells pre-doxycycline induction. In this experiment, Renilla luciferase activity from the pCheck2-p53 plasmid served as the internal control since neither Renilla nor p53 were targeted by AKT2 or Firefly luciferase specific shRNAs. Following up to five days of doxycycline treatment, cells were lysed and assayed for luciferase activity. Again, pLEG and pTREG produced efficient knockdown of the intended target and both vectors produced similar levels knockdown. Again, pLEG shRNA expression produced slightly greater knockdown of Firefly luciferase than pTREG inducible shRNA expression (Figure 3.5B).

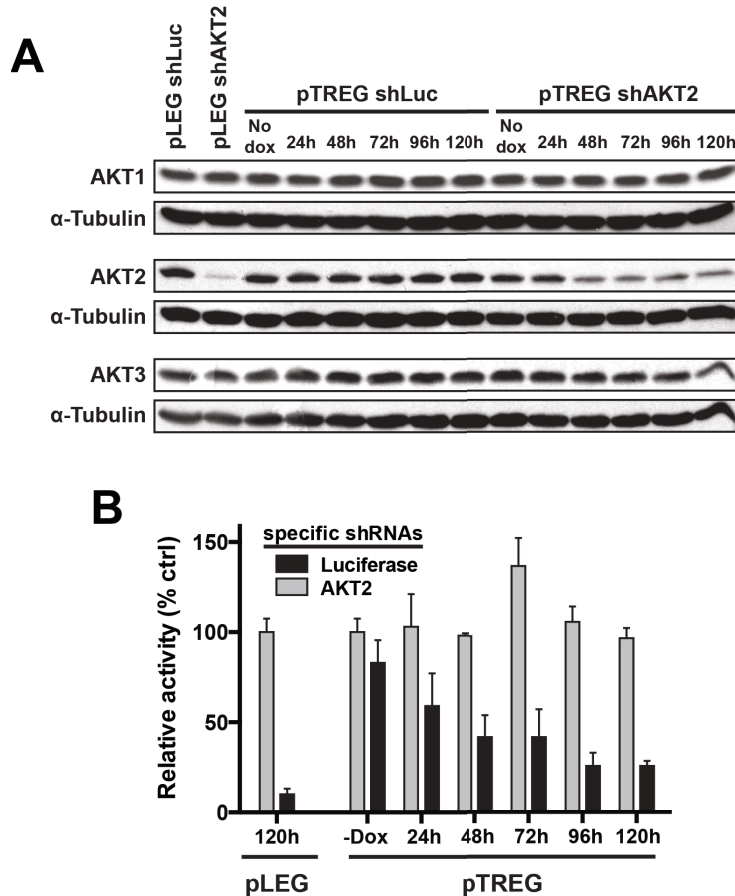


Figure 3.5. pLEG and pTREG shRNA-mediated knockdown of targeted genes. (A) HEK-293T cells were transduced with the pLEG or pTREG lentiviral vectors expressing shRNAs targeting AKT2 or firefly luciferase. After doxycycline-induced pTREG shRNA expression for up to five days, cell lysates were obtained for assessment of expression of the indicated proteins by Western blot analysis. (B) In parallel, pLEG and pTREG transduced HEK-293T cells were transfected with the pCheck2-p53 firefly and renilla luciferase reporter plasmid. After doxycycline-induced pTREG shRNA expression for up to five days, cells were lysed and assayed for firefly and renilla luciferase activity. In this case, the AKT2 shRNA samples served as the negative control for firefly-luciferase knockdown by the luciferase targeting shRNA. Unlike the aforementioned luciferase assays, Renilla luciferase was not targeted here, and thus could serve as the internal control to normalize for transfection efficiency.

After this preliminary test to functionally verify the efficacy of the pLEG and pTREG shRNA expression systems, shRNAs targeting each of the PTEN proximal genes were cloned into the pLEG and pTREG vectors using Gateway recombination as laid out above (Figure 3.5). Once cloned into the pLEG vectors, shRNA efficacy and specificity for targeted protein knockdown was tested in A375 melanoma cells (BRAF^{V600E}, PTEN wildtype) and 293T cells.

A375 cells were chosen as they expressed the majority of the target proteins at well detected levels (Figure 3.6A). Also, it should be noted that none of the melanoma cells or 293T cells expressed p110- γ at detectable levels. Thus, efficacy of the PIK3CG shRNAs and p110- γ antibody was verified by expressing the PIK3CG cDNA in 293T cells via lentiviral transduction (not shown). A375 and 293T cells were infected with lentivirus for each pLEG shRNA. Western blot analysis of lysates from each shRNA cell line validated the efficacy and specificity of shRNA-mediated knockdown (Figure 3.6B and C). These results indicate that sufficient

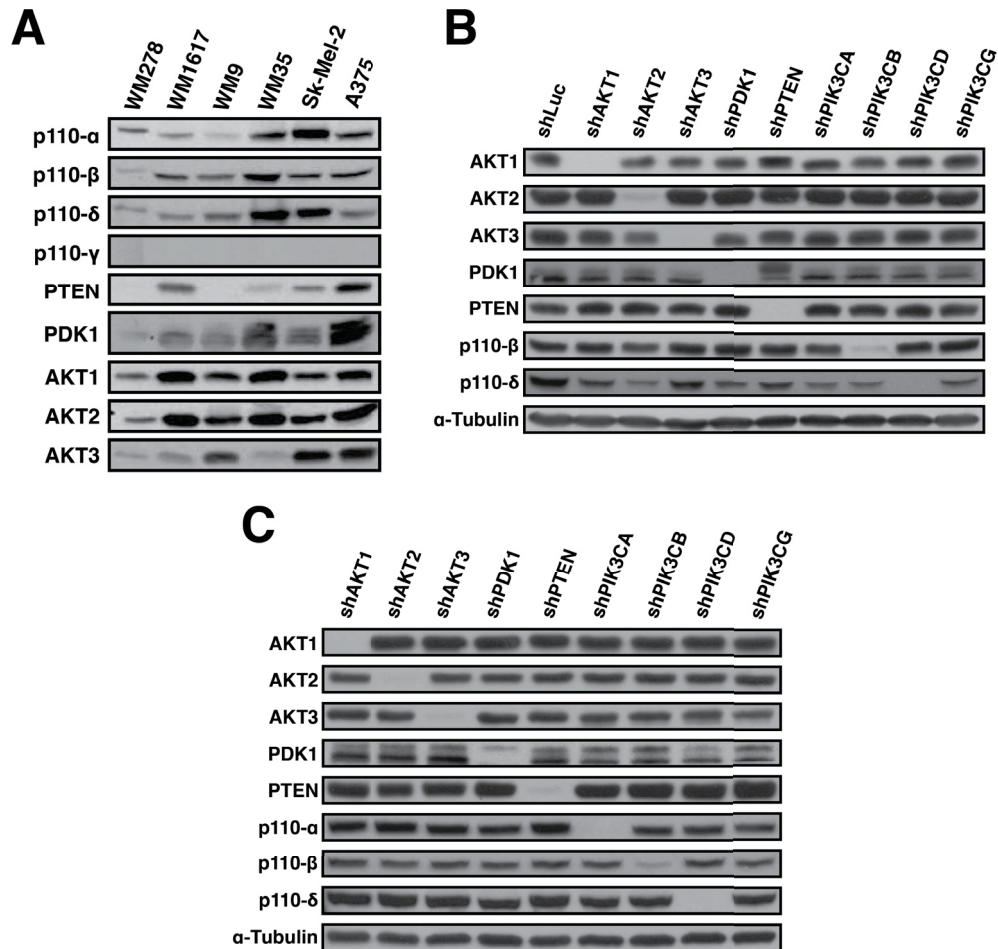


Figure 3.6. Western blot analysis of PTEN Proximal protein expression in melanoma cells and knockdown in pLEG shRNA cell lines. (A) Western blot analysis of PTEN Proximal protein expression in WM278, WM1617, WM9, WM35, Sk-mel-2, and A375 melanoma cell lines. Each lane was loaded with 55 μ g of protein except for the WM278 lane (16 μ g per well) and the Sk-Mel-2 lane (30 μ g per well) because the lysates were not concentrated enough. (B) 293T pLEG shRNA knockdown (C) A375 pLEG shRNA knockdown. Note: p110- α and p110- γ proteins are not expressed at detectable levels in 293T cells. p110- γ protein is not expressed in A375 cells.

knockdown is attainable with the pLEG shRNA infection. Unfortunately, I encountered issues when trying to achieve similar results with the pTREG shRNA expression system. These issues (inadequate target knockdown, lentiviral toxicity encountered when attempting to infect at higher multiplicity of infection (MOI), underestimation of pTREG viral titer, toxicity of doxycycline treatment) and how I assessed them are addressed in the appendix.

3.1.3. The miRNA-E Backbone

Recently, a research group demonstrated that a modified version of the miRNA-30 backbone, termed miRNA-E (miR-E), resulted in more efficient endogenous processing of the shRNAmirs and thus increased knockdown levels from single-copy shRNA expression[207]. To determine if the miR-E backbone could produce improved knockdown from the pTREG vector, miR-E knockdown was compared to miR-30 knockdown first via luciferase assays with transient shRNA expression from the shTEST plasmid and then by inducible pTREG shRNA expression. To accomplish this, the modified miR-E backbone was cloned into the shTEST plasmid replacing the miR-30 cassette. Because the core of the shRNA stem-loop structure is not affected by the design features of the miR-E backbone, the existing ~100 nt miR-30 compatible shRNA oligonucleotides can be easily converted to be compatible with the miR-E through PCR subcloning. Three sets of shRNAs targeting P53, AKT1, and PTEN (8 shRNAs total) were chosen to compare the reporter knockdown efficacy of the miR-30 and miR-E backbones via luciferase assay (Figure 3.7A). shRNAs with different knockdown capabilities (medium to highly effective) were chosen to determine if knockdown can be improved with the miR-E backbone for shRNAs at either level of performance (i.e. if an shRNA already produces efficient knockdown can the miR-E backbone further improve it or will the miR-E backbone only appreciably improve knockdown for less effective shRNAs?).

With the luciferase assay, it appeared that miR-E-based shRNAs functioned similarly to miR30-based shRNAs, yet for one miR-E-shRNA (AKT1 shRNA #5) which displayed enhanced reporter knockdown over the miR-30 backbone. To determine its effect on protein knockdown, the miR-30 and miR-E version of AKT1 shRNA #5 were cloned into pTREG. WM9 cells infected with these vectors and protein knockdown was assessed after doxycycline induction of shRNA expression for various time intervals (Figure 3.7B). Indeed, expression of the miR-E embedded shRNA#5 produced improved knockdown of AKT1 over the miR-30 embedded

version. These results indicate that the miR-E backbone functions as well as miR-30 based shRNAs and it can enhance the knockdown produced by certain shRNAs. The reason for success in this single case is not immediately obvious although increased efficacy has been reported for miR-E[207]. With the assays performed it appears that the miR-E backbone generally never worsened knockdown efficacy. Taking this into consideration, the miR-E backbone should replace the miR-30 backbone for future shRNA triaging and subsequent cloning into lentiviral expression vectors.

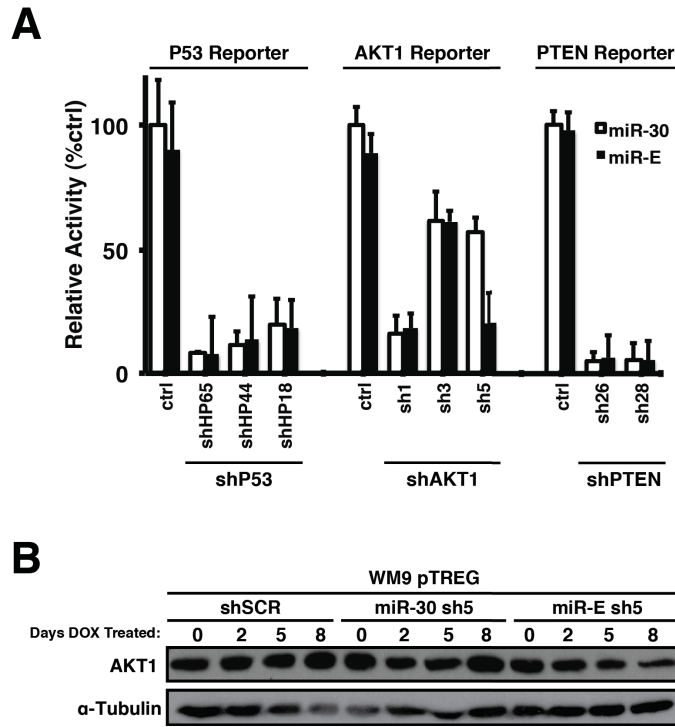


Figure 3.7. Evaluating the efficacy of shRNA-mediated target knockdown in the miRNA-30 and miRNA-E backbones.(A) Dual-luciferase assays assessing the reporter knockdown efficiency of miR-E and miR-30 embedded shRNAs targeting P53, AKT1, and PTEN. Renilla/Firefly activity for all miR-30 and miR-E shRNAs was normalized to the miR-30 controls for direct comparison of mRNA knockdown. Transfections were performed in triplicate. Error bars represent relative standard error. (B) Western blot analysis of AKT1 protein knockdown in WM9 pTREG cells containing AKT1 shRNA #5 embedded in the miR-E or miR-30 backbone. Expression of the shRNA was induced by

4. Discussion

4.1. Optimization of shRNA Delivery

This work describes the use of a unique, rapid, and efficient shRNA triaging system involving a dual-luciferase reporter assay to find shRNAs that would effectively and specifically knockdown PTEN proximal genes in the PI3K-AKT pathway. The triaging process was developed and based on work done previously in the Dankort lab. Before using this system to triage shRNAs targeting the PTEN Proximal genes of interest for the purpose of this project, limited work was done to ensure that successful shRNA candidates could effectively and specifically knockdown protein expression of intended targets *in vitro*. With this work I have demonstrated that this is indeed possible with vector delivery of either transient or stable expression into several mammalian cell lines. As mentioned before, once the target cDNA has been cloned into the pCheck2 dual-luciferase reporter plasmid and the ordered shRNA oligonucleotides are received, cloning the shRNA into the pBEG shTest plasmid and assessing target knockdown efficacy via luciferase assay could be completed in as little as five days. Now that the shRNA triaging process has been evaluated for functionality, we hope to publish this method of finding and rapidly assessing shRNA efficacy and specificity in this manner.

Another advantage to this system is that successful shRNA candidates can be readily cloned from the pBEG shTest plasmid into Gateway compatible lentiviral vectors by recombination to create constructs for the stable knockdown of endogenous protein. In this work I describe the use of two different lentiviral vectors, pLEG shRNA and pTREG shRNA, for the *in vitro* delivery of constitutive or inducible shRNA expression, respectively. After infection with pLEG shRNA lentivirus, endogenous protein in pLEG expressing 293T and melanoma cells was successfully knocked down. Of course to assess targeting efficiency, antibodies that effectively detected the expression of PTEN Proximal proteins were identified. Also, primers were designed to detect PTEN proximal gene expression by quantitative reverse transcriptase polymerase chain reaction (qRT-PCR) for future analysis mRNA knockdown efficacy (See Appendix, Table 6). Unfortunately, I experienced some difficulty in producing effective knockdown with the pTREG inducible system. More recently, Clustered Regularly Interspaced Short Palindromic Repeats Associated protein (CRISPR-Cas) systems for gene targeting have been developed and commercialized with which one can create gene deletions/knockouts of

target genes rather than knocking down expression of genetic targets via shRNA-mediated technologies[208-211]. CRISPR-Cas presents an alternative approach to down-regulating the expression of PTEN proximal genes, especially for targets that prove to be more difficult to knockdown via shRNA-mediated methods. However, one would not have the option to reverse CRISPR-Cas9-mediated gene knockouts as you would with pTREG inducible shRNA expression. Additionally, implementing CRISPR-Cas technology for knockouts of all PTEN proximal genes could be a labour/cost intensive process (vector acquisition, clone selection/screening, etc.) not necessarily producing improved suppression of target expression over shRNA knockdown, which I have demonstrated can produce sufficient target knockdown. Using the pTREG system for knocking down expression of the PTEN proximal genes would be ideal for experiments involving the assessment of viability and apoptosis. One could control the timing of knockdown and thus more closely monitor these effects after treating cells with doxycycline to induce shRNA expression. Additionally, non-treated pTREG infected cells serve as a convenient built in control. Thus, ensuring the seamless use pTREG-mediated knockdown became a priority for much of the time spent on my project.

To improve pTREG knockdown efficacy, I first attempted to increase shRNA expression levels by increasing the lentiviral MOI at which melanoma cells were being infected. This proved to be problematic because at higher MOIs (MOI >1) the lentiviral infections were extremely toxic to the cells. I attempted to reduce infection cytotoxicity potentially associated with VSV-pseudotyped lentivirus by pseudotyping the virus with LCMV-WE, MokolaG, and RD114A, envelope glycoproteins reported to have reduced cytotoxic effects[212-218]. Unfortunately, the titers produced by MokolaG and RD114A pseudotyped lentivirus were insufficiently low, and LMCV-WE pseudotyped virus did not appear to reduce lentiviral toxicity compared to VSV-G pseudotyped virus. Furthermore, VSV-G infectivity on melanoma cells was much more efficient than the infectivity of LCMV-WE, with VSV-G producing cells with higher levels of construct expression. Since greater levels of construct expression is what was desired, I continued to use VSV-G to produce lentivirus for melanoma pTREG infections. As suggested in the literature, removing serum from the medium during virus production can greatly reduce the risk of introducing additional agents, some of which might be contributing to the cell death resulting from lentiviral infection[219]. Indeed, removing serum from the medium during lentivirus production was the most fruitful in terms of reducing pTREG infection cytotoxicity,

allowing for infections to be done at higher MOI. On the melanoma cells lines tested, lentivirus produced in serum-free medium was much less toxic to the cells and had an improved effect when compared to simply removing serum from the medium during infection.

To ensure the proper execution of pTREG lentiviral infections and use of inducible shRNA expression in melanoma cells, other factors involving viral titration, doxycycline induction, and the miRNA cassette were optimized. After suspecting that titring pTREG virus using limiting dilution with puromycin drug selection was producing titer results that were a gross underestimate of the actual viral titer and not always reproducible, I discovered a much more reliable and efficient method of titring pTREG virus involving limiting dilution with TurboRFP-positive colony counting after doxycycline induction[186]. With newly titered pTREG virus (produced in serum-free medium), a range of infection MOI was determined to ensure optimal knockdown and minimal cytotoxicity for future pTREG infections. Another issue that arose with the use of pTREG-mediated shRNA knockdown was the effect of doxycycline on the viability of the melanoma cells, an effect observed previously by others[220-222]. This was realized when I attempted to treat with a higher concentration of doxycycline (10 $\mu\text{g}/\text{mL}$ compared to 1 $\mu\text{g}/\text{mL}$) to try to increase shRNA expression levels. With viability assays, I determined that even at a concentration of 1 $\mu\text{g}/\text{mL}$ melanoma cell viability is reduced. At doxycycline concentrations 0.10 to 0.25 $\mu\text{g}/\text{mL}$ cell viability was minimally affected, and that doxycycline treatment with 0.25 $\mu\text{g}/\text{mL}$ produced the same level of knockdown as treatment with 1 $\mu\text{g}/\text{mL}$. Lastly, when assessed by luciferase reporter assay or pTREG mediated endogenous protein knockdown, the miRNA-E backbone was determined to produce improved knockdown (in luciferase assays and in melanoma cells) over the miRNA-30 backbone for one particular AKT1 shRNA (shRNA #5). Since miRNA-E knockdown was not any worse than miRNA-30 knockdown as determined by luciferase assay and could provide improved knockdown for certain shRNAs, moving forward, newly designed shRNAs will be cloned into expression vectors to contain the miRNA-E backbone instead.

4.2. Future Work

Now that functional shRNAs targeting the PTEN proximal genes have been identified, and the framework has been laid out for optimal use of the pLEG and pTREG shRNA lentiviral vectors, determining the contribution of PTEN proximal proteins to melanoma malignancy and

drug resistance is more feasible. It may remain difficult to knockdown the expression of certain targets with this system depending on the stability of target mRNA and protein in each melanoma cell line. In such an instance, pharmacological inhibition could be used as an alternative approach. In the past few years, many more isoform-specific PI3K and AKT inhibitors have been designed and become commercially available[154, 223, 224]. For the purposes of this research, pharmacological inhibition could also be used as a complimentary technique to confirm any biological effects observed as a result of shRNA-mediated target knockdown.

BRAF^{V600E} melanoma pTREG shRNA cell lines carrying shRNAs specific to PTEN proximal genes are being generated for these future experiments. Using these melanoma cell lines, the effect of PTEN proximal gene knockdown will be assessed via quantitative proliferation, viability, transformation analyses, such as growth curves, resazurin viability assays, colony formation assays for anchorage independent growth, and fluorescence activated cell sorting (FACS) analysis to assess cell cycle profile, proliferation, and apoptosis. To build upon what is already known about the PI3K/AKT pathway in melanoma tumourigenesis, it will be important to assess if the contribution of each PTEN proximal protein is dependent upon tumour stage (RGP, VGP, and metastasis) and PTEN-deficiency. We also have the tools to produce lentiviral vectors containing daisy-chained shRNAmirs in a single construct (described in[192]). Thus, multiple shRNAs targeting several different proteins of interest can be expressed simultaneously to determine the specific PTEN proximal proteins that cooperate with BRAF^{V600E} to contribute to melanoma's malignant characteristics.

Additionally, it remains to be determined if knocking down specific isoforms of PI3K and AKT, or PDK1 can sensitize BRAF^{V600E} melanoma cell lines to BRAF and/or MEK inhibitory drugs. It is already known that co-targeting these pathways can decrease the tumourigenic properties of melanoma in preclinical *in vitro* and *in vivo* assessments[138, 151, 155-161]. Unfortunately, clinical use of this combination to treat cancer patients has proven to be challenging due to synergistic toxicities[63, 162, 163]. Specifically, the efficacy and tolerance of pan-PI3K inhibitors has been limited due to the dosages required to successfully inhibit all PI3K isoforms. At the dosages required, clinicians see toxicities associated with adverse off-target effects of inhibitors not sufficiently selective for PI3K, and on-target effects of inhibiting all class I PI3K isoforms whose function are essential to non-tumour cells[223]. For this reason,

recently several isoform-selective inhibitors have been designed and are emerging in clinical use[223]. Using isoform-specific PI3K inhibitors has the potential to block the function of relevant PI3K isoforms at better tolerated doses by avoiding on- and off-target broad inhibition. Thus, there is a critical need to determine which inhibitors targeting specific PTEN proximal proteins should be prioritized for testing in patients, especially in the context of MAPK inhibition in BRAF mutant melanoma.

One other aspect to consider in this targeting model is that dual PI3K-mTOR targeting has been demonstrated as an effective strategy to overcome the cross-talk and feedback loops that can reactivate both the MAPK and PI3K-AKT pathway[158, 178, 225]. Similarly to how concurrent BRAF and MEK inhibition provides improved overall inhibition of the MAPK pathway activation and extended response to therapeutic inhibition in melanoma[120, 129, 226], targeting multiple nodes of the PI3K-AKT pathway might be necessary to achieve optimal inactivation of the pathway and increase clinical efficacy. In light of this observation, for future experiments PTEN proximal genes could be targeted in conjunction with genetic or pharmacological inhibition of mTOR to investigate combinations that would most effectively sensitize BRAF^{V600E} melanoma cells to MAPK inhibition. Identifying which of the PTEN proximal proteins specifically cooperate with mTOR to confer a proliferative or survival advantage could help circumvent the toxicities associated with clinical use of pan-PI3K and mTOR inhibitors for example[111, 163, 164, 179].

Mr. Lewis has begun testing the sensitivity of various BRAF^{V600E} melanoma cell lines to BRAF and MEK inhibition with the goal of determining if knockdown of specific PTEN proximal genes can further sensitize these cells to the MAPK targeting drugs. Others have demonstrated that melanoma cell lines can be differentially sensitive to BRAF and MEK inhibition[227, 228]. Future work in the lab will be geared towards determining how PTEN proximal genes contribute to this intrinsic nature of resistance with regard to tumour stage and PTEN-deficiency. To determine contributors to acquired resistance, PTEN proximal genes will be targeted with concurrent BRAF and/or MEK-inhibition in melanoma cell lines made resistant to BRAF and MEK inhibition. These cell lines can be created by chronic treatment with these drugs as described previously[155, 157, 229]. With shRNA-mediated knockdown of PTEN proximal genes in melanoma cells sensitive and resistance to BRAF and MEK inhibition, it will be determined which of these proteins cooperate to contribute to intrinsic and acquired resistance

to MAPK inhibition. An improved understanding of the PTEN proximal proteins critical to development of resistance will facilitate decision making when determining which combinations of MAPK and PI3K-AKT targeting drugs will be prioritized for clinically testing in the treatment of BRAF mutant melanoma.

5. Conclusion

In summary, using a unique shRNA triage method based on a dual-luciferase reporter system, I have identified shRNAs that are effective and specific in targeting PTEN proximal proteins that function in the PI3K-AKT signaling pathway. In this work, methods to detect the mRNA and protein expression of these targets have been established. I validated that the successful shRNA candidates were functional in ablating their intended target via delivery of transient shRNA expression with the pBEG shTest plasmid and with stable shRNA expression with the pLEG shRNA lentiviral plasmid. Lentiviral targeting plasmids were constructed via the use of Gateway cloning technologies, the pLEG shRNA plasmids for constitutive shRNA expression, and the pTREG shRNA plasmids for doxycycline inducible shRNA expression. After some difficulty with obtaining adequate knockdown with the inducible system, attempts were made to improve and enhance lentiviral delivery of pTREG to achieve greater targeting efficiency. In these attempts, I determined that using serum-less medium for virus production reduced the cytotoxicity of lentiviral infection on melanoma cells, allowing for infection at higher MOI, and thus increased shRNA expression. Also, an efficient method of titering pTREG lentivirus was identified and replaced a less efficient and less reliable method. For induction of pTREG shRNA expression, appropriate doxycycline treatment concentrations were determined for multiple melanoma cell lines that would minimize off-target effects on viability but maintain adequate levels of knockdown. Further assessment of this is required, but a reportedly improved miRNA-30 backbone, termed miRNA-E, was tested and shown to produce better target knockdown when used in the pTREG inducible system. All of this work contributes to the greater goal of interrogating the role of PTEN proximal genes in BRAF^{V600E}-driven melanoma malignancy *in vitro*.

6. Bibliography

1. Geiling B, G Vandal, AR Posner, A de Bruyns, KL Dutchak, S Garnett, and D Dankort, *A Modular Lentiviral and Retroviral Construction System to Rapidly Generate Vectors for Gene Expression and Gene Knockdown In Vitro and In Vivo*. *Plos One* (2013). **8**(10).
2. Ferlay J, I Soerjomataram, R Dikshit, S Eser, C Mathers, M Rebelo, DM Parkin, D Forman, and F Bray, *Cancer incidence and mortality worldwide: sources, methods and major patterns in GLOBOCAN 2012*. *Int J Cancer* (2015). **136**(5): p. E359-86.
3. Lawrence MS, P Stojanov, CH Mermel, JT Robinson, LA Garraway, TR Golub, M Meyerson, SB Gabriel, ES Lander, and G Getz, *Discovery and saturation analysis of cancer genes across 21 tumour types*. *Nature* (2014). **505**(7484): p. 495-501.
4. Goel VK, AJ Lazar, CL Warneke, MS Redston, and FG Haluska, *Examination of mutations in BRAF, NRAS, and PTEN in primary cutaneous melanoma*. *J Invest Dermatol* (2006). **126**(1): p. 154-60.
5. Tsao H, V Goel, H Wu, G Yang, and FG Haluska, *Genetic interaction between NRAS and BRAF mutations and PTEN/MMAC1 inactivation in melanoma*. *J Invest Dermatol* (2004). **122**(2): p. 337-41.
6. Tsao H, X Zhang, K Fowlkes, and FG Haluska, *Relative reciprocity of NRAS and PTEN/MMAC1 alterations in cutaneous melanoma cell lines*. *Cancer Res* (2000). **60**(7): p. 1800-4.
7. Gast A, D Scherer, B Chen, S Bloethner, S Melchert, A Sucker, K Hemminki, D Schadendorf, and R Kumar, *Somatic alterations in the melanoma genome: a high-resolution array-based comparative genomic hybridization study*. *Genes Chromosomes Cancer* (2010). **49**(8): p. 733-45.
8. Chapman PB, et al., *Improved survival with vemurafenib in melanoma with BRAF V600E mutation*. *N Engl J Med* (2011). **364**(26): p. 2507-16.
9. Flaherty KT, I Puzanov, KB Kim, A Ribas, GA McArthur, JA Sosman, PJ O'Dwyer, RJ Lee, JF Grippo, K Nolop, and PB Chapman, *Inhibition of mutated, activated BRAF in metastatic melanoma*. *N Engl J Med* (2010). **363**(9): p. 809-19.
10. Sosman JA, et al., *Survival in BRAF V600-mutant advanced melanoma treated with vemurafenib*. *N Engl J Med* (2012). **366**(8): p. 707-14.
11. Kim HS, EK Kim, HJ Jun, SY Oh, KW Park, H Lim do, SI Lee, JH Kim, KM Kim, DH Lee, and J Lee, *Noncutaneous malignant melanoma: a prognostic model from a retrospective multicenter study*. *BMC Cancer* (2010). **10**: p. 167.
12. Wilkins DK and PD Nathan, *Therapeutic opportunities in noncutaneous melanoma*. *Ther Adv Med Oncol* (2009). **1**(1): p. 29-36.
13. WorldHealthOrganization. *How common is skin cancer?* Access Date: April 13, 2015. Available from: <http://www.who.int/uv/faq/skincancer/en/index1.html>.
14. Jerant AF, JT Johnson, CD Sheridan, and TJ Caffrey, *Early detection and treatment of skin cancer*. *Am Fam Physician* (2000). **62**(2): p. 357-68, 375-6, 381-2.
15. Lozano R, et al., *Global and regional mortality from 235 causes of death for 20 age groups in 1990 and 2010: a systematic analysis for the Global Burden of Disease Study 2010*. *Lancet* (2012). **380**(9859): p. 2095-128.
16. Jemal A, SS Devesa, P Hartge, and MA Tucker, *Recent trends in cutaneous melanoma incidence among whites in the United States*. *J Natl Cancer Inst* (2001). **93**(9): p. 678-83.

17. Semizarov D, L Frost, A Sarthy, P Kroeger, DN Halbert, and SW Fesik, *Specificity of short interfering RNA determined through gene expression signatures. Proc Natl Acad Sci U S A* (2003). **100**(11): p. 6347-52.
18. Chin L, G Merlino, and RA DePinho, *Malignant melanoma: modern black plague and genetic black box. Genes Dev* (1998). **12**(22): p. 3467-81.
19. AmericanCancerSociety. *Cancer Facts & Figures 2015*. Access Date: April 13, 2015. Available from: <http://www.cancer.org/acs/groups/content/@editorial/documents/document/acspc-044552.pdf>.
20. Berger MF, et al., *Melanoma genome sequencing reveals frequent PREX2 mutations. Nature* (2012). **485**(7399): p. 502-6.
21. Pleasance ED, et al., *A comprehensive catalogue of somatic mutations from a human cancer genome. Nature* (2010). **463**(7278): p. 191-6.
22. Gray-Schopfer V, C Wellbrock, and R Marais, *Melanoma biology and new targeted therapy. Nature* (2007). **445**(7130): p. 851-7.
23. Lomas J, P Martin-Duque, M Pons, and M Quintanilla, *The genetics of malignant melanoma. Front Biosci* (2008). **13**: p. 5071-93.
24. Miller AJ and MC Mihm, Jr., *Melanoma. N Engl J Med* (2006). **355**(1): p. 51-65.
25. Bennett DC, *Human melanocyte senescence and melanoma susceptibility genes. Oncogene* (2003). **22**(20): p. 3063-9.
26. Braig M and CA Schmitt, *Oncogene-induced senescence: putting the brakes on tumor development. Cancer Res* (2006). **66**(6): p. 2881-4.
27. Ha L, G Merlino, and EV Sviderskaya, *Melanomagenesis: overcoming the barrier of melanocyte senescence. Cell Cycle* (2008). **7**(13): p. 1944-8.
28. Goldstein AM, et al., *High-risk melanoma susceptibility genes and pancreatic cancer, neural system tumors, and uveal melanoma across GenoMEL. Cancer Res* (2006). **66**(20): p. 9818-28.
29. Serrano M, GJ Hannon, and D Beach, *A new regulatory motif in cell-cycle control causing specific inhibition of cyclin D/CDK4. Nature* (1993). **366**(6456): p. 704-7.
30. Pomerantz J, N Schreiber-Agus, NJ Liegeois, A Silverman, L Alland, L Chin, J Potes, K Chen, I Orlow, HW Lee, C Cordon-Cardo, and RA DePinho, *The Ink4a tumor suppressor gene product, p19Arf, interacts with MDM2 and neutralizes MDM2's inhibition of p53. Cell* (1998). **92**(6): p. 713-23.
31. Zhang Y, Y Xiong, and WG Yarbrough, *ARF promotes MDM2 degradation and stabilizes p53: ARF-INK4a locus deletion impairs both the Rb and p53 tumor suppression pathways. Cell* (1998). **92**(6): p. 725-34.
32. Kamijo T, JD Weber, G Zambetti, F Zindy, MF Roussel, and CJ Sherr, *Functional and physical interactions of the ARF tumor suppressor with p53 and Mdm2. Proc Natl Acad Sci U S A* (1998). **95**(14): p. 8292-7.
33. Zuo L, J Weger, Q Yang, AM Goldstein, MA Tucker, GJ Walker, N Hayward, and NC Dracopoli, *Germline mutations in the p16INK4a binding domain of CDK4 in familial melanoma. Nat Genet* (1996). **12**(1): p. 97-9.
34. Molven A, MB Grimstvedt, SJ Steine, M Harland, MF Avril, NK Hayward, and LA Akslen, *A large Norwegian family with inherited malignant melanoma, multiple atypical nevi, and CDK4 mutation. Genes Chromosomes Cancer* (2005). **44**(1): p. 10-8.

35. Pjanova D, L Engele, JA Randerson-Moor, M Harland, DT Bishop, JA Newton Bishop, C Taylor, T Debniak, J Lubinski, R Kleina, and O Heisele, *CDKN2A and CDK4 variants in Latvian melanoma patients: analysis of a clinic-based population. Melanoma Res* (2007). **17**(3): p. 185-91.
36. Majore S, P De Simone, A Crisi, L Eibenschutz, F Binni, I Antignoni, C De Bernardo, C Catricala, and P Grammatico, *CDKN2A/CDK4 molecular study on 155 Italian subjects with familial and/or primary multiple melanoma. Pigment Cell Melanoma Res* (2008). **21**(2): p. 209-11.
37. Puntervoll HE, et al., *Melanoma prone families with CDK4 germline mutation: phenotypic profile and associations with MC1R variants. J Med Genet* (2013). **50**(4): p. 264-70.
38. Gilchrest BA, MS Eller, AC Geller, and M Yaar, *The pathogenesis of melanoma induced by ultraviolet radiation. N Engl J Med* (1999). **340**(17): p. 1341-8.
39. Hussein MR, *Ultraviolet radiation and skin cancer: molecular mechanisms. J Cutan Pathol* (2005). **32**(3): p. 191-205.
40. Palmer JS, DL Duffy, NF Box, JF Aitken, LE O'Gorman, AC Green, NK Hayward, NG Martin, and RA Sturm, *Melanocortin-1 receptor polymorphisms and risk of melanoma: is the association explained solely by pigmentation phenotype? Am J Hum Genet* (2000). **66**(1): p. 176-86.
41. Kennedy C, J ter Huurne, M Berkhout, N Gruis, M Bastiaens, W Bergman, R Willemze, and JN Bavinck, *Melanocortin 1 receptor (MC1R) gene variants are associated with an increased risk for cutaneous melanoma which is largely independent of skin type and hair color. J Invest Dermatol* (2001). **117**(2): p. 294-300.
42. Kadarko AL, H Kanto, R Kavanagh, and Z Abdel-Malek, *Significance of the melanocortin 1 receptor in regulating human melanocyte pigmentation, proliferation, and survival. Ann N Y Acad Sci* (2003). **994**: p. 359-65.
43. Naysmith L, K Waterston, T Ha, N Flanagan, Y Bisset, A Ray, K Wakamatsu, S Ito, and JL Rees, *Quantitative measures of the effect of the melanocortin 1 receptor on human pigmentary status. J Invest Dermatol* (2004). **122**(2): p. 423-8.
44. Valverde P, E Healy, I Jackson, JL Rees, and AJ Thody, *Variants of the melanocyte-stimulating hormone receptor gene are associated with red hair and fair skin in humans. Nat Genet* (1995). **11**(3): p. 328-30.
45. Healy E, SA Jordan, PS Budd, R Suffolk, JL Rees, and IJ Jackson, *Functional variation of MC1R alleles from red-haired individuals. Hum Mol Genet* (2001). **10**(21): p. 2397-402.
46. Bastiaens M, J ter Huurne, N Gruis, W Bergman, R Westendorp, BJ Vermeer, and JN Bouwes Bavinck, *The melanocortin-1-receptor gene is the major freckle gene. Hum Mol Genet* (2001). **10**(16): p. 1701-8.
47. Valverde P, E Healy, S Sikkink, F Haldane, AJ Thody, A Carothers, IJ Jackson, and JL Rees, *The Asp84Glu variant of the melanocortin 1 receptor (MC1R) is associated with melanoma. Hum Mol Genet* (1996). **5**(10): p. 1663-6.
48. Florell SR, KM Boucher, G Garibotti, J Astle, R Kerber, G Mineau, C Wiggins, RD Noyes, A Tsodikov, LA Cannon-Albright, JJ Zone, WE Samlowski, and SA Leachman, *Population-based analysis of prognostic factors and survival in familial melanoma. J Clin Oncol* (2005). **23**(28): p. 7168-77.

49. Grafstrom E, S Egyhazi, U Ringborg, J Hansson, and A Platz, *Biallelic deletions in INK4 in cutaneous melanoma are common and associated with decreased survival. Clin Cancer Res* (2005). **11**(8): p. 2991-7.
50. Straume O, J Smeds, R Kumar, K Hemminki, and LA Akslen, *Significant impact of promoter hypermethylation and the 540 C>T polymorphism of CDKN2A in cutaneous melanoma of the vertical growth phase. Am J Pathol* (2002). **161**(1): p. 229-37.
51. Cachia AR, JO Indsto, KM McLaren, GJ Mann, and MJ Arends, *CDKN2A mutation and deletion status in thin and thick primary melanoma. Clin Cancer Res* (2000). **6**(9): p. 3511-5.
52. Forbes SA, D Beare, P Gunasekaran, K Leung, N Bindal, H Boutselakis, M Ding, S Bamford, C Cole, S Ward, CY Kok, M Jia, T De, JW Teague, MR Stratton, U McDermott, and PJ Campbell, *COSMIC: exploring the world's knowledge of somatic mutations in human cancer. Nucleic Acids Res* (2015). **43**(Database issue): p. D805-11.
53. Marais R and CJ Marshall, *Control of the ERK MAP kinase cascade by Ras and Raf. Cancer Surv* (1996). **27**: p. 101-25.
54. Robinson MJ and MH Cobb, *Mitogen-activated protein kinase pathways. Curr Opin Cell Biol* (1997). **9**(2): p. 180-6.
55. Gray-Schopfer VC, S da Rocha Dias, and R Marais, *The role of B-RAF in melanoma. Cancer Metastasis Rev* (2005). **24**(1): p. 165-83.
56. Wellbrock C, M Karasarides, and R Marais, *The RAF proteins take centre stage. Nat Rev Mol Cell Biol* (2004). **5**(11): p. 875-85.
57. Orgaz JL and V Sanz-Moreno, *Emerging molecular targets in melanoma invasion and metastasis. Pigment Cell Melanoma Res* (2013). **26**(1): p. 39-57.
58. Cohen C, A Zavala-Pompa, JH Sequeira, M Shoji, DG Sexton, G Cotsonis, F Cerimele, B Govindarajan, N Macaron, and JL Arbiser, *Mitogen-activated protein kinase activation is an early event in melanoma progression. Clin Cancer Res* (2002). **8**(12): p. 3728-33.
59. Satyamoorthy K, G Li, MR Gerrero, MS Brose, P Volpe, BL Weber, P Van Belle, DE Elder, and M Herlyn, *Constitutive mitogen-activated protein kinase activation in melanoma is mediated by both BRAF mutations and autocrine growth factor stimulation. Cancer Res* (2003). **63**(4): p. 756-9.
60. Davies H, et al., *Mutations of the BRAF gene in human cancer. Nature* (2002). **417**(6892): p. 949-54.
61. Hocker T and H Tsao, *Ultraviolet radiation and melanoma: a systematic review and analysis of reported sequence variants. Hum Mutat* (2007). **28**(6): p. 578-88.
62. Liang J and JM Slingerland, *Multiple roles of the PI3K/PKB (Akt) pathway in cell cycle progression. Cell Cycle* (2003). **2**(4): p. 339-45.
63. Liu P, H Cheng, TM Roberts, and JJ Zhao, *Targeting the phosphoinositide 3-kinase pathway in cancer. Nat Rev Drug Discov* (2009). **8**(8): p. 627-44.
64. Engelman JA, J Luo, and LC Cantley, *The evolution of phosphatidylinositol 3-kinases as regulators of growth and metabolism. Nat Rev Genet* (2006). **7**(8): p. 606-19.
65. Hodis E, et al., *A landscape of driver mutations in melanoma. Cell* (2012). **150**(2): p. 251-63.
66. Haluska FG, H Tsao, H Wu, FS Haluska, A Lazar, and V Goel, *Genetic alterations in signaling pathways in melanoma. Clin Cancer Res* (2006). **12**(7 Pt 2): p. 2301s-2307s.
67. Sensi M, G Nicolini, C Petti, I Bersani, F Lozupone, A Molla, C Vegetti, D Nonaka, R Mortarini, G Parmiani, S Fais, and A Anichini, *Mutually exclusive NRASQ61R and*

- BRAFV600E mutations at the single-cell level in the same human melanoma. Oncogene* (2006). **25**(24): p. 3357-64.
68. Wu S, H Kuo, WQ Li, AL Canales, J Han, and AA Qureshi, *Association between BRAFV600E and NRASQ61R mutations and clinicopathologic characteristics, risk factors and clinical outcome of primary invasive cutaneous melanoma. Cancer Causes Control* (2014). **25**(10): p. 1379-86.
 69. Edlundh-Rose E, S Egyhazi, K Omholt, E Mansson-Brahme, A Platz, J Hansson, and J Lundeberg, *NRAS and BRAF mutations in melanoma tumours in relation to clinical characteristics: a study based on mutation screening by pyrosequencing. Melanoma Res* (2006). **16**(6): p. 471-8.
 70. Ellerhorst JA, VR Greene, S Ekmekcioglu, CL Warneke, MM Johnson, CP Cooke, LE Wang, VG Prieto, JE Gershenwald, Q Wei, and EA Grimm, *Clinical correlates of NRAS and BRAF mutations in primary human melanoma. Clin Cancer Res* (2011). **17**(2): p. 229-35.
 71. Lee JH, JW Choi, and YS Kim, *Frequencies of BRAF and NRAS mutations are different in histological types and sites of origin of cutaneous melanoma: a meta-analysis. Br J Dermatol* (2011). **164**(4): p. 776-84.
 72. Wan PT, MJ Garnett, SM Roe, S Lee, D Niculescu-Duvaz, VM Good, CM Jones, CJ Marshall, CJ Springer, D Barford, and R Marais, *Mechanism of activation of the RAF-ERK signaling pathway by oncogenic mutations of B-RAF. Cell* (2004). **116**(6): p. 855-67.
 73. Michaloglou C, LC Vredeveld, WJ Mooi, and DS Peeper, *BRAF(E600) in benign and malignant human tumours. Oncogene* (2008). **27**(7): p. 877-95.
 74. Sharma A, NR Trivedi, MA Zimmerman, DA Tuveson, CD Smith, and GP Robertson, *Mutant V599EB-Raf regulates growth and vascular development of malignant melanoma tumors. Cancer Res* (2005). **65**(6): p. 2412-21.
 75. Pollock PM, UL Harper, KS Hansen, LM Yudt, M Stark, CM Robbins, TY Moses, G Hostetter, U Wagner, J Kakareka, G Salem, T Pohida, P Heenan, P Duray, O Kallioniemi, NK Hayward, JM Trent, and PS Meltzer, *High frequency of BRAF mutations in nevi. Nat Genet* (2003). **33**(1): p. 19-20.
 76. Michaloglou C, LC Vredeveld, MS Soengas, C Denoyelle, T Kuilman, CM van der Horst, DM Majoor, JW Shay, WJ Mooi, and DS Peeper, *BRAFE600-associated senescence-like cell cycle arrest of human naevi. Nature* (2005). **436**(7051): p. 720-4.
 77. Dankort D, DP Curley, RA Cartlidge, B Nelson, AN Karnezis, WE Damsky, Jr., MJ You, RA DePinho, M McMahon, and M Bosenberg, *Braf(V600E) cooperates with Pten loss to induce metastatic melanoma. Nat Genet* (2009). **41**(5): p. 544-52.
 78. Muthusamy V, S Duraisamy, CM Bradbury, C Hobbs, DP Curley, B Nelson, and M Bosenberg, *Epigenetic silencing of novel tumor suppressors in malignant melanoma. Cancer Res* (2006). **66**(23): p. 11187-93.
 79. Chin L, LA Garraway, and DE Fisher, *Malignant melanoma: genetics and therapeutics in the genomic era. Genes Dev* (2006). **20**(16): p. 2149-82.
 80. Sharpless E and L Chin, *The INK4a/ARF locus and melanoma. Oncogene* (2003). **22**(20): p. 3092-8.
 81. Davies MA, *The role of the PI3K-AKT pathway in melanoma. Cancer J* (2012). **18**(2): p. 142-7.

82. Altomare DA and JR Testa, *Perturbations of the AKT signaling pathway in human cancer. Oncogene* (2005). **24**(50): p. 7455-64.
83. Cantley LC, *The phosphoinositide 3-kinase pathway. Science* (2002). **296**(5573): p. 1655-7.
84. Manning BD and LC Cantley, *AKT/PKB signaling: navigating downstream. Cell* (2007). **129**(7): p. 1261-74.
85. Sarbassov DD, SM Ali, and DM Sabatini, *Growing roles for the mTOR pathway. Curr Opin Cell Biol* (2005). **17**(6): p. 596-603.
86. Yecies JL and BD Manning, *mTOR links oncogenic signaling to tumor cell metabolism. J Mol Med (Berl)* (2011). **89**(3): p. 221-8.
87. Restuccia DF and BA Hemmings, *From man to mouse and back again: advances in defining tumor AKTivities in vivo. Dis Model Mech* (2010). **3**(11-12): p. 705-20.
88. Maehama T and JE Dixon, *The tumor suppressor, PTEN/MMAC1, dephosphorylates the lipid second messenger, phosphatidylinositol 3,4,5-trisphosphate. J Biol Chem* (1998). **273**(22): p. 13375-8.
89. Wu H, V Goel, and FG Haluska, *PTEN signaling pathways in melanoma. Oncogene* (2003). **22**(20): p. 3113-22.
90. Pilarski R and C Eng, *Will the real Cowden syndrome please stand up (again)? Expanding mutational and clinical spectra of the PTEN hamartoma tumour syndrome. J Med Genet* (2004). **41**(5): p. 323-6.
91. Robertson GP, *Functional and therapeutic significance of Akt deregulation in malignant melanoma. Cancer Metastasis Rev* (2005). **24**(2): p. 273-85.
92. Dhawan P, AB Singh, DL Ellis, and A Richmond, *Constitutive activation of Akt/protein kinase B in melanoma leads to up-regulation of nuclear factor-kappaB and tumor progression. Cancer Res* (2002). **62**(24): p. 7335-42.
93. Stahl JM, A Sharma, M Cheung, M Zimmerman, JQ Cheng, MW Bosenberg, M Kester, L Sandirasegarane, and GP Robertson, *Deregulated Akt3 activity promotes development of malignant melanoma. Cancer Res* (2004). **64**(19): p. 7002-10.
94. Curtin JA, MS Stark, D Pinkel, NK Hayward, and BC Bastian, *PI3-kinase subunits are infrequent somatic targets in melanoma. J Invest Dermatol* (2006). **126**(7): p. 1660-3.
95. Omholt K, D Krockel, U Ringborg, and J Hansson, *Mutations of PIK3CA are rare in cutaneous melanoma. Melanoma Res* (2006). **16**(2): p. 197-200.
96. Davies MA, K Stemke-Hale, C Tellez, TL Calderone, W Deng, VG Prieto, AJ Lazar, JE Gershenwald, and GB Mills, *A novel AKT3 mutation in melanoma tumours and cell lines. Br J Cancer* (2008). **99**(8): p. 1265-8.
97. Beadling C, E Jacobson-Dunlop, FS Hodi, C Le, A Warrick, J Patterson, A Town, A Harlow, F Cruz, 3rd, S Azar, BP Rubin, S Muller, R West, MC Heinrich, and CL Corless, *KIT gene mutations and copy number in melanoma subtypes. Clin Cancer Res* (2008). **14**(21): p. 6821-8.
98. Curtin JA, K Busam, D Pinkel, and BC Bastian, *Somatic activation of KIT in distinct subtypes of melanoma. J Clin Oncol* (2006). **24**(26): p. 4340-6.
99. Prickett TD, NS Agrawal, X Wei, KE Yates, JC Lin, JR Wunderlich, JC Cronin, P Cruz, SA Rosenberg, and Y Samuels, *Analysis of the tyrosine kinome in melanoma reveals recurrent mutations in ERBB4. Nat Genet* (2009). **41**(10): p. 1127-32.

100. Slipicevic A, R Holm, MT Nguyen, PJ Bohler, B Davidson, and VA Florenes, *Expression of activated Akt and PTEN in malignant melanomas: relationship with clinical outcome. Am J Clin Pathol* (2005). **124**(4): p. 528-36.
101. Aguisa-Toure AH and G Li, *Genetic alterations of PTEN in human melanoma. Cell Mol Life Sci* (2012). **69**(9): p. 1475-91.
102. Zhou XP, O Gimm, H Hampel, T Niemann, MJ Walker, and C Eng, *Epigenetic PTEN silencing in malignant melanomas without PTEN mutation. Am J Pathol* (2000). **157**(4): p. 1123-8.
103. Tsao H, X Zhang, E Benoit, and FG Haluska, *Identification of PTEN/MMAC1 alterations in uncultured melanomas and melanoma cell lines. Oncogene* (1998). **16**(26): p. 3397-402.
104. Stewart AL, AM Mhashilkar, XH Yang, S Ekmekcioglu, Y Saito, K Sieger, R Schrock, E Onishi, X Swanson, JB Mumm, L Zumstein, GJ Watson, D Snary, JA Roth, EA Grimm, R Ramesh, and S Chada, *PI3 kinase blockade by Ad-PTEN inhibits invasion and induces apoptosis in RGP and metastatic melanoma cells. Mol Med* (2002). **8**(8): p. 451-61.
105. Stahl JM, M Cheung, A Sharma, NR Trivedi, S Shanmugam, and GP Robertson, *Loss of PTEN promotes tumor development in malignant melanoma. Cancer Res* (2003). **63**(11): p. 2881-90.
106. Madhunapantula SV and GP Robertson, *The PTEN-AKT3 signaling cascade as a therapeutic target in melanoma. Pigment Cell Melanoma Res* (2009). **22**(4): p. 400-19.
107. Vredeveld LC, PA Possik, MA Smit, K Meissl, C Michaloglou, HM Horlings, A Ajouaou, PC Kortman, D Dankort, M McMahon, WJ Mooi, and DS Peeper, *Abrogation of BRAFV600E-induced senescence by PI3K pathway activation contributes to melanomagenesis. Genes Dev* (2012). **26**(10): p. 1055-69.
108. Cheung M, A Sharma, SV Madhunapantula, and GP Robertson, *Akt3 and mutant V600E B-Raf cooperate to promote early melanoma development. Cancer Res* (2008). **68**(9): p. 3429-39.
109. Shin SS, BA Wall, JS Goydos, and S Chen, *AKT2 is a downstream target of metabotropic glutamate receptor 1 (Grm1). Pigment Cell Melanoma Res* (2010). **23**(1): p. 103-11.
110. Nogueira C, KH Kim, H Sung, KH Paraiso, JH Dannenberg, M Bosenberg, L Chin, and M Kim, *Cooperative interactions of PTEN deficiency and RAS activation in melanoma metastasis. Oncogene* (2010). **29**(47): p. 6222-32.
111. Girotti MR, G Saturno, P Lorigan, and R Marais, *No longer an untreatable disease: how targeted and immunotherapies have changed the management of melanoma patients. Mol Oncol* (2014). **8**(6): p. 1140-58.
112. Kudchadkar RR, KS Smalley, LF Glass, JS Trimble, and VK Sondak, *Targeted therapy in melanoma. Clin Dermatol* (2013). **31**(2): p. 200-8.
113. Bollag G, et al., *Clinical efficacy of a RAF inhibitor needs broad target blockade in BRAF-mutant melanoma. Nature* (2010). **467**(7315): p. 596-9.
114. Joseph EW, CA Pratilas, PI Poulikakos, M Tadi, W Wang, BS Taylor, E Halilovic, Y Persaud, F Xing, A Viale, J Tsai, PB Chapman, G Bollag, DB Solit, and N Rosen, *The RAF inhibitor PLX4032 inhibits ERK signaling and tumor cell proliferation in a V600E BRAF-selective manner. Proc Natl Acad Sci U S A* (2010). **107**(33): p. 14903-8.
115. Jang S and MB Atkins, *Treatment of BRAF-mutant melanoma: the role of vemurafenib and other therapies. Clin Pharmacol Ther* (2014). **95**(1): p. 24-31.

116. Eggermont AM and JM Kirkwood, *Re-evaluating the role of dacarbazine in metastatic melanoma: what have we learned in 30 years?* *Eur J Cancer* (2004). **40**(12): p. 1825-36.
117. Atkins MB, L Kunkel, M Sznol, and SA Rosenberg, *High-dose recombinant interleukin-2 therapy in patients with metastatic melanoma: long-term survival update.* *Cancer J Sci Am* (2000). **6 Suppl 1**: p. S11-4.
118. Jonasch E and FG Haluska, *Interferon in oncological practice: review of interferon biology, clinical applications, and toxicities.* *Oncologist* (2001). **6**(1): p. 34-55.
119. Hauschild A, et al., *Dabrafenib in BRAF-mutated metastatic melanoma: a multicentre, open-label, phase 3 randomised controlled trial.* *Lancet* (2012). **380**(9839): p. 358-65.
120. Flaherty KT, et al., *Combined BRAF and MEK inhibition in melanoma with BRAF V600 mutations.* *N Engl J Med* (2012). **367**(18): p. 1694-703.
121. Mattei PL, MB Alora-Palli, S Kraft, DP Lawrence, KT Flaherty, and AB Kimball, *Cutaneous effects of BRAF inhibitor therapy: a case series.* *Ann Oncol* (2013). **24**(2): p. 530-7.
122. Oberholzer PA, D Kee, P Dziunycz, A Sucker, N Kamsukom, R Jones, C Roden, CJ Chalk, K Ardlie, E Palescandolo, A Piris, LE MacConaill, C Robert, GF Hofbauer, GA McArthur, D Schadendorf, and LA Garraway, *RAS mutations are associated with the development of cutaneous squamous cell tumors in patients treated with RAF inhibitors.* *J Clin Oncol* (2012). **30**(3): p. 316-21.
123. Su F, et al., *RAS mutations in cutaneous squamous-cell carcinomas in patients treated with BRAF inhibitors.* *N Engl J Med* (2012). **366**(3): p. 207-15.
124. Gibney GT, JL Messina, IV Fedorenko, VK Sondak, and KS Smalley, *Paradoxical oncogenesis--the long-term effects of BRAF inhibition in melanoma.* *Nat Rev Clin Oncol* (2013). **10**(7): p. 390-9.
125. Freeman AK, DA Ritt, and DK Morrison, *Effects of Raf dimerization and its inhibition on normal and disease-associated Raf signaling.* *Mol Cell* (2013). **49**(4): p. 751-8.
126. Hu J, EC Stites, H Yu, EA Germino, HS Meharena, PJ Stork, AP Kornev, SS Taylor, and AS Shaw, *Allosteric activation of functionally asymmetric RAF kinase dimers.* *Cell* (2013). **154**(5): p. 1036-46.
127. Luo Z, G Tzivion, PJ Belshaw, D Vavvas, M Marshall, and J Avruch, *Oligomerization activates c-Raf-1 through a Ras-dependent mechanism.* *Nature* (1996). **383**(6596): p. 181-5.
128. Rebocho AP and R Marais, *ARAF acts as a scaffold to stabilize BRAF:CRAF heterodimers.* *Oncogene* (2013). **32**(26): p. 3207-12.
129. Paraiso KH, IV Fedorenko, LP Cantini, AC Munko, M Hall, VK Sondak, JL Messina, KT Flaherty, and KS Smalley, *Recovery of phospho-ERK activity allows melanoma cells to escape from BRAF inhibitor therapy.* *Br J Cancer* (2010). **102**(12): p. 1724-30.
130. Wellbrock C, *MAPK pathway inhibition in melanoma: resistance three ways.* *Biochem Soc Trans* (2014). **42**(4): p. 727-32.
131. Nazarian R, H Shi, Q Wang, X Kong, RC Koya, H Lee, Z Chen, MK Lee, N Attar, H Sazegar, T Chodon, SF Nelson, G McArthur, JA Sosman, A Ribas, and RS Lo, *Melanomas acquire resistance to B-RAF(V600E) inhibition by RTK or N-RAS upregulation.* *Nature* (2010). **468**(7326): p. 973-7.
132. Shi H, G Moriceau, X Kong, MK Lee, H Lee, RC Koya, C Ng, T Chodon, RA Scolyer, KB Dahlman, JA Sosman, RF Kefford, GV Long, SF Nelson, A Ribas, and RS Lo,

- Melanoma whole-exome sequencing identifies (V600E)B-RAF amplification-mediated acquired B-RAF inhibitor resistance. Nat Commun* (2012). **3**: p. 724.
133. Poulidakos PI, et al., *RAF inhibitor resistance is mediated by dimerization of aberrantly spliced BRAF(V600E). Nature* (2011). **480**(7377): p. 387-90.
 134. Girotti MR and R Marais, *Deja Vu: EGF receptors drive resistance to BRAF inhibitors. Cancer Discov* (2013). **3**(5): p. 487-90.
 135. Girotti MR, M Pedersen, B Sanchez-Laorden, A Viros, S Turajlic, D Niculescu-Duvaz, A Zambon, J Sinclair, A Hayes, M Gore, P Lorigan, C Springer, J Larkin, C Jorgensen, and R Marais, *Inhibiting EGF receptor or SRC family kinase signaling overcomes BRAF inhibitor resistance in melanoma. Cancer Discov* (2013). **3**(2): p. 158-67.
 136. Shi H, X Kong, A Ribas, and RS Lo, *Combinatorial treatments that overcome PDGFRbeta-driven resistance of melanoma cells to V600EB-RAF inhibition. Cancer Res* (2011). **71**(15): p. 5067-74.
 137. Vergani E, V Vallacchi, S Frigerio, P Deho, P Mondellini, P Perego, G Cassinelli, C Lanzi, MA Testi, L Rivoltini, I Bongarzone, and M Rodolfo, *Identification of MET and SRC activation in melanoma cell lines showing primary resistance to PLX4032. Neoplasia* (2011). **13**(12): p. 1132-42.
 138. Villanueva J, et al., *Acquired resistance to BRAF inhibitors mediated by a RAF kinase switch in melanoma can be overcome by cotargeting MEK and IGF-1R/PI3K. Cancer Cell* (2010). **18**(6): p. 683-95.
 139. Emery CM, KG Vijayendran, MC Zipser, AM Sawyer, L Niu, JJ Kim, C Hatton, R Chopra, PA Oberholzer, MB Karpova, LE MacConaill, J Zhang, NS Gray, WR Sellers, R Dummer, and LA Garraway, *MEK1 mutations confer resistance to MEK and B-RAF inhibition. Proc Natl Acad Sci U S A* (2009). **106**(48): p. 20411-6.
 140. Trunzer K, et al., *Pharmacodynamic effects and mechanisms of resistance to vemurafenib in patients with metastatic melanoma. J Clin Oncol* (2013). **31**(14): p. 1767-74.
 141. Montagut C, SV Sharma, T Shioda, U McDermott, M Ulman, LE Ulkus, D Dias-Santagata, H Stubbs, DY Lee, A Singh, L Drew, DA Haber, and J Settleman, *Elevated CRAF as a potential mechanism of acquired resistance to BRAF inhibition in melanoma. Cancer Res* (2008). **68**(12): p. 4853-61.
 142. Robert C, et al., *Improved overall survival in melanoma with combined dabrafenib and trametinib. N Engl J Med* (2015). **372**(1): p. 30-9.
 143. Flaherty KT, FS Hodi, and DE Fisher, *From genes to drugs: targeted strategies for melanoma. Nat Rev Cancer* (2012). **12**(5): p. 349-61.
 144. Garraway LA, HR Widlund, MA Rubin, G Getz, AJ Berger, S Ramaswamy, R Beroukhi, DA Milner, SR Granter, J Du, C Lee, SN Wagner, C Li, TR Golub, DL Rimm, ML Meyerson, DE Fisher, and WR Sellers, *Integrative genomic analyses identify MITF as a lineage survival oncogene amplified in malignant melanoma. Nature* (2005). **436**(7047): p. 117-22.
 145. Haq R, S Yokoyama, EB Hawryluk, GB Jonsson, DT Frederick, K McHenry, D Porter, TN Tran, KT Love, R Langer, DG Anderson, LA Garraway, LM Duncan, DL Morton, DS Hoon, JA Wargo, JS Song, and DE Fisher, *BCL2A1 is a lineage-specific antiapoptotic melanoma oncogene that confers resistance to BRAF inhibition. Proc Natl Acad Sci U S A* (2013). **110**(11): p. 4321-6.

146. Smith MP, J Ferguson, I Arozarena, R Hayward, R Marais, A Chapman, A Hurlstone, and C Wellbrock, *Effect of SMURF2 targeting on susceptibility to MEK inhibitors in melanoma. J Natl Cancer Inst* (2013). **105**(1): p. 33-46.
147. Fedorenko IV, KH Paraiso, and KS Smalley, *Acquired and intrinsic BRAF inhibitor resistance in BRAF V600E mutant melanoma. Biochem Pharmacol* (2011). **82**(3): p. 201-9.
148. Turajlic S, SJ Furney, G Stamp, S Rana, G Ricken, Y Oduko, G Saturno, C Springer, A Hayes, M Gore, J Larkin, and R Marais, *Whole-genome sequencing reveals complex mechanisms of intrinsic resistance to BRAF inhibition. Ann Oncol* (2014). **25**(5): p. 959-67.
149. Paraiso KH, Y Xiang, VW Rebecca, EV Abel, YA Chen, AC Munko, E Wood, IV Fedorenko, VK Sondak, AR Anderson, A Ribas, MD Palma, KL Nathanson, JM Koomen, JL Messina, and KS Smalley, *PTEN loss confers BRAF inhibitor resistance to melanoma cells through the suppression of BIM expression. Cancer Res* (2011). **71**(7): p. 2750-60.
150. Shao Y and AE Aplin, *Akt3-mediated resistance to apoptosis in B-RAF-targeted melanoma cells. Cancer Res* (2010). **70**(16): p. 6670-81.
151. Gopal YN, W Deng, SE Woodman, K Komurov, P Ram, PD Smith, and MA Davies, *Basal and treatment-induced activation of AKT mediates resistance to cell death by AZD6244 (ARRY-142886) in Braf-mutant human cutaneous melanoma cells. Cancer Res* (2010). **70**(21): p. 8736-47.
152. Wu P and YZ Hu, *PI3K/Akt/mTOR pathway inhibitors in cancer: a perspective on clinical progress. Curr Med Chem* (2010). **17**(35): p. 4326-41.
153. Martini M, E Ciraolo, F Gulluni, and E Hirsch, *Targeting PI3K in Cancer: Any Good News? Front Oncol* (2013). **3**: p. 108.
154. Porta C, C Paglino, and A Mosca, *Targeting PI3K/Akt/mTOR Signaling in Cancer. Front Oncol* (2014). **4**: p. 64.
155. Atefi M, E von Euw, N Attar, C Ng, C Chu, D Guo, R Nazarian, B Chmielowski, JA Glaspy, B Comin-Anduix, PS Mischel, RS Lo, and A Ribas, *Reversing melanoma cross-resistance to BRAF and MEK inhibitors by co-targeting the AKT/mTOR pathway. Plos One* (2011). **6**(12): p. e28973.
156. Deng W, YN Gopal, A Scott, G Chen, SE Woodman, and MA Davies, *Role and therapeutic potential of PI3K-mTOR signaling in de novo resistance to BRAF inhibition. Pigment Cell Melanoma Res* (2012). **25**(2): p. 248-58.
157. Jiang CC, F Lai, RF Thorne, F Yang, H Liu, P Hersey, and XD Zhang, *MEK-independent survival of B-RAFV600E melanoma cells selected for resistance to apoptosis induced by the RAF inhibitor PLX4720. Clin Cancer Res* (2011). **17**(4): p. 721-30.
158. Marone R, D Erhart, AC Mertz, T Bohnacker, C Schnell, V Cmiljanovic, F Stauffer, C Garcia-Echeverria, B Giese, SM Maira, and MP Wymann, *Targeting melanoma with dual phosphoinositide 3-kinase/mammalian target of rapamycin inhibitors. Mol Cancer Res* (2009). **7**(4): p. 601-13.
159. Perna D, FA Karreth, AG Rust, PA Perez-Mancera, M Rashid, F Iorio, C Alifrangis, MJ Arends, MW Bosenberg, G Bollag, DA Tuveson, and DJ Adams, *BRAF inhibitor resistance mediated by the AKT pathway in an oncogenic BRAF mouse melanoma model. Proc Natl Acad Sci U S A* (2015). **112**(6): p. E536-45.

160. Sanchez-Hernandez I, P Baquero, L Calleros, and A Chiloehes, *Dual inhibition of (V600E)BRAF and the PI3K/AKT/mTOR pathway cooperates to induce apoptosis in melanoma cells through a MEK-independent mechanism. Cancer Lett* (2012). **314**(2): p. 244-55.
161. Yang JY, CJ Chang, W Xia, Y Wang, KK Wong, JA Engelman, Y Du, M Andreeff, GN Hortobagyi, and MC Hung, *Activation of FOXO3a is sufficient to reverse mitogen-activated protein/extracellular signal-regulated kinase kinase inhibitor chemoresistance in human cancer. Cancer Res* (2010). **70**(11): p. 4709-18.
162. Infante JR, KP Papadopoulos, JC Bendell, A Patnaik, HA Burris, 3rd, D Rasco, SF Jones, L Smith, DS Cox, M Durante, KM Bellew, JJ Park, NT Le, and AW Tolcher, *A phase Ib study of trametinib, an oral Mitogen-activated protein kinase kinase (MEK) inhibitor, in combination with gemcitabine in advanced solid tumours. Eur J Cancer* (2013). **49**(9): p. 2077-85.
163. Shimizu T, AW Tolcher, KP Papadopoulos, M Beeram, DW Rasco, LS Smith, S Gunn, L Smetzer, TA Mays, B Kaiser, MJ Wick, C Alvarez, A Cavazos, GL Mangold, and A Patnaik, *The clinical effect of the dual-targeting strategy involving PI3K/AKT/mTOR and RAS/MEK/ERK pathways in patients with advanced cancer. Clin Cancer Res* (2012). **18**(8): p. 2316-25.
164. Kwong LN and MA Davies, *Navigating the Therapeutic Complexity of PI3K Pathway Inhibition in Melanoma. Clinical Cancer Research* (2013). **19**(19): p. 5310-5319.
165. Kim DH, DD Sarbassov, SM Ali, JE King, RR Latek, H Erdjument-Bromage, P Tempst, and DM Sabatini, *MTOR interacts with Raptor to form a nutrient-sensitive complex that signals to the cell growth machinery. Cell* (2002). **110**(2): p. 163-175.
166. Shi Y, H Yan, P Frost, J Gera, and A Lichtenstein, *Mammalian target of rapamycin inhibitors activate the AKT kinase in multiple myeloma cells by up-regulating the insulin-like growth factor receptor/insulin receptor substrate-1/phosphatidylinositol 3-kinase cascade. Mol Cancer Ther* (2005). **4**(10): p. 1533-40.
167. O'Reilly KE, F Rojo, QB She, D Solit, GB Mills, D Smith, H Lane, F Hofmann, DJ Hicklin, DL Ludwig, J Baselga, and N Rosen, *mTOR inhibition induces upstream receptor tyrosine kinase signaling and activates Akt. Cancer Res* (2006). **66**(3): p. 1500-8.
168. Carracedo A, L Ma, J Teruya-Feldstein, F Rojo, L Salmena, A Alimonti, A Egia, AT Sasaki, G Thomas, SC Kozma, A Papa, C Nardella, LC Cantley, J Baselga, and PP Pandolfi, *Inhibition of mTORC1 leads to MAPK pathway activation through a PI3K-dependent feedback loop in human cancer. J Clin Invest* (2008). **118**(9): p. 3065-74.
169. Soares HP, Y Ni, K Kisfalvi, J Sinnott-Smith, and E Rozengurt, *Different patterns of Akt and ERK feedback activation in response to rapamycin, active-site mTOR inhibitors and metformin in pancreatic cancer cells. Plos One* (2013). **8**(2): p. e57289.
170. Davies MA, et al., *Phase I study of the combination of sorafenib and temsirolimus in patients with metastatic melanoma. Clin Cancer Res* (2012). **18**(4): p. 1120-8.
171. Margolin K, J Longmate, T Baratta, T Synold, S Christensen, J Weber, T Gajewski, I Quirt, and JH Doroshow, *CCI-779 in metastatic melanoma: a phase II trial of the California Cancer Consortium. Cancer* (2005). **104**(5): p. 1045-8.
172. Margolin KA, J Moon, LE Flaherty, CD Lao, WL Akerley, 3rd, M Othus, JA Sosman, JM Kirkwood, and VK Sondak, *Randomized phase II trial of sorafenib with temsirolimus*

- or tipifarnib in untreated metastatic melanoma (S0438). *Clin Cancer Res* (2012). **18**(4): p. 1129-37.
173. Sarbassov DD, SM Ali, DH Kim, DA Guertin, RR Latek, H Erdjument-Bromage, P Tempst, and DM Sabatini, *Rictor, a novel binding partner of mTOR, defines a rapamycin-insensitive and raptor-independent pathway that regulates the cytoskeleton*. *Current Biology* (2004). **14**(14): p. 1296-1302.
174. Scortegagna M, C Ruller, Y Feng, R Lazova, H Kluger, JL Li, SK De, R Rickert, M Pellecchia, M Bosenberg, and ZA Ronai, *Genetic inactivation or pharmacological inhibition of Pdk1 delays development and inhibits metastasis of Braf(V600E)::Pten(-/-) melanoma*. *Oncogene* (2014). **33**(34): p. 4330-9.
175. Chakrabarty A, V Sanchez, MG Kuba, C Rinehart, and CL Arteaga, *Feedback upregulation of HER3 (ErbB3) expression and activity attenuates antitumor effect of PI3K inhibitors*. *Proc Natl Acad Sci U S A* (2012). **109**(8): p. 2718-23.
176. Chandarlapaty S, A Sawai, M Scaltriti, V Rodrik-Outmezguine, O Grbovic-Huezo, V Serra, PK Majumder, J Baselga, and N Rosen, *AKT inhibition relieves feedback suppression of receptor tyrosine kinase expression and activity*. *Cancer Cell* (2011). **19**(1): p. 58-71.
177. Serra V, M Scaltriti, L Prudkin, PJ Eichhorn, YH Ibrahim, S Chandarlapaty, B Markman, O Rodriguez, M Guzman, S Rodriguez, M Gili, M Russillo, JL Parra, S Singh, J Arribas, N Rosen, and J Baselga, *PI3K inhibition results in enhanced HER signaling and acquired ERK dependency in HER2-overexpressing breast cancer*. *Oncogene* (2011). **30**(22): p. 2547-57.
178. Aziz SA, LB Jilaveanu, C Zito, RL Camp, DL Rimm, P Conrad, and HM Kluger, *Vertical targeting of the phosphatidylinositol-3 kinase pathway as a strategy for treating melanoma*. *Clin Cancer Res* (2010). **16**(24): p. 6029-39.
179. Lemech C, J Infante, and HT Arkenau, *Combination molecularly targeted drug therapy in metastatic melanoma: progress to date*. *Drugs* (2013). **73**(8): p. 767-77.
180. Khan MOF and CL Ramos, *An Update on BRAF Inhibitors and Other New Molecular Targets for the Treatment of Malignant Melanoma of the Skin*. *Clinical Medicine Insights: Dermatology* (2013). **2013**(6): p. 1-7.
181. Vadas O, JE Burke, X Zhang, A Berndt, and RL Williams, *Structural basis for activation and inhibition of class I phosphoinositide 3-kinases*. *Sci Signal* (2011). **4**(195): p. re2.
182. Dow LE, PK Premririt, J Zuber, C Fellmann, K McJunkin, C Miething, Y Park, RA Dickins, GJ Hannon, and SW Lowe, *A pipeline for the generation of shRNA transgenic mice*. *Nature Protocols* (2012). **7**(2): p. 374-93.
183. Chang K, SJ Elledge, and GJ Hannon, *Lessons from Nature: microRNA-based shRNA libraries*. *Nat Methods* (2006). **3**(9): p. 707-14.
184. Hampf M and M Gossen, *A protocol for combined Photinus and Renilla luciferase quantification compatible with protein assays*. *Anal Biochem* (2006). **356**(1): p. 94-9.
185. Dyer BW, FA Ferrer, DK Klinedinst, and R Rodriguez, *A noncommercial dual luciferase enzyme assay system for reporter gene analysis*. *Anal Biochem* (2000). **282**(1): p. 158-61.
186. Thermo Fisher Scientific I. *Thermo Scientific Inducible TRIPZ Lentiviral shRNA*. Available from: http://itd.unair.ac.id/files/thermoscientific/pTRIPZ%20Lentiviral%20shRNA_Technical%20Manual.pdf.

187. Bassik MC, RJ Lebbink, LS Churchman, NT Ingolia, W Patena, EM LeProust, M Schuldiner, JS Weissman, and MT McManus, *Rapid creation and quantitative monitoring of high coverage shRNA libraries*. *Nat Methods* (2009). **6**(6): p. 443-5.
188. Li L, X Lin, A Khvorova, SW Fesik, and Y Shen, *Defining the optimal parameters for hairpin-based knockdown constructs*. *RNA* (2007). **13**(10): p. 1765-74.
189. Taxman DJ, LR Livingstone, J Zhang, BJ Conti, HA Iocca, KL Williams, JD Lich, JP Ting, and W Reed, *Criteria for effective design, construction, and gene knockdown by shRNA vectors*. *BMC Biotechnol* (2006). **6**: p. 7.
190. Stegmeier F, G Hu, RJ Rickles, GJ Hannon, and SJ Elledge, *A lentiviral microRNA-based system for single-copy polymerase II-regulated RNA interference in mammalian cells*. *Proc Natl Acad Sci U S A* (2005). **102**(37): p. 13212-7.
191. Wiznerowicz M, J Szulc, and D Trono, *Tuning silence: conditional systems for RNA interference*. *Nat Methods* (2006). **3**(9): p. 682-8.
192. Geiling B, G Vandal, AR Posner, A de Bruyns, KL Dutchak, S Garnett, and D Dankort, *A modular lentiviral and retroviral construction system to rapidly generate vectors for gene expression and gene knockdown in vitro and in vivo*. *PLoS One* (2013). **8**(10): p. e76279.
193. Tarun SZ, Jr. and AB Sachs, *Association of the yeast poly(A) tail binding protein with translation initiation factor eIF-4G*. *Embo J* (1996). **15**(24): p. 7168-77.
194. Le H, RL Tanguay, ML Balasta, CC Wei, KS Browning, AM Metz, DJ Goss, and DR Gallie, *Translation initiation factors eIF-iso4G and eIF-4B interact with the poly(A)-binding protein and increase its RNA binding activity*. *J Biol Chem* (1997). **272**(26): p. 16247-55.
195. Hartley JL, GF Temple, and MA Brasch, *DNA cloning using in vitro site-specific recombination*. *Genome Res* (2000). **10**(11): p. 1788-95.
196. Nash HA, K Mizuuchi, LW Enquist, and RA Weisberg, *Strand exchange in lambda integrative recombination: genetics, biochemistry, and models*. *Cold Spring Harb Symp Quant Biol* (1981). **45 Pt 1**: p. 417-28.
197. Sasaki Y, T Sone, S Yoshida, K Yahata, J Hotta, JD Chesnut, T Honda, and F Imamoto, *Evidence for high specificity and efficiency of multiple recombination signals in mixed DNA cloning by the Multisite Gateway system*. *J Biotechnol* (2004). **107**(3): p. 233-43.
198. Olson A, N Sheth, JS Lee, G Hannon, and R Sachidanandam, *RNAi Codex: a portal/database for short-hairpin RNA (shRNA) gene-silencing constructs*. *Nucleic Acids Res* (2006). **34**(Database issue): p. D153-7.
199. Qin JY, L Zhang, KL Clift, I Hulur, AP Xiang, BZ Ren, and BT Lahn, *Systematic comparison of constitutive promoters and the doxycycline-inducible promoter*. *Plos One* (2010). **5**(5): p. e10611.
200. Cruz S. *PI 3-kinase p110 γ (h): 293T Lysate: sc-115447* Access Date: January 14. Available from: <http://www.scbt.com/datasheet-115447-pi-3-kinase-p110gamma-h-293t-lysate.html>.
201. Aksoy E, W Vanden Berghe, S Detienne, Z Amraoui, KA Fitzgerald, G Haegeman, M Goldman, and F Willems, *Inhibition of phosphoinositide 3-kinase enhances TRIF-dependent NF-kappa B activation and IFN-beta synthesis downstream of Toll-like receptor 3 and 4*. *Eur J Immunol* (2005). **35**(7): p. 2200-9.
202. Manjunath N, H Wu, S Subramanya, and P Shankar, *Lentiviral delivery of short hairpin RNAs*. *Adv Drug Deliv Rev* (2009). **61**(9): p. 732-45.

203. Kennedy SG, AJ Wagner, SD Conzen, J Jordan, A Bellacosa, PN Tschlis, and N Hay, *The PI 3-kinase/Akt signaling pathway delivers an anti-apoptotic signal. Genes Dev* (1997). **11**(6): p. 701-13.
204. Greger JG, SD Eastman, V Zhang, MR Bleam, AM Hughes, KN Smitheman, SH Dickerson, SG Laquerre, L Liu, and TM Gilmer, *Combinations of BRAF, MEK, and PI3K/mTOR inhibitors overcome acquired resistance to the BRAF inhibitor GSK2118436 dabrafenib, mediated by NRAS or MEK mutations. Mol Cancer Ther* (2012). **11**(4): p. 909-20.
205. Smalley KS, NK Haass, PA Brafford, M Lioni, KT Flaherty, and M Herlyn, *Multiple signaling pathways must be targeted to overcome drug resistance in cell lines derived from melanoma metastases. Mol Cancer Ther* (2006). **5**(5): p. 1136-44.
206. Gossen M, S Freundlieb, G Bender, G Muller, W Hillen, and H Bujard, *Transcriptional activation by tetracyclines in mammalian cells. Science* (1995). **268**(5218): p. 1766-9.
207. Fellmann C, T Hoffmann, V Sridhar, B Hopfgartner, M Muhar, M Roth, DY Lai, IA Barbosa, JS Kwon, Y Guan, N Sinha, and J Zuber, *An optimized microRNA backbone for effective single-copy RNAi. Cell Rep* (2013). **5**(6): p. 1704-13.
208. Mali P, KM Esvelt, and GM Church, *Cas9 as a versatile tool for engineering biology. Nat Methods* (2013). **10**(10): p. 957-63.
209. Mali P, L Yang, KM Esvelt, J Aach, M Guell, JE DiCarlo, JE Norville, and GM Church, *RNA-guided human genome engineering via Cas9. Science* (2013). **339**(6121): p. 823-6.
210. Ran FA, PD Hsu, J Wright, V Agarwala, DA Scott, and F Zhang, *Genome engineering using the CRISPR-Cas9 system. Nature Protocols* (2013). **8**(11): p. 2281-308.
211. Shalem O, NE Sanjana, E Hartenian, X Shi, DA Scott, TS Mikkelsen, D Heckl, BL Ebert, DE Root, JG Doench, and F Zhang, *Genome-scale CRISPR-Cas9 knockout screening in human cells. Science* (2014). **343**(6166): p. 84-7.
212. Cronin J, XY Zhang, and J Reiser, *Altering the tropism of lentiviral vectors through pseudotyping. Curr Gene Ther* (2005). **5**(4): p. 387-98.
213. Kobinger GP, S Deng, JP Louboutin, M Vatamaniuk, F Matschinsky, JF Markmann, SE Raper, and JM Wilson, *Transduction of human islets with pseudotyped lentiviral vectors. Hum Gene Ther* (2004). **15**(2): p. 211-9.
214. Sena-Estevés M, JC Tebbets, S Steffens, T Crombleholme, and AW Flake, *Optimized large-scale production of high titer lentivirus vector pseudotypes. J Virol Methods* (2004). **122**(2): p. 131-9.
215. Watson DJ, GP Kobinger, MA Passini, JM Wilson, and JH Wolfe, *Targeted transduction patterns in the mouse brain by lentivirus vectors pseudotyped with VSV, Ebola, Mokola, LCMV, or MuLV envelope proteins. Mol Ther* (2002). **5**(5 Pt 1): p. 528-37.
216. Zhang XY, VF La Russa, and J Reiser, *Transduction of bone-marrow-derived mesenchymal stem cells by using lentivirus vectors pseudotyped with modified RD114 envelope glycoproteins. J Virol* (2004). **78**(3): p. 1219-29.
217. Ricks DM, R Kutner, XY Zhang, DA Welsh, and J Reiser, *Optimized lentiviral transduction of mouse bone marrow-derived mesenchymal stem cells. Stem Cells Dev* (2008). **17**(3): p. 441-50.
218. Kutner RH, XY Zhang, and J Reiser, *Production, concentration and titration of pseudotyped HIV-1-based lentiviral vectors. Nat Protoc* (2009). **4**(4): p. 495-505.

219. Segura MM, A Garnier, Y Durocher, H Coelho, and A Kamen, *Production of lentiviral vectors by large-scale transient transfection of suspension cultures and affinity chromatography purification. Biotechnol Bioeng* (2007). **98**(4): p. 789-99.
220. Ahler E, WJ Sullivan, A Cass, D Braas, AG York, SJ Bensinger, TG Graeber, and HR Christofk, *Doxycycline Alters Metabolism and Proliferation of Human Cell Lines. Plos One* (2013). **8**(5).
221. Xie J, A Nair, and TW Hermiston, *A comparative study examining the cytotoxicity of inducible gene expression system ligands in different cell types. Toxicology in Vitro* (2008). **22**(1): p. 261-266.
222. Zakrzewska KE, A Samluk, KD Pluta, and DG Pijanowska, *Evaluation of the effects of antibiotics on cytotoxicity of EGFP and DsRed2 fluorescent proteins used for stable cell labeling. Acta Biochim Pol* (2014). **61**(4): p. 809-13.
223. Fruman DA and C Rommel, *PI3K and cancer: lessons, challenges and opportunities. Nat Rev Drug Discov* (2014). **13**(2): p. 140-56.
224. Kwong LN and MA Davies, *Navigating the therapeutic complexity of PI3K pathway inhibition in melanoma. Clin Cancer Res* (2013). **19**(19): p. 5310-9.
225. Maira SM, F Stauffer, J Brueggen, P Furet, C Schnell, C Fritsch, S Brachmann, P Chene, A De Pover, K Schoemaker, D Fabbro, D Gabriel, M Simonen, L Murphy, P Finan, W Sellers, and C Garcia-Echeverria, *Identification and characterization of NVP-BEZ235, a new orally available dual phosphatidylinositol 3-kinase/mammalian target of rapamycin inhibitor with potent in vivo antitumor activity. Mol Cancer Ther* (2008). **7**(7): p. 1851-63.
226. Sturm OE, R Orton, J Grindlay, M Birtwistle, V Vyshemirsky, D Gilbert, M Calder, A Pitt, B Kholodenko, and W Kolch, *The mammalian MAPK/ERK pathway exhibits properties of a negative feedback amplifier. Sci Signal* (2010). **3**(153): p. ra90.
227. Schayowitz A, G Bertenshaw, E Jeffries, T Schatz, J Cotton, J Villanueva, M Herlyn, C Krepler, A Vultur, W Xu, GH Yu, L Schuchter, and DP Clark, *Functional profiling of live melanoma samples using a novel automated platform. Plos One* (2012). **7**(12): p. e52760.
228. Stones CJ, JE Kim, WR Joseph, E Leung, ES Marshall, GJ Finlay, AN Shelling, and BC Baguley, *Comparison of responses of human melanoma cell lines to MEK and BRAF inhibitors. Front Genet* (2013). **4**: p. 66.
229. Yadav V, X Zhang, J Liu, S Estrem, S Li, XQ Gong, S Buchanan, JR Henry, JJ Starling, and SB Peng, *Reactivation of mitogen-activated protein kinase (MAPK) pathway by FGF receptor 3 (FGFR3)/Ras mediates resistance to vemurafenib in human B-RAF V600E mutant melanoma. J Biol Chem* (2012). **287**(33): p. 28087-98.
230. Logan AC, SJ Nightingale, DL Haas, GJ Cho, KA Pepper, and DB Kohn, *Factors influencing the titer and infectivity of lentiviral vectors. Hum Gene Ther* (2004). **15**(10): p. 976-88.
231. Zhang B, P Metharom, H Jullie, KA Ellem, G Cleghorn, MJ West, and MQ Wei, *The significance of controlled conditions in lentiviral vector titration and in the use of multiplicity of infection (MOI) for predicting gene transfer events. Genet Vaccines Ther* (2004). **2**(1): p. 6.
232. Jackson AL, SR Bartz, J Schelter, SV Kobayashi, J Burchard, M Mao, B Li, G Cavet, and PS Linsley, *Expression profiling reveals off-target gene regulation by RNAi. Nat Biotechnol* (2003). **21**(6): p. 635-7.

233. Fedorov Y, EM Anderson, A Birmingham, A Reynolds, J Karpilow, K Robinson, D Leake, WS Marshall, and A Khvorova, *Off-target effects by siRNA can induce toxic phenotype*. *RNA* (2006). **12**(7): p. 1188-96.
234. Lin X, X Ruan, MG Anderson, JA McDowell, PE Kroeger, SW Fesik, and Y Shen, *siRNA-mediated off-target gene silencing triggered by a 7 nt complementation*. *Nucleic Acids Res* (2005). **33**(14): p. 4527-35.
235. Grimm D, *The dose can make the poison: lessons learned from adverse in vivo toxicities caused by RNAi overexpression*. *Silence* (2011). **2**: p. 8.
236. Cronin J, XY Zhang, and J Reiser, *Altering the tropism of lentiviral vectors through pseudotyping (vol 5, pg 387, 2005)*. *Current Gene Therapy* (2005). **5**(5): p. 531-531.
237. Cronin J, XY Zhang, and J Reiser, *Altering the tropism of lentiviral vectors through pseudotyping*. *Current Gene Therapy* (2005). **5**(4): p. 387-398.
238. Kobinger GP, SP Deng, JP Louboutin, M Vatamaniuk, F Matschinsky, JF Markmann, SE Raper, and JM Wilson, *Transduction of human islets with pseudotyped lentiviral vectors*. *Human Gene Therapy* (2004). **15**(2): p. 211-219.
239. Watson DJ, GP Kobinger, MA Passini, JM Wilson, and JH Wolfe, *Targeted transduction patterns in the mouse brain by lentivirus vectors pseudotyped with VSV, Ebola, Mokola, LCMV, or MuLV envelope proteins*. *Molecular Therapy* (2002). **5**(5): p. 528-537.
240. Zhang XY, VF La Russa, and J Reiser, *Transduction of bone-marrow-derived mesenchymal stem cells by using lentivirus vectors pseudotyped with modified RD114 envelope glycoproteins*. *Journal of Virology* (2004). **78**(3): p. 1219-1229.
241. Cloyd MW and WS Lynn, *Perturbation of host-cell membrane is a primary mechanism of HIV cytopathology*. *Virology* (1991). **181**(2): p. 500-11.
242. Lynn WS, A Tweedale, and MW Cloyd, *Human immunodeficiency virus (HIV-1) cytotoxicity: perturbation of the cell membrane and depression of phospholipid synthesis*. *Virology* (1988). **163**(1): p. 43-51.
243. Danthi P, *Enter the kill zone: initiation of death signaling during virus entry*. *Virology* (2011). **411**(2): p. 316-24.
244. Cimarelli A, S Sandin, S Hoglund, and J Luban, *Basic residues in human immunodeficiency virus type 1 nucleocapsid promote virion assembly via interaction with RNA*. *Journal of Virology* (2000). **74**(7): p. 3046-3057.
245. Lingappa JR, MA Newman, KC Klein, and JE Dooher, *Comparing capsid assembly of primate lentiviruses and hepatitis B virus using cell-free systems*. *Virology* (2005). **333**(1): p. 114-123.
246. Kim SH, HJ Jun, SI Jang, and JC You, *The Determination of Importance of Sequences Neighboring the Psi Sequence in Lentiviral Vector Transduction and Packaging Efficiency*. *Plos One* (2012). **7**(11).
247. Jere D, HL Jiang, R Arote, YK Kim, YJ Choi, MH Cho, T Akaike, and CS Chot, *Degradable polyethylenimines as DNA and small interfering RNA carriers*. *Expert Opinion on Drug Delivery* (2009). **6**(8): p. 827-834.
248. Lu H, Y Dai, L Lv, and H Zhao, *Chitosan-graft-polyethylenimine/DNA nanoparticles as novel non-viral gene delivery vectors targeting osteoarthritis*. *PLoS One* (2014). **9**(1): p. e84703.
249. Wang YQ, J Su, F Wu, P Lu, LF Yuan, WE Yuan, J Sheng, and T Jin, *Biscarbamate cross-linked polyethylenimine derivative with low molecular weight, low cytotoxicity, and high efficiency for gene delivery*. *Int J Nanomedicine* (2012). **7**: p. 693-704.

250. Balazs DA and W Godbey, *Liposomes for use in gene delivery*. *J Drug Deliv* (2011). **2011**: p. 326497.
251. Sandrin V, B Boson, P Salmon, W Gay, D Negre, R Le Grand, D Trono, and FL Cosset, *Lentiviral vectors pseudotyped with a modified RD114 envelope glycoprotein show increased stability in sera and augmented transduction of primary lymphocytes and CD34+ cells derived from human and nonhuman primates*. *Blood* (2002). **100**(3): p. 823-32.
252. Millington M, A Arndt, M Boyd, T Applegate, and S Shen, *Towards a Clinically Relevant Lentiviral Transduction Protocol for Primary Human CD34(+) Hematopoietic Stem/Progenitor Cells*. *Plos One* (2009). **4**(7).
253. Uchida N, MM Hsieh, J Hayakawa, C Madison, KN Washington, and JF Tisdale, *Optimal conditions for lentiviral transduction of engrafting human CD34(+) cells*. *Gene Therapy* (2011). **18**(11): p. 1078-1086.
254. Valtink M, L Knels, N Stanke, K Engelmann, RHW Funk, and D Lindemann, *Overexpression of Human HMW FGF-2 but Not LMW FGF-2 Reduces the Cytotoxic Effect of Lentiviral Gene Transfer in Human Corneal Endothelial Cells*. *Investigative Ophthalmology & Visual Science* (2012). **53**(6): p. 3207-3214.
255. Hackl H, A Rommer, TA Konrad, C Nassimbeni, and R Wieser, *Tetracycline regulator expression alters the transcriptional program of mammalian cells*. *Plos One* (2010). **5**(9): p. e13013.
256. Bryja V, J Pachernik, L Kubala, A Hampl, and P Dvorak, *The reverse tetracycline-controlled transactivator rtTA2s-S2 is toxic in mouse embryonic stem cells*. *Reprod Nutr Dev* (2003). **43**(6): p. 477-86.
257. Perl AK, L Zhang, and JA Whitsett, *Conditional expression of genes in the respiratory epithelium in transgenic mice: cautionary notes and toward building a better mouse trap*. *Am J Respir Cell Mol Biol* (2009). **40**(1): p. 1-3.
258. Benabdellah K, M Cobo, P Munoz, MG Toscano, and F Martin, *Development of an all-in-one lentiviral vector system based on the original TetR for the easy generation of Tet-ON cell lines*. *Plos One* (2011). **6**(8): p. e23734.
259. Baron U, M Gossen, and H Bujard, *Tetracycline-controlled transcription in eukaryotes: novel transactivators with graded transactivation potential*. *Nucleic Acids Res* (1997). **25**(14): p. 2723-9.
260. Zhou J, J Lin, C Zhou, X Deng, and B Xia, *Cytotoxicity of red fluorescent protein DsRed is associated with the suppression of Bcl-xL translation*. *FEBS Lett* (2011). **585**(5): p. 821-7.

7. Appendix

7.1. Optimizing pTREG shRNA Knockdown

Soon after starting to use pTREG-mediated shRNA expression in melanoma cells, it became evident that it would be more difficult to successfully target some of the PTEN Proximal genes than originally thought based on the preliminary experiments done in the 293T cells. I initially chose to target a subset of the PTEN Proximal genes, the AKT isoforms, in experiments wherein I would induce AKT shRNA expression in melanoma pTREG shRNA cells with doxycycline for several days and count the number of cells at the end point of doxycycline induction. By comparing cell counts between + and – doxycycline samples, I could assess if knockdown of any of the AKT isoforms had an effect on overall cell number (called “cell counting assays” from here on). Since I needed to elucidate the role of each of the PTEN proximal genes on malignancy in several BRAF^{V600E} melanoma cell lines, these cell counting assays were to serve the purpose of a medium/high- throughput method to screen each target for its potential role in sustaining proliferation and viability. Unfortunately, with the experimental conditions used for these initial assays, doxycycline treatment appeared to reduce cell number even when using a non-targeting shRNA control, Also, I was unable to achieve suitable levels of knockdown for AKT2 and AKT3 in some of the melanoma cell lines. Once these issues with the pTREG system were realized, I pursued many avenues to try to resolve the problems surrounding proper controls and insufficient knockdown. Efforts to improve pTREG-mediated shRNA expression are discussed in detail in the following sections.

7.1.1. Insufficient Knockdown with pTREG

Initially, I chose to do the pTREG shRNA cell counting assays with two BRAF^{V600E}/PTEN mutant cell lines, WM9 and WM278 melanoma cells. These cells were transduced with a 1:1 mix of unconcentrated lentivirus to culture media, as was usually the procedure for other lentiviral infections performed in the lab. After this first set of infections, it became apparent that even though the same volume of each pTREG shRNA virus was being used to do the infections, expression levels of the lentiviral insert differed between the AKT1, AKT2, and AKT3 shRNA-expressing cells (as visualized by accompanying doxycycline-induced

expression of TurboRFP, not shown). This was most likely due to differences in lentiviral titer between the pTREG shRNA viruses resulting in varying infection efficiencies. Although virus producing 293T cells are initially transfected with a standard amount of lentiviral DNA for virus production, invariably viral titer can differ between viral preparations as a result of differences in such things as quality of the DNA preparations, inoculum volume of the vector, and producer cell number [230, 231]. Variable levels of RNA interference (i.e shRNA or siRNA) can cause variable degrees off-target effects including phenotypic changes (e.g. changes in cell viability) [17, 232] [233-235]. To avoid the potentially confounding results of different degrees of off-target shRNA effects in assessing knockdown phenotype, I decided to infect cells at the same multiplicity of infection (MOI) to reduce variability in shRNA expression levels.

For the first round of transductions done at a standardized MOI, I transduced cells with unconcentrated pTREG AKT shRNA lentiviruses at an MOI of 1. To do so, pTREG shRNA lentiviruses had to be titered to know the exact concentration of transducing viral units of each viral preparation. For the titration, 293T cells were infected with serial dilutions of lentivirus and then subjected to puromycin selection. Viral titer was calculated by counting crystal violet stained colonies at the end point of puromycin selection. Using the titer data, melanoma cells were subsequently infected with a standard amount of infectious units to infect cells at a standard MOI of 1. Successfully transduced melanoma cells were selected for using puromycin and then split evenly into two separate wells to either serve as the doxycycline-free control (“-DOX”) or doxycycline-treated sample (“+DOX”). After five days of shRNA expression induction with doxycycline, neither the AKT2 nor AKT3 proteins were knocked down in either of the WM9 or WM278 cell lines (Figure 7.1).

I considered many reasons for why knockdown was not achieved under these experimental conditions. As indicated by TurboRFP expression, similar levels of each AKT shRNA should have been expressed (Figure 7.1B). This suggests that unsuccessful knockdown could be the result of overwhelming levels of mRNA and/or protein. Perhaps mRNA and/or protein for AKT2 and AKT3 is more stable or produced at higher levels than AKT1, thus potentially requiring higher levels of shRNA to target AKT2 and AKT3 mRNA more effectively or an extended period of treatment time with doxycycline to ensure enough time for degradation of existing protein. It is possible that if the duration of doxycycline-induction time was extended, suitable knockdown could be achieved by the end-point of the assay. Another possibility is that

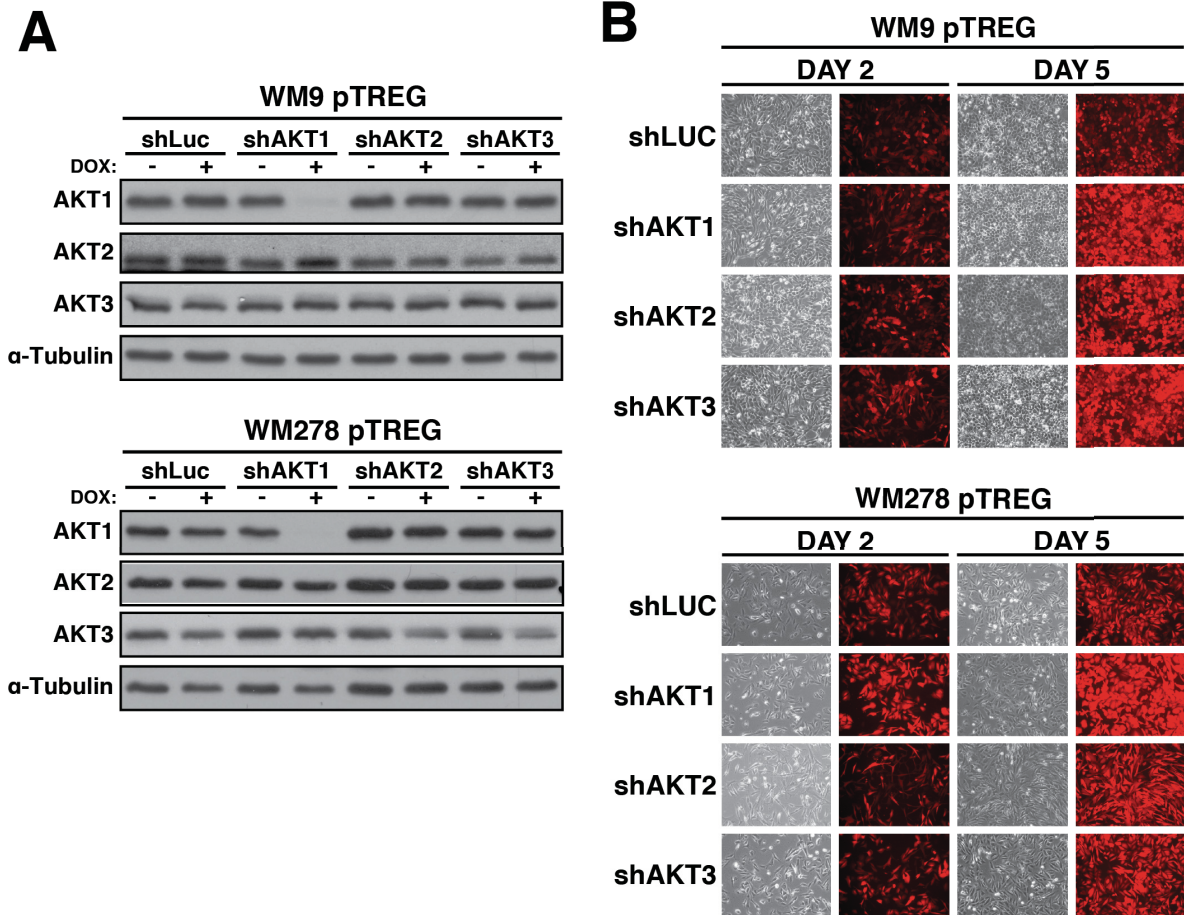


Figure 7.1. pTREG-mediated knockdown in melanoma cells.(A) Western blot analysis of WM9 and WM278 pTREG AKT shRNA cells after 5 days of treatment with doxycycline (1 μ g/mL). (B) TurboRFP expression in WM9 and WM279 pTREG AKT shRNA cells after two and five days of treatment with doxycycline.

AKT2 and *AKT3* are transcribed at a faster/more frequent rate creating a pool of mRNA that is too great for the amount of shRNA produced to target effectively.

Although lengthening shRNA-induction time could potentially alleviate the issue of insufficient protein knockdown, this course of action might not be optimal for future experimental set-ups. If target knockdown elicits a biological response (e.g. cell death), it would be preferable for knockdown to occur more immediately after doxycycline induction, thus allowing me to assay for this response soon after shRNA expression has been turned on. This would be more convenient for experimental design as it would allow for assays to be completed in a more time efficient manner. Therefore, I first tried to improve pTREG-mediated knockdown

by means that would essentially result in higher levels of shRNA expression. Initially, I attempted to produce more substantial shRNA levels by infecting melanoma cells at a higher MOI with the pTREG shRNA lentivirus. A higher MOI should generate more pTREG shRNA integration events per cell and as a result, should translate to higher levels of shRNA expression upon doxycycline induction. Carrying out infections at higher MOIs proved to be more difficult than initially anticipated because of issues that arose regarding cytotoxicity of lentiviral infections on melanoma cells. I had previously been able to infect 293T and A375 cells with unconcentrated pLEG lentivirus, obtaining efficient target knockdown without any viral toxicity (Figure 3.6). Additionally, preliminary infections of 293T cells with unconcentrated pTREG AKT2 shRNA virus produced no noticeable cell death due to the infections and I successfully obtained sufficient knockdown of AKT2 after induction of shRNA expression with doxycycline in these cells (Figure 3.5). I suspect that toxicity was not an issue when infecting with unconcentrated virus because the viral load (i.e. MOI) was below a toxic threshold or perhaps 293T and A375 cells could be more resilient to viral infection than the melanoma cells I infected thereafter. Also, at this MOI, levels of shRNA expression appeared to be sufficient for target knockdown in these cells. Achieving adequate knockdown could be dependent on how strongly expression is driven from the promoter controlling shRNA expression in different cells types. Indeed, levels of expression produced from the inducible TRE promoter has been shown to vary in different mammalian cell types with levels of expression produced in 293T cells being on the higher end of the spectrum[199]. These issues and the methods I used to try to overcome the cytotoxicity matter will be addressed in the next section (Section 7.1.2). In addition to trying a higher MOI to improve target knockdown, I also experimented with using higher concentrations of doxycycline to induce increased shRNA expression (Section 7.1.3) and using a reportedly optimized version of the miRNA-30 backbone, the miRNA-E cassette, for improved knockdown (Section 3.1.3).

7.1.2. Lentiviral Infection Cytotoxicity

Lentivirus produced for the aforementioned infections was pseudotyped with vesicular stomatitis virus G (VSV-G) glycoprotein envelope. For a host of reasons, VSV-G is the most popular envelope pseudotype used for delivery of lentiviral vectors. VSV-G pseudotyped virus is known to have a broad host-cell range, can produce high viral titers, and confers high infectivity

and high vector particle stability allowing for virus concentration by ultracentrifugation [214, 236]. Indeed, pTREG shRNA lentivirus had to be concentrated by ultracentrifugation to use for infections at higher MOIs, since with unconcentrated virus one would have to use impractically large volumes of virus to accomplish this. Unfortunately, when attempting to infect WM9 melanoma cells at a higher MOI, an MOI of 10, virtually none of the cells survived the infection. Cytotoxicity of infection with VSV-G pseudotyped lentivirus has been previously reported. This cell death response has been observed with many different cell types, especially when infecting with increased viral loads (i.e. higher MOI)[237-240]. A search of the literature revealed that lentiviral infection can culminate in cell death as a result of programmed innate immunity in response to viral entry. Viral entry into a cell can cause “prodeath” signaling as a result of attachment to cell receptors, perturbation of the cell membrane, or other events that occur following membrane penetration (e.g virus uncoating in endosomes, genomic integration, etc.)[241-243].

Because of the cytotoxicity issues associated with transducing with an increased viral load, it was necessary to determine the appropriate MOI at which to transduce melanoma cells in order to produce optimal target knockdown with minimal cytotoxicity. Whilst doing this, I performed lentiviral infections in a manner that would allow me to further explore and attempt to understand the observed cell death post-infection in hopes that my results would reveal a way to perhaps mitigate the cell death response. To this end, I first attempted infection of WM9 and 293T cells with pTREG lentivirus at MOIs of 1, 5, and 10. Infections were done with two different lentiviral preps (pTREG shSCR and pTREG shAKT3), including heat-inactivated versions of each. With these different infection parameters I would be able to shed light on the effect of cell type, MOI, pTREG prep, and inactive virus on the infection cytotoxicity. As expected, cytotoxicity increased with increasing MOI for both cell lines (Figure 7.2A). 293T cells did appear to be more tolerant to infection at higher MOIs than the WM9 cells. For the 293T cells, cells survived after infection at MOI 1, 5, and 10, whereas only the WM9 cells infected at an MOI of 1 survived. This was the first indication that some cells might be variably tolerant to infection with lentivirus than others. This might be governed by variations in susceptibility to the “prodeath” signaling discussed above. Cytotoxicity does not appear to be attributable to shRNA-specific effects since similar cytotoxicities were observed for either of the pTREG shRNA viruses, the non-targeting scramble shRNA (shSCR) and AKT3-targeting

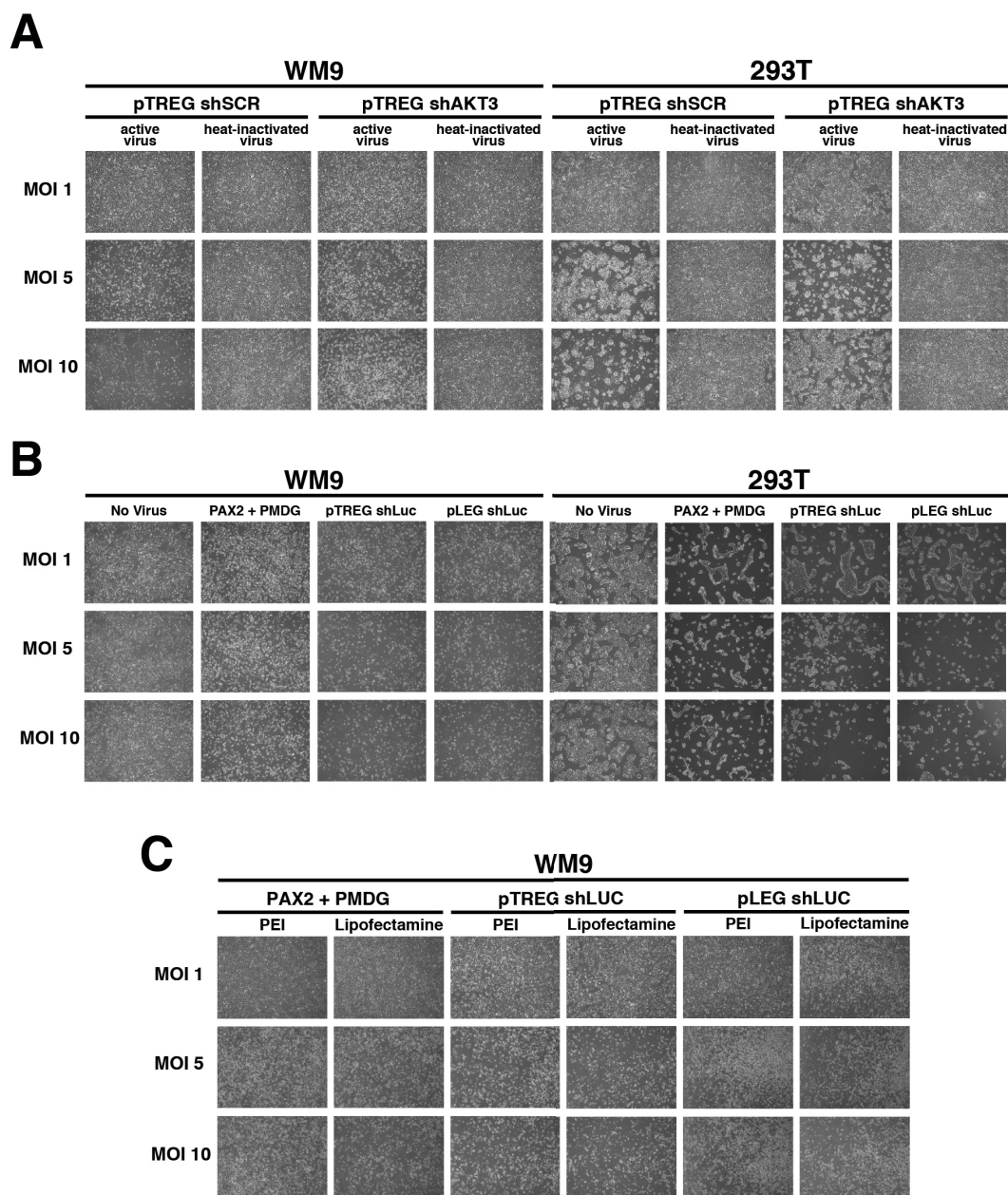


Figure 7.2. Troubleshooting cytotoxicity associated with lentiviral transduction. (A) WM9 and 293T cells infected at MOI 1, 5, and 10 with pTREG shSCR or shAKT3 lentivirus, active and heat-inactivated. (B) WM9 and 293T cells infected at an MOI of 1, 5, and 10 with a no virus control, PAX2/PMDG-produced virus, and pTREG or pLEG shLuc lentivirus. (C) WM9 cells infected at an MOI of 1, 5, and 10 with PAX2/PMDG, pTREG shLuc, or pLEG shLuc virus produced with either PEI or Lipofectamine transfection. All photographs were taken three days after the infection before puromycin selection was started.

shRNA (shAKT3). However, one would not expect an shRNA-specific effect since shRNA expression is inducible and these infections were carried out in doxycycline-free conditions. Of

note is that no cell death was observed in cells “infected” with heat-inactivated samples of the pTREG lentiviruses. Lentiviruses are completely inactivated at high temperatures, in other words, rendered completely incapable of infecting cells. The absence of cell death after exposure to heat-inactivated viral preps strongly suggests that lentiviral entry and/or integration is the cause of the observed lentiviral toxicity, and not simply a response to a toxic component secreted by 293T producer cells or present in 293T cell growth medium that might be concentrated along with the virus in the viral supernatant. However, it could be argued that such a toxic component is also destroyed by the heat-inactivation process, hence the absence of cell death after heat-inactivating the viral prep. To confirm toxicity is due to the lentivirus, I did mock infections with virus-free 293T growth medium prepared and concentrated in the same way as regular lentiviral preps, but without transfection of packaging plasmids and lentiviral vectors. No cell death was observed with this mock infection, ensuring that the culture medium itself is not toxic when concentrated (Figure 7.2B). However, it is possible that the 293T cells could be producing a toxic compound only when producing virus.

To further investigate the root cause of cytotoxicity, cells were infected with viral preps collected from 293T cells transfected with only the packaging plasmids (i.e. PAX2 and PMDG, and no lentiviral vector). According to the literature, virus is in fact assembled in 293T cells transfected with just the packaging plasmids. It has been reported that lentiviral RNA is not required for virion assembly[244, 245]. Non-specific interactions of capsid proteins (Gag, encoded for by PAX2) with endogenous RNA promotes Gag polymerization and virion assembly because it is thought that this RNA is used as scaffolding during assembly. Because of the associations that form between Gag and the endogenous RNA, some of this RNA is incorporated into virions. This is the same method by which lentiviral RNA is packaged, by association with the Gag protein. Although in the case of viral RNA, the lentiviral RNA is preceded by a psi sequence which has a strong affinity to the nucleocapsid (NC) domain of the Gag[246]. This specific interaction is critical for viral RNA packaging and efficient gene delivery[246]. Once released into a recipient cell, unlike lentiviral RNA, non-lentiviral endogenous RNA is non-integrating because it lacks the required 5' and 3' LTR recognized by integrase. With this in mind, I could use virus produced with just the packaging plasmids to infect cells and observe the extent of cell death to determine if it is the process of lentiviral integration into the genome or the process of lentiviral entry that is eliciting the cytotoxic response. These infections were

compared to infections performed with pTREG and pLEG shRNA lentivirus produced and concentrated in parallel. The pLEG lentivirus was included in this experiment to find out if cells are more prone to cell death when infected with the pTREG vector. The extent of cell death resulting from packaging plasmid viral infection was very similar to that resulting from infection with pTREG or pLEG shRNA lentivirus (Figure 7.2B). These suggest that the process of lentiviral entry (including events prior to integration) could be mediating the cell death phenotype rather than the process of lentiviral integration into the genome. If cell death was slightly greater in pTREG or pLEG infected cells I speculated that it was because virion assembly should be more efficient in 293T cells transfected with the packaging plasmids and a lentiviral vector as compared to the packaging plasmids alone. Based on the fact that RNA can be used as scaffolding for the assembly of the viral capsid, and that lentiviral RNA would have more of an affinity for the Gag capsid protein than random endogenous RNA, one could imagine that virion production would be more efficient in cells transfected with packaging plasmids and a lentiviral construct as compared with cells transfected with just the packaging plasmids. Viral RNA would be directed and more available for Gag polymerization scaffolds compared to non-specifically interacting endogenous RNA. If more virus is assembled in the former, this could explain the additional cytotoxicity seen in the pTREG and pLEG infections. These experiments also confirmed that infection cytotoxicity is not a specific to the pTREG lentiviral construct.

In another attempt to reduce cytotoxicity, Lipofectamine was used instead of polyethylenimine (PEI), as the transfecting agent to deliver the packaging plasmids and lentiviral construct into the 293T producer cells. Lipofectamine serves as a cationic lipid carrier for DNA, whereas PEI is a cationic polymer carrier. Because these agents are non-degradable, they can bioaccumulate resulting in cytotoxicity[247-250]. Out of concern that residual PEI was differentially affecting the virus production process or concentrating along with the virus in such a way that would be more toxic to the recipient cells during transduction, melanoma cells were transduced with concentrated lentivirus produced using Lipofectamine transfection. Unfortunately virus produced with Lipofectamine transfection proved to be just as cytotoxic as that produced with PEI (Figure 7.2C).

After these initial rounds of troubleshooting, I was able to better understand the source of lentiviral infection cytotoxicity. By using concentrated virus I could attempt to infect cells at a higher MOI. Viral overloading, and not specific viral preparation procedures, seemed to be the most likely cause for the observed cytotoxicity. Also, increasing the viral load for higher MOI infections appears to produce a variable degree of excessive cytotoxicity among different cell types. 293T cells were more tolerant to lentiviral infection, withstanding pLEG and pTREG shRNA infections up to an MOI of 10. With the resulting 293T pLEG shRNA cells infected at an MOI of 1, 5, and 10, I was able to demonstrate that at increasing MOIs, greater levels of pTREG expression, and thus target knockdown, can be achieved (Figure 7.3). The difference in knockdown produced by increasing MOI appeared to be more noticeable after a longer period of shRNA induction, albeit a modest difference.

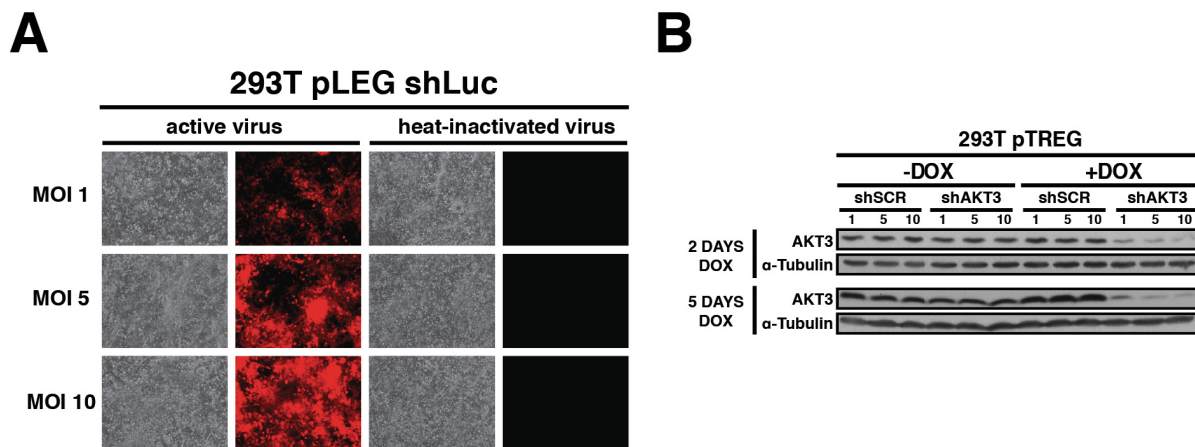


Figure 7.3. Affect of increased MOI on pTREG-mediated TurboRFP expression and target knockdown. (A) TurboRFP expression of 293T cells 5 days post-infection with pLEG shLuc lentivirus at MOI 1, 5, and 10. Also shown are cells that were exposed to heat-inactivated samples of the virus (for infections with heat-inactivated virus, equivalent volumes of virus to that used with active virus samples were used). Western blot analysis of 293T pTREG shSCR and shAKT3 cells infected at MOIs of 1, 5, and 10 +/- doxycycline treatment (1 μ g/mL doxycycline for a total of two or five days).

7.1.2.1. Viral Pseudotyping and Serum-less Medium for Virus Production and Infection

A search of the literature revealed that others have overcome the issue of cytotoxicity associated with VSV-G pseudotyped lentivirus by using lentivirus pseudotyped with alternative envelope (Env) glycoproteins (GPs) derived from other viruses [212-216]. Unfortunately,

specific research on viral pseudotyping for melanoma cells could not be found in the literature. In hopes of reducing infection cytotoxicity on melanoma cells, lentivirus was produced using three other viral Env glycoproteins: a modified version of the feline endogenous RD114 virus Env GP (RD114A), Lymphocytic choriomeningitis virus strain WE Env GP (LCMV-WE), and Mokola virus Env GP (MokolaG). These pseudotypes were chosen because they were suggested by multiple sources as alternatives to VSV-G for lentiviral production and had previously reported to successfully produce high viral titers and reduced cytotoxicity[212-218]. An initial infection of 293T cells with unconcentrated pLEG-eGFP-iPuro lentivirus pseudotyped with either of the four Env GPs was carried out to obtain a rough indication of relative titer production by assessing infection efficiency. The pLEG-eGFP-iPuro vector was used for this round of infections to allow for rapid assessment of infection efficiency by visualization of constitutive eGFP expression. In line with what has been previously reported, VSV-G yielded the highest infectivity (i.e. highest titer), followed by LCMV-WE, MokolaG, then RD114A (Figure 7.4A)[214, 215, 251]. Increasing the ratio of LCMV-WE, MokolaG, and RD114A-encoding plasmid DNA transfected for virus production, as suggested by Kutner *et al.*, did not markedly improve infectivity either[218]. WM9 cells were also infected using the unconcentrated virus to roughly assess infectivity and cytotoxicity that might result from the various pseudotypes. As expected, infection efficiency was very poor for MokolaG and RD114A pseudotyped virus (not shown), and was relatively high for VSV and LCMV-WE pseudotyped virus, with VSV having slightly higher infectivity than LCMV-WE (Figure 7.4B). Interestingly, the WM9 cells infected with the VSV lentivirus had all died a few days after infection, whereas those infected with the LCMV-WE virus were still viable, even though the cells appeared to have been infected at similar efficiencies (Figure 7.4B). This initial assessment of the infection of melanoma cells showed that LCMV-WE pseudotyped lentivirus held promise for producing similar titers to that of the VSV pseudotyped virus, and for having a less cytotoxic effect on melanoma cells.

We then proceeded to produce and concentrate (by ultracentrifugation) pLEG-eGFP-iPuro virus on a large scale for all four viral pseudotypes. This virus was to be used to infect melanoma cells at different MOIs to compare the cytotoxic effects of each of the viral pseudotypes. Since our initial infections with unconcentrated virus indicated that the viral titer with LCMV-WE would be slightly lower than with VSV, we transfected double the amount the LCMV-WE Env encoding plasmid for virus production compared to VSV. Likewise, since the

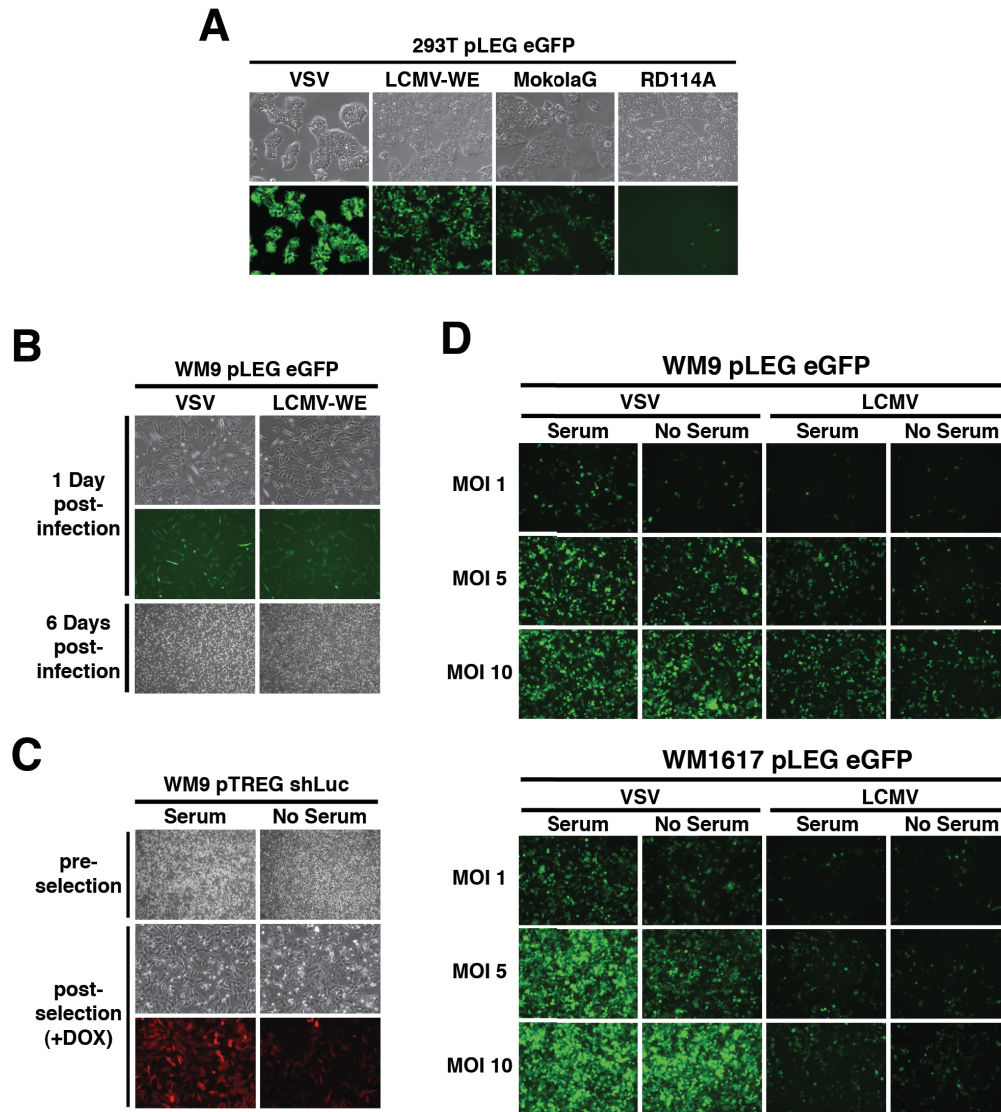


Figure 7.4. Affect of lentiviral vector pseudotyping and serum-less media on the infectivity and cytotoxicity of infection. (A) eGFP visualization of 293T cells infected with unconcentrated pLEG eGFP lentivirus produced with VSV-G, LCMV-WE, MokolaG, and RD114A pseudotypes. (B) WM9 cells infected with unconcentrated VSV and LCMV-WE pseudotyped pLEG eGFP lentivirus. One day post-infection: upper two panels, 100X magnification. Six days post-infection: bottom panel, 40X magnification. (C) WM9 cells infected with pTREG shLUC lentivirus at an MOI of 3 in serum-containing or serum-free media. Five days post-infection: top panel, 40X magnification. Post-selection and treatment with doxycycline (1 μ g/mL DOX for 5 days): bottom two panels, TurboRFP visualization at 100X magnification. (D) WM9 and WM1617 cells infected in serum-containing or serum-free medium with VSV or LCMV-WE pseudotyped pLEG eGFP lentivirus. eGFP expression was visualized two days post-infection.

titers MokolaG, and RD114A were considerably lower than VSV and LCMV-WE as indicated by the unconcentrated virus infection, for these two Env plasmids we transfected 10X as much

DNA compared to VSV. Viral titers of the MokolaG and RD114A pseudotyped lentivirus were still considerably lower ($\sim 10^4 - 10^5$ transducing units(TU)/mL) compared to the titers produced by LCMV-WE ($\sim 10^7$ TU/mL) and VSV ($\sim 10^8$ TU/mL). The titers for RD114A and MokolaG were so much lower that we decided not to continue on with testing these two pseudotypes in the cytotoxicity assessment. Our concern with using these viruses was that we would need to use much greater volumes of virus to infect the melanoma cells at the MOIs we wanted to test for infections (MOI 1, 5, and 10). This would not be practical considering the small volume of virus (~ 1 mL) you get using the ultracentrifugation concentration process.

Following this, concentrated VSV and LCMV-WE pseudotyped pLEG-eGFP-iPuro lentivirus was used to infect WM9 and WM1617 cells at an MOI of 1, 5, and 10 to qualitatively compare the cytotoxic effects on those melanoma cells. To assess the effect that presence of serum during transduction might have on melanoma cell toxicity post-transduction, we also compared conducting the infections in serum-containing and serum-free medium. It has been previously reported that in some cell types, when attempting to transduce at higher MOIs, using serum-free medium can not only improve lentiviral transduction efficiency but also decrease levels of cytotoxicity when compared to transduction in serum-containing media[252-254]. I had previously tested the affect of presence of serum in the infection medium on WM9 cells infected with pTRIPz shLUC at an MOI of 3 (Figure 7.4C). With serum, lentiviral infection was clearly more cytotoxic to the cells as compared to without serum. Five days post-infection (pre-selection), there was extensive cell death occurring in the cells infected in serum-containing medium and the remaining living population of cells looked generally unhealthy (abnormal morphology and slow growth/proliferation), in contrast to the cells infected in serum-free conditions in which the cells appeared relatively healthy (normal morphology and growth/proliferation rate). After puromycin selection, infection efficiency was assessed through visualization of doxycycline-induced TurboRFP expression to determine if the cells infected in serum-free conditions were being infected as efficiently as those infected in serum-containing media (Figure 7.4C). Visualization of TurboRFP revealed that cells were infected at a seemingly higher MOI with serum in the media, and this could possibly account for the observable increased cell mortality compared to the cells infected under serum-free conditions. The VSV and LMCV-WE pLEG-eGFP-iPuro infections were conducted in serum-containing or serum-free

medium to further explore the effect of serum on infection cytotoxicity when infecting at higher MOIs.

By visually examining the cells after transduction, it appeared that LCMV-WE pseudotyped virus was only marginally less cytotoxic to WM9 cells than VSV pseudotyped virus (not shown). Viral pseudotype had no noticeable difference on WM1617 cell mortality post-transduction either. However, it appeared that VSV pseudotyped virus consistently infected both WM9 and WM1617 cells more efficiently at any MOI (Figure 7.4D). Any additional cytotoxicity observed could then potentially be attributed to infection at an effectively greater MOI. Also, performing the infections in serum-free medium only marginally decreased WM9 and WM1617 cell mortality post-transduction (not shown). Having serum in the media for transduction increased the infectivity of the virus at MOI 1 and 5 (as previously seen with the pTREG infections, Figure 7.4C), but at an MOI of 10, transduction efficiencies appeared to be about equal between the two serum conditions when judged by eGFP expression. Perhaps the few cells that are dying from the serum-transduced conditions are those that have been infected at a higher rate, high enough to elicit the cell death response. If those cells were still viable after transduction, one could imagine how there might be higher levels of eGFP expression observed compared to what was observed for the cells transduced in serum-free media.

In conclusion, it seems that at lower MOIs (1-5), if we want greater transduction efficiencies with VSV-pseudotyped virus, it is best to use serum-containing media. Beyond a certain point (somewhere MOI of >5), cell mortality post-transduction could increase due to higher infection rate per cell, and this seems to impede our ability to acquire cells expressing higher levels of the lentiviral insert. In other words, there appears to be an upper limit to how many infections one cell can handle in serum-containing media. In serum-free media, this upper limit of infections per cell seems to be higher. This is in line with what others have reported in lentiviral transduction studies. In a study by Uchida *et al.*, at an MOI of 5 transduction of CD34+ hemopoietic stem cells with a lentiviral insert encoding for eGFP resulted in greater eGFP expression when transduced in serum-containing media as compared to serum-free media[253]. But at an MOI of 50, having serum in the media yielded much lower transduction rates and most of the cells died post-transduction in contrast to cells transduced in serum-free conditions which had markedly higher transduction rates at an MOI of 50 and cell viabilities similar to that of the no viral control [253].

Overall, using LCMV-WE pseudotyped virus and/or serum-less transduction had only a minor, if any, effect on reducing infection cytotoxicity. In fact, barely any cell death was observed with either pseudotype, even at an MOI of 10. This was unlike what I had observed previously with pTREG shRNA and pLEG shRNA transductions at higher MOIs, wherein WM9 cells could not tolerate infections at MOIs of 5 and 10, leaving only the cells infected at an MOI of 1 viable post-transduction (Figure 7.2). It could be that cytotoxicity is partially mediated by the type of viral vector transduced. Besides the fact that pTREG shRNA and pLEG shRNA encode shRNAmirs, these vectors also differ from pLEG-eGFP-iPuro in other ways in what they encode for under control of a constitutive promoter. Once integrated, they all constitutively express puromycin resistance gene, but additionally, the pTREG shRNA vector expresses rTta protein, and the pLEG shRNA vector expresses dsRED instead of eGFP. Interestingly, constitutive expression of a transactivator domain can reportedly cause phenotypic changes in mammalian cells, including cytotoxicity[255-259]. Also, dsRED expression has associated cytotoxic effects and has been shown to be more cytotoxic to cells than eGFP[222, 260]. Perhaps these elements, the rTta and dsRED, are the cause for the additional cell mortality observed post-transduction compared to what was observed with the pLEG-eGFP-iPuro lentiviral transductions.

To further investigate the effect of serum on pTREG infection cytotoxicity, I tested if there would be any additional benefit to removing serum from the medium when producing the virus. As suggested in the literature, removing serum from the medium during virus production can greatly reduce the risk of introducing adventitious agents, some of which might be contributing to the cell death resulting from lentiviral infection[219]. To investigate this, pTREG shSCR virus produced in serum-containing and serum-free medium was used to perform infections on WM9 and WM1617 cells at an MOI of 1, 5, and 10. Additionally, the cells were infected with or without serum present in the infection medium. Visual examination of the viable cells post-infection revealed that using serum-less medium for virus production appreciably decreases cell death caused by pTREG lentiviral infection (Figure 7.5).

Performing infections in serum-free conditions did not appear to additionally reduce cell death. Following these results, it could be that serum components being concentrated along with the lentivirus during ultracentrifugation and/or serum components present in infection medium are complexing with the lentivirus in a way that elicits a cytotoxic response during the infection process. Alternatively, serum could be increasing the infectivity of the virus, resulting in an

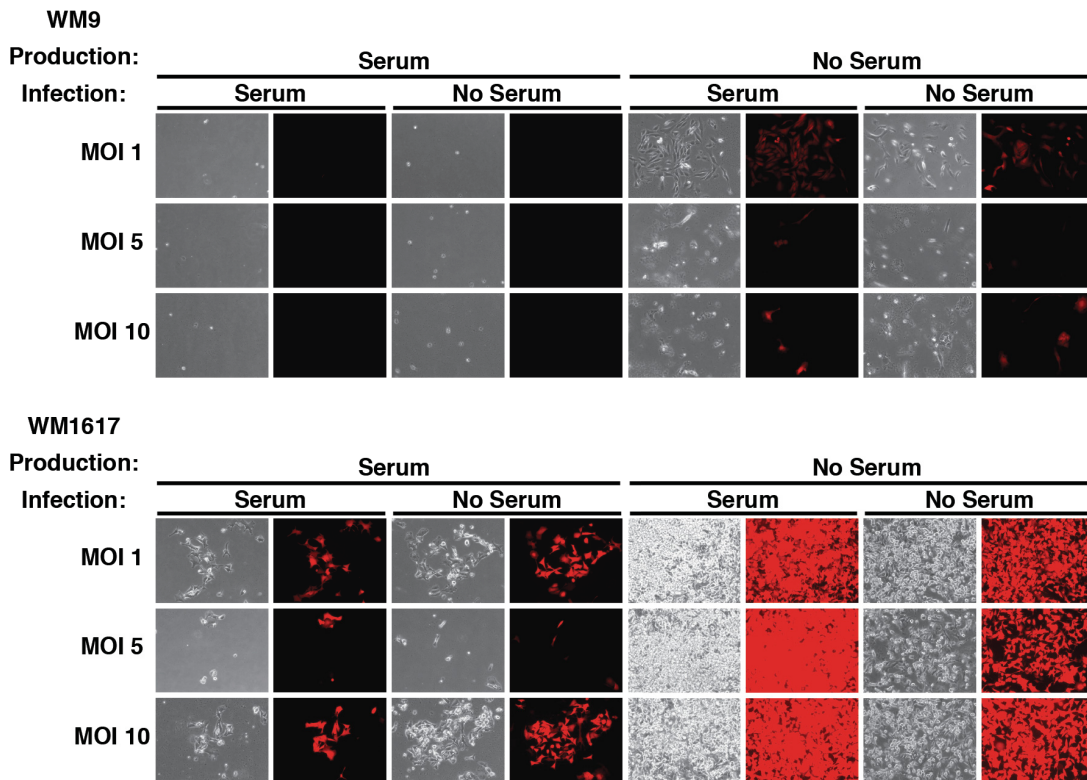


Figure 7.5. Presence of serum in virus production and transduction affects viral cytotoxicity. WM9 and WM1617 cells infected with pTREG shSCR lentivirus at MOI 1, 5, and 10. Virus produced with or without serum in the medium was used to perform transductions with or without serum in the transduction medium. Photos were taken six days post-infection and pre-selection. TurboRFP expression was induced with 1 $\mu\text{g}/\text{mL}$ doxycycline for two days before visualization with the fluorescence microscope.

excessive amount of infections per cell and eventual cell death because of elicited pro-death signaling. This could also explain why WM1617 cells appear to be more tolerant of lentiviral infection than WM9 cells. The biology of WM9 cells (e.g membrane composition, downstream signaling, etc.) could be more amenable to viral infection leading to higher infection rates resulting in higher susceptibility to cell death-related signaling. Nevertheless, the removal of serum during viral production seemed to mitigate the extent of cell death caused by lentiviral infection, and as a result was adopted as common practice for future production of concentrated lentivirus.

7.1.2.1. Underestimation of Lentiviral Titer/Redefining MOI

In the last set of infections described, the viral load appeared to be too high for the WM9 infections at any of the MOIs attempted (Figure 7.5). For all of the infection conditions, barely any of the cells survived, even at infection at an MOI of 1. The extent of cell death was much greater than any I had observed previously (Figure 7.2). This led me to believe that potentially the viral titers were being grossly underestimated, resulting in infection at MOIs effectively much greater than intended. Typically titration by drug selection/limiting dilution yields significantly lower estimated titers than titration with fluorescence activated cell sorting (FACS) analysis of a vector-encoded fluorophore. Unfortunately, I was unable to titer pTREG lentivirus by FACS because the FACS machines at my disposal were not equipped to detect TurboRFP expression sufficiently. Also, the process would be complicated by having to induce TurboRFP expression with doxycycline prior to FACS analysis. Another concern was that concurrent induction of shRNA expression would have secondary effects on determination of titer. Thus, titration with drug selection/colony counting was the method used for initial titrations of concentrated lentivirus. This method takes about 12-14 days since one has to wait on successfully infected 293T cells to grow out as colonies large enough to stain and count. Growth medium (containing selection drug) is changed several times before the cells are ready for staining. During medium changes or pre-staining rinses, invariably some colonies are washed off, even if the plates were pre-coated with an attachment factor (poly-D-lysine). The extent of colony loss due to washing off would vary from one titration to the next. Not only would this contribute to the underestimation of viral titer, it could also introduce variability into the titer estimates. Variability of titer results could also be partially responsible for variable toxicity from one infection to the next.

In search of a new method to more precisely and accurately determine pTREG lentiviral titer, I came across a method involving manual counting of pTREG TurboRFP expressing colonies. This method is the suggested method of titration for pTRIPz (precursor to pTREG) as described in the pTRIPz Technical Manual (ThermoScientific)[186]. It requires that 293T cells be transduced with serial dilutions of pTREG lentivirus, followed by incubation in doxycycline-containing medium. After three days of growth, TurboRFP positive colonies are manually counted for calculating viral titer. This method is advantageous over drug selection/colony counting for multiple reasons: (1) It takes 5 days rather than 12- 14 days to complete the titration protocol (2) The media only changed once during the whole process (to remove virus post-

transduction), thus reducing the risk of washing off transduced cells and underestimating the titer, and (3) 293T cells are transduced in 24-well plate format instead of 6-well format and serial dilutions are prepared in a 96-well plate (using multichannel pipettor) instead of microtubes, so it is more feasible to titer several viruses at the same time. One potential drawback to the TurboRFP colony count method is that concurrent shRNA expression could conceivably deleteriously affect 293T cell growth and/or viability. This could ultimately impact the titer result from one shRNA to the next. However, 293T cells had been previously infected with pLEG shRNA lentivirus, and none of the shRNAs targeting PTEN proximal genes appeared to adversely affect 293T cell growth and viability

After finding a more reliable method of titering virus, pTREG shRNA was produced (in serum-free medium), concentrated, and titered using this new method. To avoid issues with insufficient target knockdown (i.e. MOI too low) or extensive cell death following transduction (i.e. MOI too high), I infected WM9 and WM1617 cells with a subset of shRNA vectors (pTREG shAKT1 and shAKT3) at MOIs of differing orders of magnitude (MOI 0.01, 0.1, 1, 10) and assessed infection efficiency, cytotoxicity, and target knockdown. Characterizing pTREG functionality in this way would help identify the ideal range of MOI at which to infect cells to obtain optimal knockdown with minimal cytotoxicity. No cell death was observed post-transduction when infecting at an MOI of 0.01 and 0.1, but infection efficiency was extremely low, lower than what would be required for sufficient knockdown (Figure 7.6A). Conversely, a considerable amount of cell death occurred when cells were infected at an MOI of 10 and the overall health of surviving cells had clearly been compromised (morphologically abnormal and retarded proliferation). However, a number of cells survived the infection, unlike with previous pTREG infections with virus produced in serum-containing medium and titered using drug selection/colony counting. This indicates that removing serum from virus production staved the extent of post-transduction cell death and/or a more appropriate viral load was used for the infection because the new titration method more accurately determines viral titer. Infections at an MOI of 1 produced the best results as judged by infection efficiency and overall cell health post-transduction.

Next, the WM9 and WM1617 pTREG cells (MOI1) were used to determine if adequate protein knockdown could be achieved after various time intervals of doxycycline induction (WM9: Figure 7.6B, WM1617 with 2 doxycycline concentrations: Figure 7.7D). AKT1 was

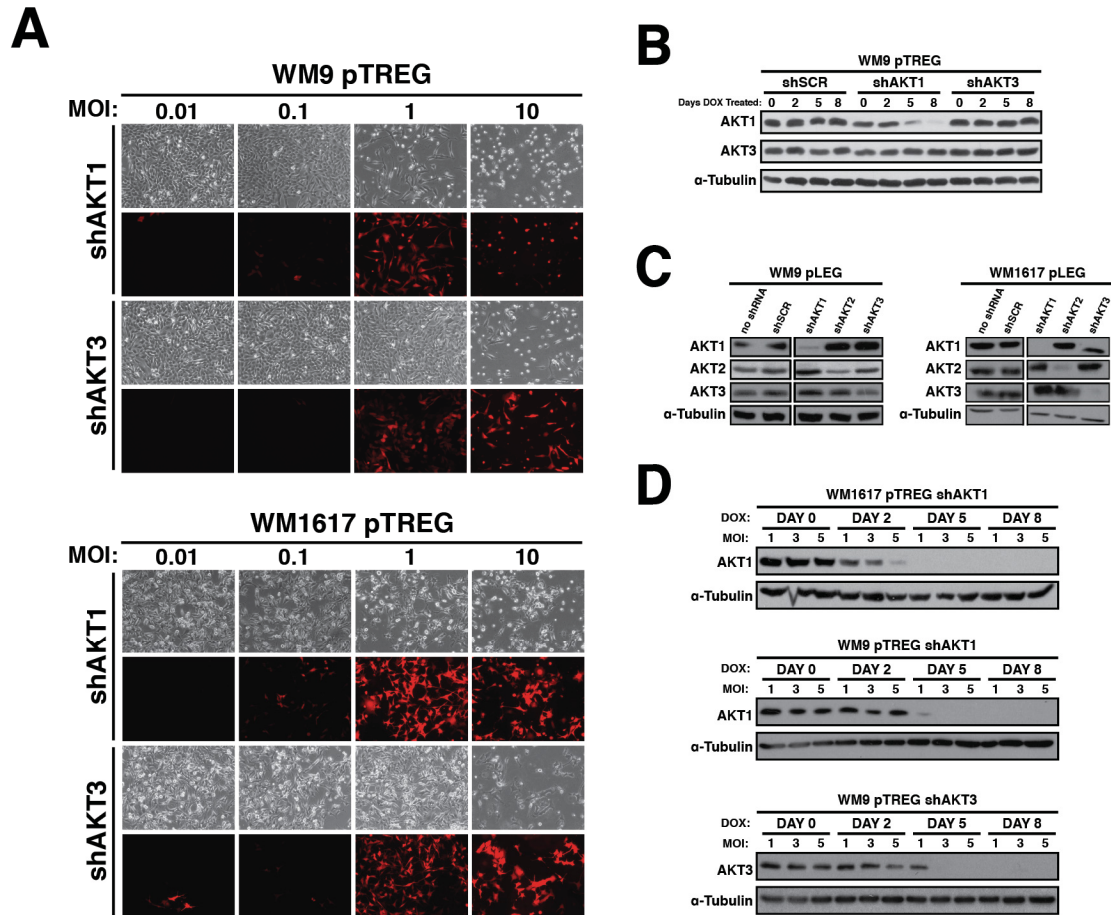


Figure 7.6. Characterization of pTREG-mediated target knockdown at different MOIs. (A) pTREG shAKT1 and shAKT3 virus, titered via the TurboRFP colony count method, was used to infect WM9 and WM1617 cells at an MOI of 0.01, 0.1, 1 and 10. Doxycycline (0.5 $\mu\text{g}/\text{mL}$) was added one day post-infection. TurboRFP expression was visualized 3 days post-infection. (B) Western blot analysis of WM9 pTREG shSCR, shAKT1, and shAKT3 (MOI of 1) cells treated with doxycycline (1 $\mu\text{g}/\text{mL}$) for the indicated amount of time. (C) Western blot analysis of WM9 and WM1617 pLEG shRNA cells. Controls were run on the same gel with the other samples, but lanes were separated by other samples not shown. (D) Western blot analysis of WM1617 pTREG shAKT1 cells infected at an MOI of 1, 3, or 5. Knockdown of AKT1 was assessed after the indicated length of doxycycline treatment times (0.25 $\mu\text{g}/\text{mL}$).

successfully targeted in WM9 and WM1617 cells, with noticeable knockdown being obtained by Day 5 and 2, respectively. In WM1617 shAKT3 cells, AKT3 protein levels were noticeably knocked down by Day 8 of doxycycline treatment, but the knockdown produced was not as effective as compared to AKT1 knockdown. Unfortunately, AKT3 knockdown was unsuccessful in WM9 shAKT3 cells, even after 8 days of doxycycline treatment. Again, AKT3 proved to be more difficult to target in these cells. We know that knockdown is possible in these cells using

the pLEG shRNA vector targeting AKT3 (Figure 7.6C), so it appears that inadequate targeting with pTREG can be attributed to insufficient levels of shRNA expression. WM9 and WM1617 cells were infected at an MOI of 1, 3, and 5 with the pTREG shAKT lentiviruses to determine if increasing MOI (to a tolerable level) would allow for the effective targeting of all AKT proteins. Even though more cell death was observed for infections at MOI of 3 and 5, the infections were well tolerated and survived for further subculturing. We are currently in the process of assessing knockdown efficacy in these cell lines. Initial results indicate that with this newly infected set of cells, inducible knockdown of AKT3 was finally achieved in WM9 pTREG cells (Figure 7.6D). Also, as expected, increasing infection MOI to 3 and 5 allows for more prompt ablation of targeted protein (Figure 7.6D). This would be useful for future experiments as it would reduce the time required before assaying for a biological response to knockdown. Also,

7.1.3. Doxycycline Toxicity

In another attempt to improve efficacy of pTREG mediated knockdown, higher concentrations of doxycycline treatment was used to elicit increased shRNA transcription from the TRE promoter. In preliminary tests wherein higher concentrations of doxycycline were used, treatment of 293T pTREG cells with 10 $\mu\text{g}/\text{mL}$ of doxycycline resulted in elevated expression of TurboRFP, as compared to treatment with 1 $\mu\text{g}/\text{mL}$ of doxycycline (Figure 7.7A). This was the first indication that boosting doxycycline concentration could indeed drive increased transcription off the TRE promoter to produce more TurboRFP, and presumably more shRNA. Unfortunately, when attempting to treat WM9 pTREG cells with 10 $\mu\text{g}/\text{mL}$ of doxycycline, not only did this impede TurboRFP expression, it was toxic to the cells causing cell death, major growth retardation, and changes in cell morphology (Figure 7.7B). It had also become evident that even with treatment at 1 $\mu\text{g}/\text{mL}$ of doxycycline in pTREG cell counting assays, doxycycline treated wells would have decreased cell number when compared to doxycycline-free wells for all shRNAs including the control (not shown). Others have found that doxycycline treatment can have deleterious effects on cell metabolism, viability, and proliferation *in vitro*[220-222].

The emergence of doxycycline toxicity necessitated the need to find a safe concentration of doxycycline for treatment of pTREG cells. This would ensure that at the onset of doxycycline treatment, any effects on viability, proliferation, and transformation would be attributable to induced shRNA expression. Viability assays were performed with 293T, A375, WM1617, and

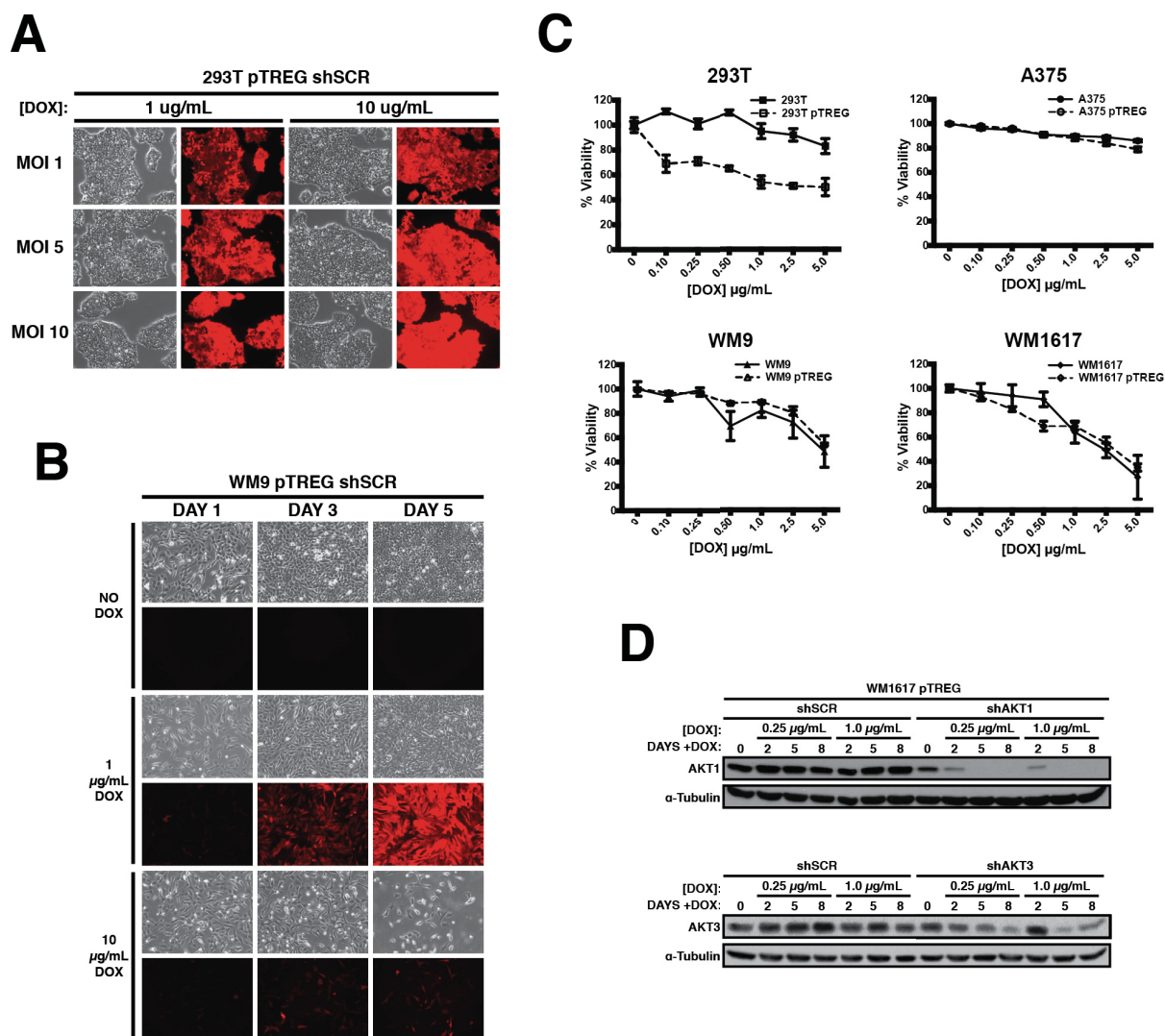


Figure 7.7. Effect of doxycycline concentration on pTREG expression and cell viability. (A) 293T pTREG shSCR cells (post-selection) after 2 days of doxycycline treatment at 1 µg/mL or 10 µg/mL. (B) WM9 pTREG shSCR cells (MOI 3) treated with either 1 µg/mL or 10 µg/mL of doxycycline for 5 days. (C) Resazurin viability analysis of 293T cells and various melanoma cell lines and the pTREG shSCR (MOI3) infected versions of these cells when treated with various concentrations of doxycycline for five days. Error bars represent relative standard error. (D) Western blot analysis of pTREG-mediated AKT1 and AKT3 knockdown in WM1617 cells (MOI1) when treated with 0.25 µg/mL or 1 µg/mL doxycycline for the indicated times.

WM9 cells and their pTREG shSCR infected equivalents. As expected, cell viability decreased with increasing doxycycline concentration. Doxycycline toxicity on pTREG cells compared to uninfected cells was similar, except for 293T pTREG cells which were much more sensitive to

doxycycline treatment at any concentration. For the melanoma cell lines, WM1617 cell viability appeared to be the most affected, followed by WM9 cells and then A375 cells. At the standard doxycycline treatment concentration of 1 $\mu\text{g}/\text{mL}$, decreased viability of WM1617 cells was quite apparent. Treatment at this concentration produced a marginal decrease in viability for A375 and WM9 cells. Following these results, lower concentrations of doxycycline (0.10 to 0.25 $\mu\text{g}/\text{mL}$) were used for induction of shRNA expression from pTREG for future experiments. Importantly, Western blot analysis of WM1617 pTREG shAKT1 and shAKT3 cells confirmed that doxycycline treatment with 0.25 $\mu\text{g}/\text{mL}$ produced the same level of knockdown as treatment with 1 $\mu\text{g}/\text{mL}$ (Figure 7.7D). If using higher concentrations of doxycycline does not in fact improve knockdown efficacy in pTREG cells, use of lower concentrations of doxycycline is further justified.

7.2. Appendix Tables

Table 1. Sequencing primers for shRNA sequence confirmation in shRNAmir containing plasmids.

Primer Name	Primer Target	Sequence (5' – 3')
AD0058	pBEG shRNA (Fwd)	TGAGCAAAGACCCCAACGAG
AD0057	pBEG shRNA (Rev)	GTCATTTTCAGGTCCTTGGG
AD0060	pLEG shRNA (Rev)	AGCAGCGTATCCACATAGCG
AD0051	pTREG shRNA (Fwd)	AGAACCTCAAGATGCCCGGCT
AD0052	pTREG shRNA (Rev)	TAAGGCCGAGTCTTATGAGCA

Table 2. Cloning primers to construct TOPO compatible AKT2 cDNA PCR product.

Primer Name	Primer Target	Sequence (5' – 3')
KD0052	pDNR-Dual AKT2 (Fwd)	CACCATGGGATCCCCCCCAGGGAGCACT AAGCGAGC
KD0053	pDNR-Dual AKT2 (Rev)	CCCCCCCCTCGAGTCACAATTGGTCTGA GTCAGGCCCTTC

Table 3. DNA oligonucleotides for shRNA sequences used in the pBEG system. Underlined are the sequences homologous to the universal PCR primers. The sense and antisense strands are highlighted in grey. The bolded letter in the sense strand was changed to be uncomplimentary to the bolded letter in the antisense strand.

Target	shRNA #	Sequence (5' – 3')
Luc	-	<u>TGCTGTTGACAGTGAGCGCCCGCCTGAAGTCTCTGATTAATAGT</u> GAAGCCACAGATGTATTAATCAGAGACTTCAGGCGGTTGCCTAC <u>TGCTCGGAAT</u>
SCR	49	<u>TGCTGTTGACAGTGAGCGAGAATCTCATTCGATGCATACTAGTG</u> AAGCCACAGATGTAGTATGCATCGAATGAGATTCTGCCTACTG <u>CCTCGGAAT</u>
AKT1	1	<u>TGCTGTTGACAGTGAGCGCGACCATGAACGAGTTTGATAGTGAA</u> GCCACAGATGTATCAAACCTCGTTCATGGTCA T GCCTACTGCCTCG <u>GAAT</u>
	2	<u>TGCTGTTGACAGTGAGCGATGGACCACTGTCATCGAATAGTGAA</u> GCCACAGATGTATTCGATGACAGTGGTCCACTGCCTACTGCCTC <u>GGAAT</u>
AKT2	7	<u>TGCTGTTGACAGTGAGCGACTACTTCCTCCTCAAGAATGTAGTG</u> AAGCCACAGATGTACATTCTTGAGGAGGAAGTAGCTGCCTACTG <u>CCTCGGAAT</u>
	11	<u>TGCTGTTGACAGTGAGCGAAGAATGCCAGCTGATGAATAGTGAA</u> GCCACAGATGTATTCATCAGCTGGCATTCTGTGCCTACTGCCTCG <u>GAAT</u>
AKT3	13	<u>TGCTGTTGACAGTGAGCGAGCACTTTTGGGAAAGTTATTTAGTG</u> AAGCCACAGATGTAAAATAACTTTCCCAAAGTGCCTGCCTACT <u>GCCTCGGAAT</u>
AKT3	16	<u>TGCTGTTGACAGTGAGCGATGCCTTGGACTATCTACATTTAGTGA</u> AGCCACAGATGTAAATGTAGATAGTCCAAGGCAGTGCCTACTGC <u>CTCGGAAT</u>
PDK1	18	<u>TGCTGTTGACAGTGAGCGCGGCAAGAGACCTCGTGGAGAATAGT</u> GAAGCCACAGATGTATTCTCCACGAGGTCTCTTGCC T GCCTACT <u>GCCTCGGAAT</u>
	22	<u>TGCTGTTGACAGTGAGCGAGCAGCAACATAGAGCAGTACATAGT</u> GAAGCCACAGATGTATGTA T CTGCTCTATGTTGCTGCCTGCCTACT <u>GCCTCGGAAT</u>
PTEN	24	<u>TGCTGTTGACAGTGAGCGAAGGAACAATATTGATGATGTATAGT</u> GAAGCCACAGATGTATACATCATCAATATTGTT CCT GCCTACT <u>GCCTCGGAAT</u>
	26	<u>TGCTGTTGACAGTGAGCGAAAACATTATTGCTATGGGATTTAGT</u> GAAGCCACAGATGTAAATCCCATAGCAATAATGTT T GCCTAC <u>TGCCTCGGAAT</u>
PIK3CA	30	<u>TGCTGTTGACAGTGAGCGACCAAGAATCCTAGTAGAATGTTTAT</u> AGTGAAGCCACAGATGTATAAACATTCTACTAGGATTCTTGGG T <u>GCCTACTGCCTCGGAAT</u>
	32	<u>TGCTGTTGACAGTGAGCGCGGCTTATCTAGCTATTCGACATAGT</u> GAAGCCACAGATGTATG T CGAATAGCTAGATAAGCCT T GCCTAC <u>TGCCTCGGAAT</u>
PIK3CB	34	<u>TGCTGTTGACAGTGAGCGCGCAACAGCTTTGCATGTTAAATAGT</u> GAAGCCACAGATGTATTTAACATGCAAAGCTGTTGCATGCCTAC

		TGCCTCGGAAT
	36	<u>TGCTGTTGACAGTGAGCGACTCCTTATGGATATTGACTCCTATTA</u> GTGAAGCCACAGATGTAATAGGAGTCAATATCCATAAGGAGGT <u>GCCTACTGCCTCGGAAT</u>
PIK3CD	39	<u>TGCTGTTGACAGTGAGCGCGGCCCTGAATGACTTCGTCAATAGT</u> GAAGCCACAGATGTATTGACGAAGTCATTGAGGGCCTTGCCTAC <u>TGCCTCGGAAT</u>
	41	<u>TGCTGTTGACAGTGAGCGAAAGACTAATAATAGTGAGAAATAGT</u> GAAGCCACAGATGTATTTCTCACTATTATTAGTCTTCTGCCTACT <u>GCCTCGGAAT</u>
PIK3CG	45	<u>TGCTGTTGACAGTGAGCGCAAGCTTTAGAGTTCCATATGATAGT</u> GAAGCCACAGATGTATCATATGGAAGCTCTAAAGCTTTTGCCTAC <u>TGCCTCGGAAT</u>
	47	<u>TGCTGTTGACAGTGAGCGACCAAGTTATTTACAACCTTAATAGT</u> GAAGCCACAGATGTATTAAGTTGTGAAATAACTTGGGTGCCTAC <u>TGCCTCGGAAT</u>
P53	HP65	<u>TGCTGTTGACAGTGAGCGCCCACTACAAGTACATGTGTAATAGT</u> GAAGCCACAGATGTTACACATGTAAGTTGTAGTGGATGCCTACTG <u>CCTCGGAAT</u>
	HP44	<u>TGCTGTTGACAGTGAGCGCGGAAATTTGTATCCCGAGTATTAGT</u> GAAGCCACAGATGATACTCGGGATACAAATTTCTTGCCTACTG <u>CCTCGGAAT</u>
	HP18	<u>TGCTGTTGACAGTGAGCGACCAGTCTACTTCCCGCCATAATAGT</u> GAAGCCACAGATGTTATGGCGGGAAGTAGACTGGCTGCCTACTG <u>CCTCGGAAT</u>

Table 4. The miRNA-30 and miRNA-E backbones. The change from the BamHI site to BglII site is shown highlighted in grey. The original miRNA-30 EcoRI site is shown here underlined. This site was destroyed in the miRNA-E backbone. The new EcoRI site is shown in lowercase letters. The 5' modification to compliment this change is shown in bold.

miRNA	Sequence Ordered for Cloning (5' – 3')
miRNA-30	<u>GGATCC</u> AGCGCTGGCGCGCCATTTAAATCGATAGTTTGTGTTGAATGAGGCTTCA GTA ^{TTT} TACAGAATCGTTGCCTGCACATCTTGGAAACACTTGCTGGGATTACTT CTTCAGG TAAACCAACAGAAGGCTCGAGAAGGTATATTGCTGTTGACAGTGA GCGCACGTGATGCCTACTGCCTCGGAATTCAAGGGGCTA ^{ctttag} GAGCAATTATC TTGTTTACTAAAACCTGAATACCTTGTCTATCTCTTTGATACATTTTACAAAGCTG AATTA ^{AAA} ATGGTATAAATTAATCACTTTTTTCAATTGTTTAAACCCTGCAGG TACGTAACGCGTGGATATC
miRNA-E	<u>AGATCT</u> AGCGCTGGCGCGCCATTTAAATCGATAGTTTGTGTTGAATGAGGCTTCA GTA ^{TTT} TACAGAATCGTTGCCTGCACATCTTGGAAACACTTGCTGGGATTACTT CGACTT CTTAACCAACAGAAGGCTCGAGAAGGTATATTGCTGTTGACAGTGA GCGCACGTGATGCCTACTGCCTCGGAAGTCAAGGGGCTA ^{gaattc} GAGCAATTATC TTGTTTACTAAAACCTGAATACCTTGTCTATCTCTTTGATACATTTTACAAAGCTG AATTA ^{AAA} ATGGTATAAATTAATCACTTTTTTCAATTGTTTAAACCCTGCAGG TACGTAACGCGTGGATATC

Table 5. Melanoma lines and their mutation status.

Cell line	Type of lesion	Site	Reported mutations
WM278	primary VGP	cutis	BRAF(V600E), hemizygous deletion PTEN
WM1617	metastasis (same patient as WM278)	cutis	BRAF(V600E), hemizygous deletion PTEN
WM35	early primary RGP	scalp/neck	BRAF(V600E), PTEN mutant
WM793	primary VGP	-	BRAF(V600E), PTEN mutation/hem. del., CDK4 (K22Q)
WM9	metastasis	LN axilla	BRAF(V600E), PTEN hem. del.
WM2664	metastasis	skin	BRAF(V600D), PTEN hom. del.
WM451Lu	mouse xenograft metastasis	lung	BRAF(V600E), (PTEN WT)
Sbc12	primary RGP	-	NRAS(Q61R)
A-375	metastasis	-	BRAF(V600E), (PTEN WT)
MM485	metastasis	LN	NRAS(Q61R), CDKN2A(W110Stop)
MM370	metastasis	LN	BRAF(V600E), CDKN2A hom. deletion
Sk-mel-2	metastasis	thigh	NRAS(Q61R) (PTEN WT)

Table 6. Primers for qRT-PCR analysis of PTEN Proximal gene mRNA expression.

Target	Primer #	Sequence (5' – 3')
S28	CJ0039	TCCATCATCCGCAATGTAAAAG
	CJ0040	GCTTCTCGCTCTGACTCCAAA
GAPDH	CJ0047	TGCACCACCAACTGCTTAGC
	CJ0048	CAGCCTTGGCAGCGCCAGTA
β -Actin	CJ0037	GCAAAGACCTGTACGCCAAC
	CJ0038	AGTACTTGCGCTCAGGAGGA
PIK3CA	CJ0017	TTAGCCAGAGGTTTGGCCTG
	CJ0018	TCTGGTCGCCTCATTTGCTC
PIK3CB	CJ0023	ATCCTTGACATCTGGGCGGT
	CJ0024	GGGTAATTGTGAACTTGCTTCCA
PIK3CD	CJ0025	GCTCGCTCCACCAAGAAGAA
	CJ0026	CGCTATCCGTGTTGGGGTTA
PIK3CG	CJ0029	AGGGGAAAGCTTCATAGCCTC
	CJ0030	CCTTCGGCAGTTGTCCTCTC
PDK1	CJ0001	CAGAGAGCGGGATGTCATGT
	CJ0002	TCAGCCGTGTAAAATCGGGT
PTEN	CJ0035	AAGGCACAAGAGGCCCTAGA
	CJ0036	GATTGCAAGTTCCGCCACTG
AKT1	CJ0005	CAGGATGTGGACCAACGTGA
	CJ0006	AAGGTGCGTTTCGATGACAGT
AKT2	CJ0041	AGTGACTCCTCCACGACTGA
	CJ0042	TTCGCAGGATCTTCATGGCG
AKT3	CJ0015	CAGACAGACTGCAGAGGCAA
	CJ0016	TCCACTTGCCTTCTCTCGAAC